The Dynamics and Mass Budget of Arctic Glaciers

Extended abstracts

Workshop and GLACIODYN (IPY) meeting, 15 - 18 January 2007, Pontresina (Switzerland)

IASC Working group on Arctic Glaciology

IMAU Institute for Marine and Atmospheric research Utrecht

Institute for Marine and Atmospheric Research Utrecht
Utrecht University, The Netherlands

The Dynamics and Mass Budget of Arctic Glaciers

Extended abstracts

Workshop and GLACIODYN (IPY) Meeting, 15 - 18 January 2007, Pontresina (Switzerland)

IASC Working Group on Arctic Glaciology

Organized by J. Oerlemans and C.H. Tijm-Reijmer

Institute for Marine and Atmospheric Research Utrecht
Utrecht University, The Netherlands

CONTENTS

PREFACE

This year (2007) the annual workshop of the Working Group on Arctic Glaciology of the International Arctic Science Committee (IASC-WAG) was held once more in Pontresina, Switzerland. Apart from the traditional contributions on the mass balance of arctic glaciers there was also an appreciable number of contributions on glacier dynamics.

Over 50 participants presented 41 oral contributions and 11 posters on a wide range of subjects. Since previous reports of the workshop were received with great enthusiasm, it was decided to make a book of extended abstracts once more. Therefore many of the presentations are summarized here, and I want to thank the contributors for their efforts to produce clear and well-illustrated texts.

IASC generously provided financial means for eight young scientists to participate in the workshop. Further support was received from IMAU (Utrecht University) and the Netherlands IPY Programme (NWO), covering the costs of the congress facilities and the printing of this book.

It is clear that the IPY will strengthen existing projects and generate new projects on arctic glaciers. The issue of greenhouse warming, land ice and sea level, remains an important one. The summary of the upcoming 4th IPCC assessment makes clear that the uncertainty in sea-level projections is large. The Greenland Ice Sheet, in particular, is the subject of an intense debate.
GLACIODYN, a lead IPY project on the sensitivity of arctic glaciers to climate change, fits very well in this picture. It will help to answer questions about the stability and sensitivity of arctic ice masses. According to reports of the national representatives, funding of significant GLACIODYN projects has now been secured.
For some years to come, GLACIODYN will keep the Working Group on Arctic Glaciology busy. We expect that the annual workshop will remain a useful informal event where preliminary results can be discussed and further plans can be made.
Information on the activities of the IASC-WAG, including a description of GLACIODYN, can be found at:
http://www.phys.uu.nl/%7Ewwwimau/research/ice_climate/iasc_wag/

Finally, I thank Carleen Tijm-Reijmer for all the help in organising the workshop and editing the book of abstracts.

Johannes Oerlemans
Chairman, IASC Working Group on Arctic Glaciology

PROGRAM

Monday 15

Convener: Jon Ove Hagen

- 09:00 – 09:10 *Jon Ove Hagen:* Welcome
- 09:10 – 09.30 *Tazio Strozzi, A. Wiesmann, U. Wegmüller and C. Werner*: Estimation of the motion of arctic glaciers with satellite L-band SAR data
- 09.30 – 09:50 *Martin Lüthi*: Ice dynamics changes of Jakobshavn Isbrae
- 09.50 – 10:10 *Jason Box*: Impact of surface meltwater production in Greenland ice sheet flow
- 10:10 – 10:30 *Roderik van de Wal*: GPS observations along the K-transect, West Greenland

10:30 – 10:50 Coffee break

- 10:50 – 11:10 *Manfred Stober*: Geodetic investigations on dynamic parameters of the West Greenland inland ice
- 11:10 – 11:30 *Vicky Parry*: Variations in mass balance and density of the snowpack and firn in Greenland's percolation zone
- 11:30 – 11:50 *H. Jay Zwally, A.C. Brenner, S.B. Luthcke, D. Yi, J. Li, J.L. Saba, M.B. Giovinetto, H.G. Cornejo, M.A. Beckley, and W. Abdalati*: Mass balance of the Greenland ice sheet: Consistent results on near balance to negative
- 11:50 – 12:10 *Jonathan Bamber, M. Bougamont, R. Gladstone, J. Griggs, T. Payne, I. Rutt, E. Hanna, J. Ridley, W. Greuell*: Predicting the surface mass balance of the Greenland ice sheet: Importance of refreezing

12:10 – 14:00 LUNCH

Convener: Roderik van de Wal

- 14:00 – 14:20 *Mark Dyurgerov*: The reference state of bench mark glaciers world wide; the possible glacier monitoring concept
- 14:20 – 14:40 *Valentina Radic*: Glacier volume projections: flowline modelling vs volume-area scaling
- 14:40 – 15:00 *Regine Hock*: Intercomparison of mass balance models using ERA-40 reanalysis and climate model data
- 15:00 – 15:20 *Atsumo Ohmura*: Long-term relation between mass budget and energy balance for Arctic glaciers

15:20 – 15:50 Coffee break

- 15:50 – 16:00 *Per Holmlund*: Climate influence on ice dynamics of Mårmaglaciären, northern Sweden
- 16:00 – 16:20 *Eleri Evans*: Changing snow cover and the net mass balance of Storglaciären, Northern Sweden
- 16:20 – 16:40 *Liss Andreassen*: Observing and modelling the energy and mass balance of Storbreen, Norway

- 16:40 – 17:00 *Thomas Schuler, P. Crochet, M. Jackson and R. Hock*: Accumulation distribution across Svartisen assessed by a model of orographic precipitation
- 17:00 – 17:20 *Frank Paul and L.M. Andreassen*: A new glacier inventory for the Svartisen area (Norway) from Landsat ETM+: Methodological challenges and first results

DINNER

Tuesday 16

Convener: Tomas Johannesson

- 09:00 – 09:20 *Antoine Kies*: Natural Radioactive Isotopes in Glaciology
- 09:20 – 09:40 *Veijo Pohjola, B. Sjögren, T. Martma, E. Isaksson, J. Kohler, K. Törnblom and R.S.W. van de Wal*: A study of 18O and temperature gradients and their trends and relations over the ice field Lomonosovfonna, Svalbard
- 09:40 – 10.00 *Neil Arnold*: Topographic controls on the spatial variability of glacier surface energy balance
- 10.00 – 10:20 *Cameron Rye*: Modelling the 21st century mass balance of Svalbard glaciers using ERA-40 reanalysis and general circulation models

10:20 – 10:50 Coffee break

- 10:50 – 11:10 *Ireneusz Sobota*: Mass balance monitoring of Kaffiøyra glaciers in 1996-2006, Svalbard
- 11:10 – 11:30 *Krzysztof Migala, D. Puczko, J. Jania, P. Glowacki*: Ablation of Hansbreen (Svalbard) estimated using energy balance from the AWS data
- 11:30 – 11:50 *F. Machío, Javier Lapazaran, P. Dolnicki, M. Petlicki, P. Glowacki and F. Navarro*: Preliminary results from radio-echo sounding at Ariebreen, Hornsund, Spitsbergen
- 11:50 – 12:10 *Aleksey Sharov*: Ground control for modelling glacier changes in “Hornsundet”

12:10 – 14:00 LUNCH

Convener: Veijo Pohjola

- 14:00 – 14:20 *Ian Willis*: Changes in the Thermal Regime of the Polythermal Midre Lovénbreen, Svalbard
- 14:20 – 14:40 *Ivan Lavrentiev*: Fridtjovbreen changes in 20th century from remote sensing data
- 14:40 – 15:00 *P. Glowacki, E.V. Vasilenko, Y.Y. Macheret, A. Glazovski , J. Moore , J.O. Hagen, D. Puczko, M. Grabiec, Jacek Jania*: Surface and bedrock topography of Amundsenisen - the thickest ice mass on Svalbard
- 15:00 – 15:20 *P. Glowacki, E.V. Vasilenko, Y.Y. Macheret, Andrey Glazovsky, J. Moore, J.O. Hagen, F.J. Navarro*: Structure of Amundsenisen, Spitsbergen, from ground-based radio echo sounding

15:20 – 15:50 Coffee break

- 15:50 – 16:00 *Michael Zemp*: World Glacier Monitoring Service - Call-for-data for the observation period 2000-2005 and IPY activities

- 16:00 – 16:20 *Matt Nolan*: Volume change of glaciers in Alaska's arctic
- 16:20 – 16:40 *Felix Svoboda and F. Paul*: A new glacier inventory for Cumberland Peninsula, Canadian Arctic, from ASTER data with assessment of changes since 1975
- 16:40 – Poster Introduction and poster session

DINNER

Wednesday 17

Convener: Jacek Jania

- 09:00 – 09:20 *Tad Pfeffer*: A simple mechanism for irreversible outlet glacier retreat
- 09:20 – 09.40 *Guðfinna Aðalgeirsdóttir, H. Björnsson, F. Pálsson and S.P. Sigurðsson* : 20th century evolution and modeling of Hoffellsjökull, southeast Iceland
- 09.40 – 10:00 *Tomas Johannesson*: Mass balance modeling of Hofsjökull
- 10.00 – 10.20 *Matt Nolan*: GLACIODYN: Outreach activities

10:20 – 10:50 Coffee break

- 10:50 – 11:10 *Sverrir Guðmundsson, H. Björnsson, G. Aðalgeirsdóttir, T. Jóhannesson, F. Pálsson and O. Sigurðsson*: Climate change response of three ice caps in Iceland
- 11:10 – 11:30 *Helgi Bjornsson*: Vatnajökull 2007: reflections and outlook
- 11:30 – 11:50 *Jon Ove Hagen*: The Norwegian contribution to Glaciodyn, plans for 2007-2009
- 11:50 – 12:10 *Jonathan Bamber, T. Murray, T. James, J. Rougier, B. Krabill, J. Kohler, J.O. Hagen, P. Gogineni*: Geodetic observations of Svalbard land ice mass balance: Results and plans for IPY

12:10 – 16:30 LUNCH and skiing at Diavolezza

- 17:00 – 18:30 **National representatives meeting**

DINNER

Thursday 18

- 9:00 – Excursion to the AWS on the Morteratsch glacier

DINNER

POSTERS

- *Christina Bell*: Controls on the spatial and temporal variability in the snowpack of a High Arctic ice mass: the Devon Island Ice Cap, Nunavut, Canada
- *Marianne den Ouden, J. Oerlemans and C.H. Reijmer*: Relation of melt water and flow velocities of Arctic glaciers: Nordenskiöldbreen, Svalbard
- *Thorben Dunse*: Snow accumulation on Austfonna, northeastern Svalbard, derived by ground-penetrating radar
- *Mariusz Grabiec*: Mass balance assessment of Werenskioldbreen (SW Spitsbergen) on the basis of meteorological and cartographical data
- *Geir Moholdt*: A new DEM over Austfonna ice cap from SAR interferometry, ICESat altimetry and GPS ground profiles
- *F. Obleitner and M. Kuhn*: Measurement and simulation of the turbulent fluxes at the Greenland Summit
- *J. Oerlemans, Carleen Reijmer, M.R. van den Broeke and R.S.W. van de Wal*: Arctic Glaciers, Climate and Sea Level Change: A Contribution to GLACIODYN
- *F. Pálsson, Sverrir Guðmundsson and H. Björnsson*: The impact of volcanic and geothermal activity on the mass balance of Vatnajökull
- *Ireneusz Sobota*: Ablation and outflow from Kaffiøyra glaciers in 1996-2006, Svalbard
- *Ireneusz Sobota*: Relationship of equilibrium line altitude (ELA) and accumulation area ratio (AAR) with mass balance of Kaffiøyra glaciers, Svalbard
- *Irina Solovjanova*: Results of 4 years massbalance measurements on Svalbard glaciers (Barentsburg area)

LIST OF PARTICIPANTS

1. Guðfinna Aðalgeirsdóttir (gua@dmi.dk)
   Danish Climate Centre, Danish Meteorological Institute, Copenhagen, Denmark
2. Liss Andreassen (lma@nve.no)
   Norwegian Water Resources and Energy Directorate, Oslo, Norway
3. Neil Arnold (nsa12@cam.ac.uk)
   Scott Polar Research Institute, Cambridge, UK
4. Narelle Baker (npmb2@cam.ac.uk)
   Scott Polar Research Institute, Cambridge, UK
5. Jonathan Bamber (j.bamber@bristol.ac.uk)
   Bristol Glaciology Centre, University of Bristol, UK
6. Christina Bell (christina.bell@abdn.ac.uk)
   University of Aberdeen, Aberdeen, UK
7. Helgi Björnsson (hb@raunvis.hi.is)
   Institute of Earth Sciences, University of Iceland, Reykjavik, Iceland
8. Jason Box (box.11@osu.edu)
   Byrd Polar Research Center, Ohio State University, Columbus, Ohio, USA
9. Marianne den Ouden (M.A.G.denOuden@phys.uu.nl)
   Institute for Marine and Atmospheric Research, Utrecht University, Netherlands
10. Thorben Dunse (thorben.dunse@geo.uio.no)
    Department of Geosciences, University of Oslo, Oslo, Norway
11. Mark Dyurgerov (Mark.Dyurgerov@Colorado.EDU)
    INSTAAR, University of Colorado, Boulder, USA
    Department of Physical Geography and Quaternary Geology, Stockholm University, Sweden
12. Eleri Evans (e_evans00@yahoo.com)
    University of Wales, Aberystwyth, UK
13. Andrey Glazovsky (icemass@yandex.ru)
    Institute of Geography, Russian Academy of Sciences, Moscow, Russia
14. Piotr Glowacki (glowacki@igf.edu.pl)
    Institute of Geophysics, Polish Academy of Science, Warszawa, Poland
15. Mariusz Grabiec (mgrabiec@ultra.cto.us.edu.pl)
    University of Silesia, Sosnowiec, Poland
16. Sverrir Gudmundsson (sg@raunvis.hi.is)
    Institute of Earth Sciences, University of Iceland, Reykjavik, Iceland
17. Jon Ove Hagen (j.o.m.hagen@geo.uio.no)
    Department of Geosciences, University of Oslo, Oslo, Norway
18. Regine Hock (regine.hock@geo.uu.se)
    Department of Earth Sciences, Uppsala University, Uppsala, Sweden
19. Per Holmlund (per.holmlund@natgeo.su.se)
    Department of Physical Geography and Quaternary Geology, Stockholm University, Sweden
20. Miriam Jackson (mja@nve.no)
    Norwegian Water Resources and Energy Directorate, Oslo, Norway
21. Jacek Jania (jjania@us.edu.pl)

University of Silesia, Sosnowiec, Poland
22. Tomas Johannesson (tj@vedur.is)
Icelandic Meteorological Office, Reykjavik, Iceland
23. Antoine Kies (antoine.kies@uni.lu)
Faculty of Science, Technology and Communication, University of Luxembourg, Luxembourg
24. Michael Kuhn (michael.kuhn@uibk.ac.at)
University of Innsbruck, Austria
25. Javier Lapazaran (jjli@mat.upm.es)
Department of applied mathematics, Madrid Polytechnical University, Spain
26. Ivan Lavrentiev (i_lavrentev@mail.ru)
Institute of Geography, Russian Academy of Sciences, Moscow, Russia
27. Martin Lüthi (luethi@vaw.baug.ethz.ch)
Laboratory of Hydraulics, Hydrology and Glaciology, Swiss Federal Institute of Technology (ETH), Zurich, Switzerland
28. Yuri Macheret (macheret@gol.ru)
Institute of Geography, Russian Academy of Sciences, Moscow, Russia
29. Horst Machguth (machguth@gmx.ch)
Department of Geography, University of Zurich, Zurich, Switzerland
30. Krzysztof Migala (migalak@meteo.uni.wroc.pl)
Wroclaw University, Wraclaw, Poland
31. Geir Moholdt (geir.moholdt@geo.uio.no)
Department of Geosciences, University of Oslo, Oslo, Norway
32. Matt Nolan (fnman@uaf.edu)
Insitute of Northern Engineering, University of Alaska, Fairbanks, Alaska
33. Hans Oerlemans (J.Oerlemans@phys.uu.nl)
Institute for Marine and Atmospheric Research, Utrecht University, Netherlands
34. Atsumo Ohmura (atsumu.ohmura@env.ethz.ch)
Institute for Atmospheric and Climate Science, Swiss Federal Institute of Technology (ETH), Zurich, Switzerland
35. Vicky Parry (v.l.parry@sms.ed.ac.uk)
Geography Department, University of Edinburgh, UK
36. Frank Paul (fpaul@geo.unizh.ch)
Department of Geography, University of Zurich, Zurich, Switzerland
37. Tad Pfeffer (pfeffer@tintin.colorado.edu)
University of Colorado, Boulder, USA
38. Veijo Pohjola (veijo.pohjola@geo.uu.se)
Department of Earth Sciences, Uppsala University, Uppsala, Sweden
39. Dariusz Puczko (dp@igf.edu.pl)
Institute of Geophysics, Polish Academy of Science, Warszawa, Poland
40. Valentina Radic (valentina.radic@natgeo.su.se)
Department of Physical Geography and Quaternary Geology, Stockholm University, Sweden
41. Cameron Rye (cr362@cam.ac.uk)
Scott Polar Research Institute, Cambridge, UK
42. Thomas Schuler (t.v.schuler@geo.uio.no)
Department of Geosciences, University of Oslo, Oslo, Norway
43. Aleksey Sharov (aleksey.sharov@joanneum.at)

Institute of Digital Image Processing, Joanneum Research, Graz, Austria

44. Ireneusz Sobota (irso@geo.uni.torun.pl)
    Dept. of Cryology and Polar Research, N.Copernicus University, Torun, Poland
45. Irina Solovjanova (solir22@mail.ru)
46. Manfred Stober (manfred.stober@hft-stuttgart.de)
    Department of Surveying and Geoinformatics, Stuttgart University of Applied Sciences, Stuttgard, Germany
47. Tazio Strozzi (strozzi@gamma-rs.ch)
    Gamma Remote Sensing, Gümligen, Switzerland
48. Felix Svoboda (fsvoboda@geo.unizh.ch)
    Institute of Geography, University of Zurich-Irchel, Zurich, Switzerland
49. Carleen Tijm-reijmer (c.h.tijm-reijmer@phys.uu.nl)
    Institute for Marine and Atmospheric Research, Utrecht University, Netherlands
50. Roderik van de Wal(r.s.w.vandewal@phys.uu.nl)
    Institute for Marine and Atmospheric Research, Utrecht University, Netherlands
51. Ian Willis (iw102@cam.ac.uk)
    Scott Polar Research Institute, Cambridge, UK
52. Michael Zemp (mzemp@geo.unizh.ch)
    Department of Geography, University of Zurich, Zurich, Switzerland
53. Jay Zwally (zwally@icesat2.gsfc.nasa.gov)
    NASA Goddard SFC, USA

ABSTRACTS

20TH CENTURY EVOLUTION AND MODELLING OF HOFFELLSJÖKULL, SOUTHEAST ICELAND

GUÐFINNA AÐALGEIRSDÓTTIR[1,2], HELGI BJÖRNSSON[1], FINNUR PÁLSSON[1] AND SVEN P. SIGURÐSSON[3]

[1] Institute for Earth Sciences, University of Iceland, Reykjavik, Iceland
[2] Danish Meteorological Institute, Kopenhagen, Denmark
[3] Faculty of Engineering, University of Iceland, Reykjavik, Iceland

The maximum extent of glaciers in Iceland was reached about 1890 AD and during the 20th century most of the glaciers have been retreating. Radio-echo sounding measurements from Hoffellsjökull, a south-eastern outlet glacier of Vatnajökull ice cap, were performed in 2001 and surface mass balance measurements were done. The measured bedrock topography reveals that during the Little Ice Age advance, from about 1600-1900 AD, the glacier excavated about 1.6 km^3 deep trench over an area of 11 km^2. This trench is 300 m below sea level where it is the deepest and is now emerging as a lake in front of the glacier as it retreats. Maximum thickness of the glacier is measured 560 m. The area of the glacier at maximum extent was 234 km^2 it retreated to 227 km^2 by 1936, and to 212 km^2 in 2001, or 10% during the 20th century. The volume reduction during the same period is about 20%. The present mass balance and climate conditions are similar to observed during a Swedish-Icelandic expedition 1936-1938, about -0.5 m^{-1}.

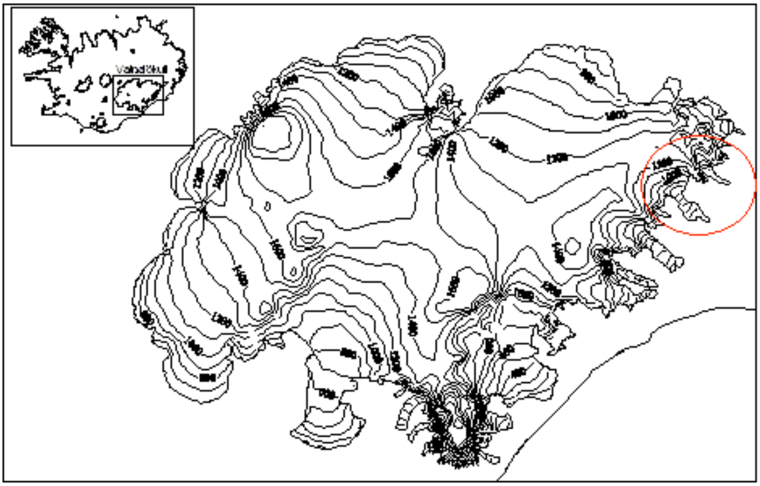

Figure 1. Surface topography of Vatnajökull ice cap on the south-east coast of Iceland. The read circle indicates the modelled area, including Hoffellsjökull and neighbouring outlet glacier.

In this study we use the measured bedrock and surface topography of Hoffellsjökull as boundary condition for a numerical ice flow model to assess the ability of coupled ice flow and mass balance model to simulate the observed changes. A degree day mass balance model developed for glaciers in Iceland (Jóhannesson, 1997), which has been calibrated and used for climate response assessment on southern Vatnajökull (Aðalgeirsdóttir et al., 2006), is coupled with a new finite element SIA dynamic flow model, which is adopted from a code that was developed for fish migration in the Atlantic ocean. In the model computations the ice divide is kept at a fixed location and no flow allowed across the boundary. A reference climate constructed from the average measurements during the period 1980-2000 is applied as the present climate condition (Aðalgeirsdóttir et al., 2004).

The present size of Hoffellsjökull and mass balance can be simulated with the coupled model. By lowering the reference temperature in the degree-day model by 0.3°C, the maximum extent at the end of the Little Ice Age can be reconstructed. This temperature decrease lowers the ELA from 1050 m a.s. to 950 m a.s. Sensitivity study shows that a moderate change in temperature (< 1°C) can cause considerable volume changes and corresponding changes in ELA.

Temperature and precipitation records from a number of locations around Iceland are available and the longest records go back to late 19th century. We plan to use these records as well as measured glacier extent and corresponding glacier surface maps of Hoffellsjökull from 1904, 1936, 1945, 1988 and 2001 to assess the ability of the coupled model to simulate the 20th century evolution. The model can then be used to make projections into the near future, given a climate change scenario for this area.

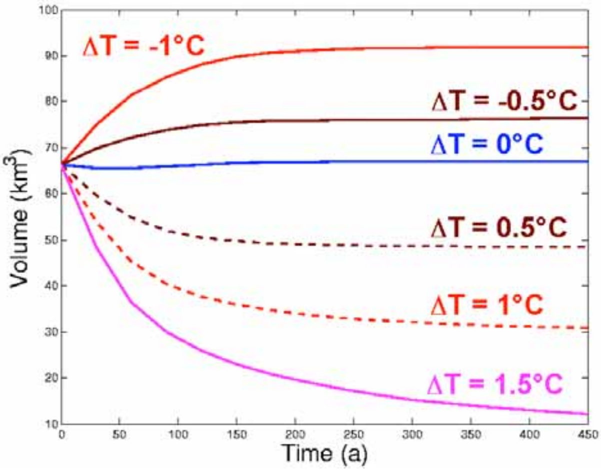

Figure 2. Sensitivity of the volume of Hoffellsjökull to changes in temperature. Step changes in temperature are applied to the mass balance model, the precipitation kept constant, and the resulting change in volume computed with the coupled mass balance-ice flow model.

References

Aðalgeirsdóttir, G., T. Jóhannesson, H. Björnsson, F. Pálsson, O. Sigurðsson. 2006. Response of Hofsjökull and southern Vatnajökull, Iceland, to climate change. J. Geophys. Res., 111, F03001, doi:10.1029/2005JF000388.

Aðalgeirsdóttir, G., Helgi Björnsson, Tómas Jóhannesson. 2004. Vatnajökull ice cap, results of computations with a dynamical model coupled with a degree-day mass-balance model. RH-11-2004, Science Institute, University of Iceland, Reykjavík.

Jóhannesson, T. 1997. The response of two Icelandic glaciers to climatic warming computed with a degree-day glacier mass balance model coupled to a dynamic glacier model. Journal of Glaciology, 43, 143, 321-327.

The surface energy balance of Storbreen

Liss M. Andreassen[1,2], Michiel van den Broeke[3], Johannes Oerlemans[3]

[1] Norwegian Water Resources and Energy Directorate, Oslo, Norway
[2] Department of Geosciences, University of Oslo, Norway
[3] *Institute of Marine and Atmospheric Research (IMAU), University of Utrecht*, the Netherlands.

The relation between meteorological quantities and the mass balance of a glacier surface is important for process understanding and for modelling the reaction of different glaciers to climate change. At Storbreen (61°36'N, 8°8'E), a small continental glacier in southern Norway, mass balance investigations began already in 1949. Since September 2001 an automatic weather station has been running in the ablation zone of Storbreen at about 1570 m a.s.l. (Figure 1). The station is part of the Institute of Marine and Atmospheric Research (IMAU) network of AWS on glaciers (http://www.phys.uu.nl/~wwwimau/research/ice_climate/aws/). The station measures all quantities needed for calculating the surface energy balance (SEB) of Storbreen, and has provided a near continuous 5-year record of micro-meteorology from September 2001 to September 2006. In this period Storbreen had a specific net balance of -1.2 m w.e per year, far more negative than the mean for the whole period, which is -0.26 m w.e. per year. The large deficit was mainly due to a combination of less snow than normal (winter balance well below the mean for four of the five years) and three years with extraordinary high summer balance (2002, 2003 and 2006).

Figure 1. The automatic weather station at Storbreen, Norway. Measurements of humidity, temperature and wind are done at two levels,about 2 m and 6 m above the ice surface.The free standing sonic ranger (to the left) measures ice melt and snow accumulation. Photo: Liss M. Andreassen.

The AWS-data were used to calculated the surface energy budget of Storbreen. The surface energy balance can be expressed as:

$Q = S{\downarrow}(1-\alpha) + L{\downarrow} - L{\uparrow} + Q_H + Q_L$

$S{\downarrow}$- short-wave incoming radiative flux, α - surface albedo, $L{\downarrow}$- long-wave incoming radiative flux, $L{\uparrow}$ - long-wave outgoing radiative flux, Q_H - sensible heat flux, Q_L- latent heat flux

The radiative fluxes were measured at the AWS. The turbulent fluxes were calculated by applying the bulk method using surface roughness values calculated from the wind measurements at the 2 and 6 m level. A subsurface model calculating refreezing was included. Comparison of the melt calculated by the model using two different methods to calculate the surface temperature and by comparison with stake readings showed good agreement.

The calculations show that the surface is at melt about 33 % of the time. The dominant melt season is from June to September, but melt episodes are not unusual in April, May and October and melt episodes have occurred in all months except January. The mean values during melt for the 5-year period (Fig. 2) reveal that the shortwave net radiation is the most important contributor to the melt, while the sensible heat flux is second most important followed by the latent heat flux. The longwave net radiative flux is negative.

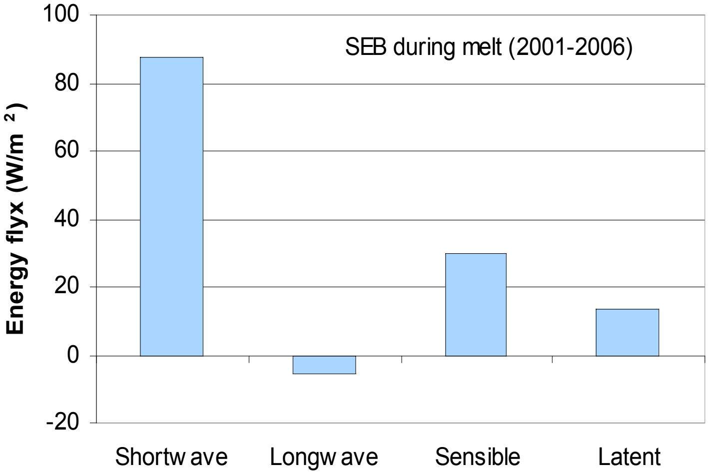

Figure 2. The mean surface energy balance budget during melt for the whole observation period September 2001-September 2006.

The importance of shortwave net radiation for the total melt implies that the albedo of the surface as well as the depth of the snow pack are very important for the SEB at Storbreen. Figure 3 illustrates the albedo development for two years, 2003 and 2005. In 2003 the winter accumulation was about 20 % below normal and in 2005 the winter accumulation was 20 % above normal (of the reference period 1971-2000). In 2003 the thin snowpack resulted in a snow free surface already in early July, while in 2005 the surface was not snow free until a month later. The Figure also shows the occurrence of several melt episodes in March 2003 lowering the albedo of the surface temporarily.

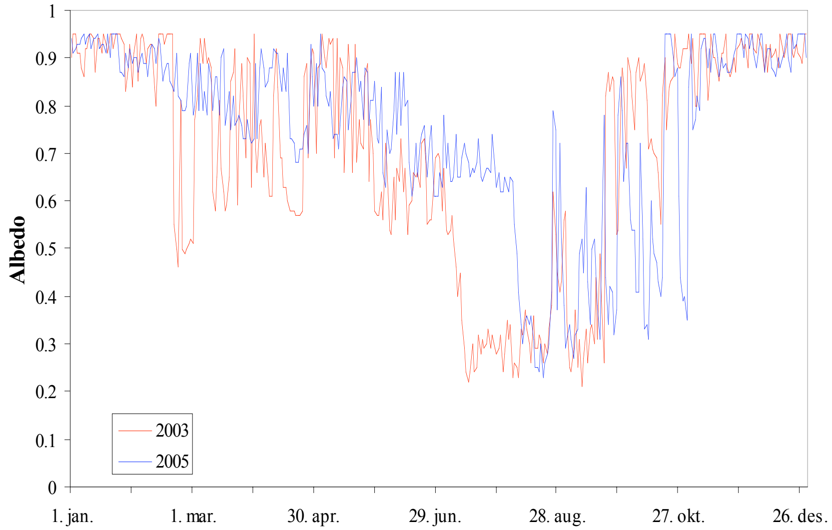

Figure 3. Development of daily albedo for 2003 and 2005.. The albedo is calculated as the ratio between outgoing and incoming shortwave radiation. The radiation data was corrected using an accumulated albedo method by Van den Broeke and others (2004).

Reference

Van den Broeke, M. R., D. van As, C. H. Reijmer and R. S. W. van de Wal, 2004: Assessing and improving the quality of unattended radiation observations in Antarctica. *Journal of Atmospheric and Oceanic Technology* **21(9)**, 1417-1431.

TOPOGRAPHIC CONTROLS ON THE SPATIAL VARIABILITY OF GLACIER SURFACE ENERGY BALANCE

NEIL ARNOLD[1], GARETH REES[1], ANDREW HODSON[2] AND JACK KOHLER[3]

[1] Scott Polar Research Institute, University of Cambridge, Cambridge, U.K.
[2] Department of Geography, University of Sheffield, Sheffield, U.K.
[3] Norwegian Polar Institute, Polar Environmental Centre, Tromsø, Norway.

Introduction

This paper presents the results of a distributed, 2-dimensional surface energy balance model used to investigate the spatial and temporal variations in the surface energy balance of Midre Lovénbreen, a small valley glacier in north-west Spitsbergen, Svalbard (Figure 1) over the summer of 2000. Small valley glaciers only contain a small fraction of the world's snow and ice, but are the most responsive to climate change. Many Svalbard glaciers in rapid retreat; for instance, Midre Lovénbreen itself has retreated by over 1km, and lost 10,000,000m^3 of ice, in the 20th century.

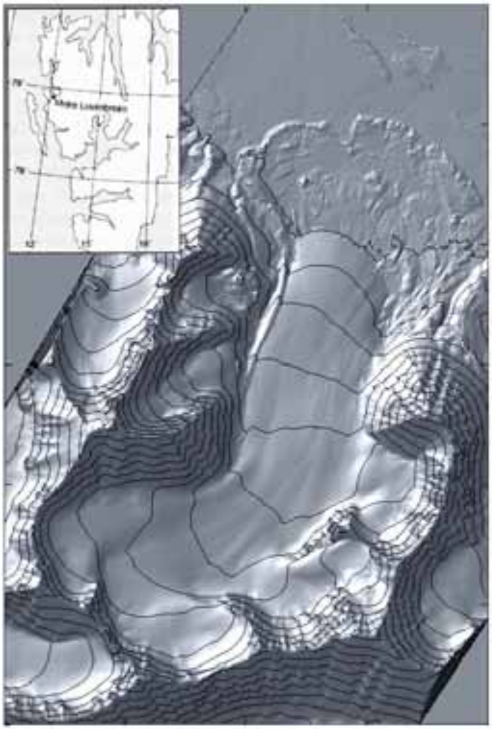

Figure 1. Location map for Midre Lovénbreen. Slope-shaded DEM from high resolution airborne LiDAR data. Contour interval is 50 m; the lowest contour is at an elevation of 50 m.

The surface energy balance of glaciers is a key control on surface melt, but the spatial resolution of energy balance models is generally constrained by the resolution (and accuracy) of the Digital Elevation Models of topography available from glaciated areas. In this paper, we utilize high resolution airborne LiDAR

(Arnold et al. 2006b) data to derive a Digital Elevation Model of the glacier and surrounding topography, which forms one input to a distributed surface energy balance model. Unlike the DEMs used in most other energy balance studies, the DEM used here is not interpolated from map or terrestrial survey data; instead it is derived from over 12 million individual height measurements. This DEM preserves small scale topographic (<100m) features which are typically lost in interpolated DEMs, and can therefore allow such local variations in slope and aspect and their impact on the surface energy balance, to be calculated.

Methods

The model is based on that used by Arnold et al. (2006a). The model assumes that there are four main components of the total surface energy balance (G); net short-wave (solar) radiation (Q*); net long-wave (terrestrial) radiation (L*); sensible turbulent heat (S); and latent turbulent heat (T). In addition to these, the model also calculates the conductive flux from the surface into the body of the glacier. These five components are calculated for each grid cell of the DEM every hour of the melt-season using the measured meteorological data and calculated solar altitude and azimuth.

As well as the DEM of the glacier surface, the model also needs hourly meteorological data, which were obtained from an automatic weather station located on the glacier surface, supplemented by data from a synoptic weather station at the nearby Ny-Ålesund research base. Start-of-season snow depths over the glacier were interpolated from 145 snow depth measurements made on 14 April 2000; an empirical relationship derived from 104 snow depth/albedo measurements was used to calculate the surface albedo within the model.

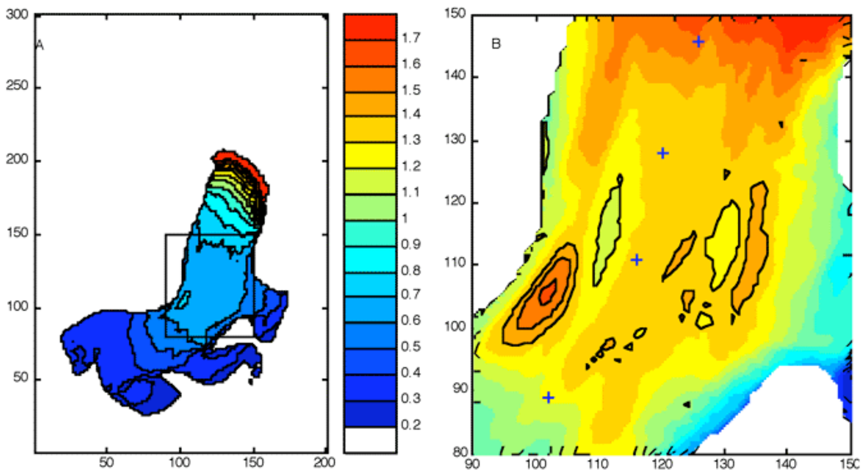

Figure 2. Modelled summer mass balance in m w.e. A. For the whole glacier; B. For the inset area shown in A. The inset shows the high spatial variability due largely to small-scale topographic variations and their impact on solar radiation receipts.

Results

The model is validated using a combination of mass balance data from the glacier, measured surface lowering at the glacier meteorological station, and by comparing the derived net all-wave radiative flux calculated by the model with the net-all wave radiative flux measured at the AWS on the glacier surface, which is not used as a driving variable. Overall, the model performance is very good. Correlation coefficients between the model output and observed values are 0.982 for the season-long stake mass balance; 0.690 for the hourly melt rate; and 0.872 for the hourly net-all wave radiation.

Glacier topography is found to play a fundamental role in determining the surface energy balance. The general summer mass balance gradient with elevation is well reproduced (Figure 2a), but this conceals a wealth of small-scale spatial variability over 10s of metres (Figure 2b), driven largely by small-scale topographic variability, and its effect on solar radiation receipts, amplified by feedbacks within the model. When averaged by elevation band across the glacier, the modelled mass balances (Figure 3) show that areally-extrapolated centre-line mass balance measurements may over-estimate the mass balance where the glacier surface is surrounded by high topography (such as the central areas of Midre Lovénbreen) due to increased shading (and consequent lower melt towards the lateral margins), but may underestimate melt in areas where the glacier is very exposed (such as the snout of Midre Lovénbreen, which protrudes onto the coastal plain).

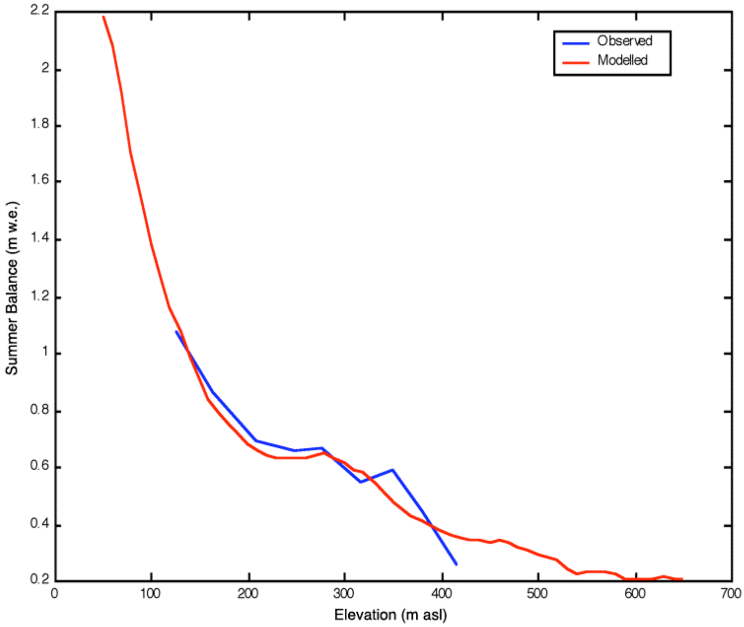

Figure 3. Areally-averaged modelled mass balance by 10m elevation band, and observed mass balance at the centre-line stake network. Between ~150 and ~300m, the centre-line measured values are larger than the areally-averaged model results due to shading of the valley sides; below ~150m, the areally-averaged model values are larger than the stake data due to the high exposure of the glacier snout to solar radiation. Above 300 m, the values measured at two of the centre-line stakes deviate from model predictions.

Discussion and Conclusions

The results of this model have shown that small-scale topographic features can have a large impact on the spatial variability of glacier surface energy balance. This has implications for the placement of mass-balance monitoring stakes; changes in stake position of only 50 to 100m can lead to differences of up to 10% in the calculated summer balance. The model results also highlight the cross-glacier variability in summer balance at any given elevation caused by, for instance, shading of the glacier margins by surrounding high topography. This has implications for the extrapolation of at-a-point stake measurements of mass balance to area-wide estimates of mass balance; it also implies that energy balance models, together with high-resolution topographic data, could be used in future to guide the placement of mass-balance stakes on monitored glaciers to ensure adequate spatial representation of mass balance variability.

We are also currently using the model and LiDAR data to investigate how topography can control the sensitivity of mass-balance elevation profiles to possible climatic change, and to evaluate methods to reduce the impact of coarse resolution DEM data on distributed mass balance calculations.

References

Arnold, N.S., Rees, W.G., Hodson, A.J. and Kohler, J. 2006a. Topographic controls on the energy balance of a high Arctic glacier. *Journal of Geophysical Research (Earth Surface)*. **111(F2),** F02011, doi:10.1029/2005JF000426.

Arnold, N.S., Rees, W.G., Devereaux, B.J. and Amable, G. 2006b Evaluating the potential of high-resolution airborne LiDAR in glaciology. *International Journal of Remote Sensing*. **27 (5-6),** 1233-1251.

PREDICTING THE SURFACE MASS BALANCE OF THE GREENLAND ICE SHEET: IMPORTANCE OF REFREEZING

JONATHAN BAMBER[1], MARION BOUGAMONT[1], RUPERT GLADSTONE[1], JENNY GRIGGS[1], TONY PAYNE[1], IAN RUTT[1], EDWARD HANNA[2], JEFF RIDLEY[3] AND WOUTER GREUELL[4]

[1] Bristol Glaciology Centre, School of Geographical Sciences, University of Bristol, UK
[2] Department of Geography, University Sheffield, UK
[3] Hadley Centre, UK Met Office, UK
[4] Institute for Marine and Atmospheric Research, Utrecht University, The Netherlands

The surface mass balance of the Greenland ice sheet has, in the past, been determined most commonly with the aid of a positive degree day model (PDDM) to estimate ablation. This is a reduced form of an energy balance model (EBM) where temperature is the sole variable that determines melt. More sophisticated EBMs exist that, for example, take account of radiative, turbulent and sensible heat fluxes explicitly but the data needed to drive them, until now, has been inadequate. Consistent global climate re-analysis data have recently been generated that show considerable skill in reproducing the observed temporal and spatial trends in key variables such as radiative fluxes and precipitation, and which are starting to be used to force EBMs of the ice sheet. We are using re-analysis data to drive a high resolution regional area atmospheric model covering Greenland to determine its surface mass balance for the last 50 years.

EBMs and PDDMs have different sensitivities to climate forcings. For example, an EBM is sensitive to changes in cloud cover as this affects both long and shortwave radiative fluxes, while a PDDM is only indirectly affected through any changes in surface temperature that may result from the different cloud cover. To investigate these differences quantitatively for a future climate warming scenario we forced an EBM and PDDM for the Greenland ice sheet with the output of a coupled atmosphere-ocean GCM, HadCM3, which was run from the present-day forward in time for 140 years assuming a 4 x $C0_2$ forcing trend. The EBM comprises two components: one that determines the energy balance and a second sub-surface snow diagenesis part that models the evolution of the snowpack and its thermal energy. The PDDM, by contrast, uses a very simple scheme for determining the proportion of melt that refreezes within the snowpack based on a fraction (Pmax) of the total snow deposited. The HadCM3 data were used to force the two models forward in time for 300 years with constant climate from year 110. Surprisingly, the amount of melt generated by the two models is remarkably similar up to year 110, despite major differences in model physics and the area over which melt was predicted. However, the two refreezing schemes showed differences of around a factor 3, accounting for almost all the difference in runoff produced by the two models.

It is the case that there are tuneable parameters in both models and that some of the difference could be reduced by changing these values. However, here we used relatively “standard” values for the PDDM and the EBM was tuned to provide agreement with *in-situ* observations of mass balance along the K-transect in southwest Greenland. There is, therefore, limited scope for tuning without moving one or other model away from observations. Increasing the value of Pmax to 0.8 gives slightly but not significantly better agreement between the two model output. The large difference in net mass balance predicted by the two models highlights the importance of refreezing rather than the method for estimating the amount of melt. To date, however, greater emphasis has perhaps been placed on the latter compared with the former possibly because of the difficulty in acquiring direct measurements of refreezing.

GEODETIC OBSERVATIONS OF SVALBARD LAND ICE MASS BALANCE: RESUTLS AND PLANS FOR IPY

JONATHAN BAMBER[1], TAVI MURRAY[2], TIM JAMES[2], JONATHAN ROUGIER[3], BILL KRABILL[4], JACK KOHLER[5], JON OVE HAGEN[6] AND PRASAD GOGINENI[7]

[1] School of Geographical Sciences, University of Bristol, UK
[2] School of the Environment and Society, University of Wales, Swansea, UK
[3] Department of Maths, University of Bristol, UK
[4] Wallops Flight Facility, NASA/GSFC, USA
[5] Norwegian Polar Institute, Tromsø, Norway
[6] Dept of Geosciences, University Oslo, Norway
[7] CReSIS, University Kansas, USA

In 1996 and 2002 NASA flew a series of flightlines over Svalbard producing estimates of elevation change during this time interval for some 17 ice masses including Austfonna (Bamber et al., 2004) and a number of glaciers on Spitsbergen (Bamber et al., 2005). Recently results of volume change from repeated stereo-photogrammetric elevation data have also been produced (James et al., 2006). We summarise this work here in the context of plans to extend the analysis to cover some 50 glaciers and ice caps across the archipelago as part of the UK contribution to the GLACIODYN IPY program. The aim of the project is to derive a time-evolving mass balance for the archipelago that is regionally differentiated, providing the most comprehensive and extensive estimate of the contribution of the ice masses in Svalbard to sea level rise between ~1950s and 2008.

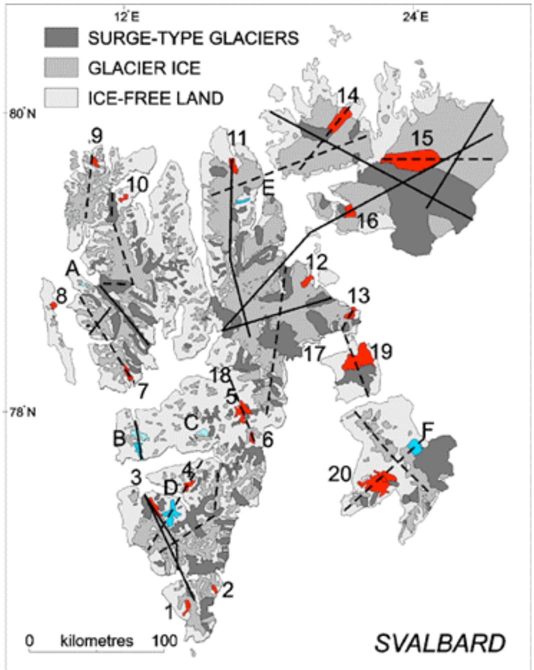

Figure 1. Map of sampling strategy. Blue areas (A-F) = dv/dt already acquired by SLICES project. Red areas (1-20) = new sites for dv/dt by stereo-photogrammetry. Solid lines = original 1996/2002 ATM lines to be repeated in 2008. Dashed lines = new ATM lines to be differenced from the NPI 1990 DEM and the photogrammetric DEMs produced in this project (not all tracks shown for clarity).

The project (Svalbard Land Ice Mass Balance From Lidar And Photogrammetry: acronym Slim) will achieve its aims by flying a comprehensive suite of flight lines across Svalbard covering a carefully selected sample of ice masses that covers the full range of glaciological, climatological and altitudinal conditions. We will combine repeat-survey airborne lidar data with stereo-photogrammetrically-derived digital elevation models for multiple epochs. The results will be upscaled using a Bayesian statistical modelling approach that accounts for the underlying physical processes in a probabilistic manner, resulting in rigorous uncertainty estimates. Here we summarise the proof-of-concept studies and our proposed fieldwork plans for spring 2008. The target ice masses are shown in Figure 1. As well as a lidar, the aircraft will also be carrying a Kansas ice penetrating radar.

References:

Bamber, J. L., Krabill, W., et al., 2004. Anomalous recent growth of part of a large Arctic ice cap: Austfonna, Svalbard. *Geophysical Research Letters,* **31,** (12), doi:10.1029/2004GL019667.

Bamber, J. L., Krabill, W., et al., 2005. Elevation changes measured on Svalbard glaciers and ice maps from airborne laser data. *Annals of Glaciology,* **42,** 202-208.

James, T. D., Murray, T., et al., 2006. Extracting photogrammetric ground control from lidar DEMs for change detection. *Photogrammetric Record,* **21,** (116), 310-326.

IMPACT OF SURFACE MELTWATER PRODUCTION ON GREENLAND ICE SHEET OUTLET GLACIER FLOW

JASON E. BOX[1,2], LEI YANG[1,2] AND ADAM HERRINGTON[1]

[1] Department of Geography, The Ohio State University, Columbus, Ohio, USA
[2] Byrd Polar Research Center, The Ohio State University, Columbus, Ohio, USA

Summary

This study evaluates links between Greenland ice sheet outlet glacier flow velocity and surface climate on seasonal to inter-annual time scales. We evaluate the statistically correlation of annual and seasonal temperature anomalies and annual positive degree days with published outlet glacier velocity values. We desired temperature time-series at the location of various Greenland outlet glaciers. To facilitate this, we use monthly surface air temperatures from the Polar MM5 regional climate model.

We find that a positive correlation exists between 1960-1991 base-period temperature anomalies at annual and seasonal timescales. The summer (June-August) correlation exceeds that for annual anomalies. A yet higher correlation is evident for annual positive degree day anomalies for the same base period. The patterns of scatter suggest a non-linear correlation.

Meltwater Input, Flow Velocities and Calving of Arctic Glaciers: Nordenskiöldbreen, Svalbard

Marianne A.G. den Ouden[1], J. Oerlemans[1], C.H. Tijm-Reijmer[1] and V. Pohjola[2]

[1] Institute for Marine and Atmospheric Research, Utrecht University, the Netherlands
[2] Department of Earth Sciences, Uppsala University, Uppsala, Sweden.

Introduction

The IPY project GLACIODYN has been initiated to assess the dynamical response of Arctic glaciers to climate change. The Dutch contribution to this large international effort focuses on the relation between meltwater input, ice-flow velocities and calving of Arctic glaciers. Current evidence suggests that increased meltwater production results in higher flow velocities, subsequently thinning glaciers and accordingly increasing melt. This positive-feedback mechanism enables glaciers to react faster than expected to rising temperatures. During the first phase of the project the focus will be on Nordenskiöldbreen, Svalbard.

Objective

To study the relation between (melt)water input and ice dynamics on several of the GLACIODYN target glaciers, focussing on seasonal and inter-annual variability in ice velocity, and including the process of calving when appropriate (Figure 1).

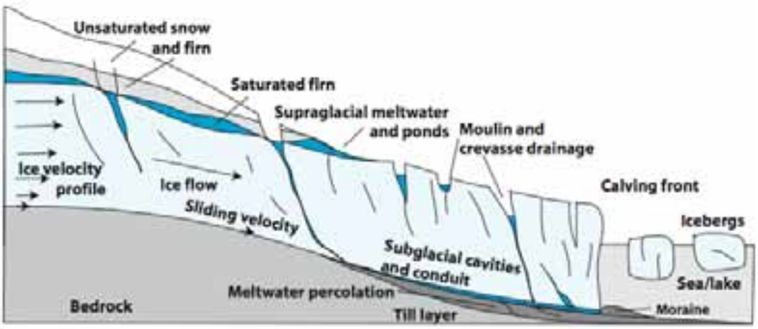

Figure 1. Illustration of the drainage pathways in a tidewater glacier. Meltwater is drained through moulins and crevasses towards the bottom of the glacier where it can enhance flow (sliding).

Target Glaciers

- Nordenskiöldbreen, Svalbard
- Kangerlussuaq basin, West Greenland
- 2-3 glaciers to be chosen

Methods

- Measure ice velocities of the target glaciers continuously by means of a low-cost GPS technique.

- Estimate meltwater input to these glaciers from meteorological data and mass-balance observations.
- Use the observational data as input and validation of mass-balance models.
- Make a theoretical interpretation of observed seasonal and inter-annual velocity fluctuations.
- Use the dataset for comparison with velocities obtained by remote-sensing techniques.

Nordenskiöldbreen, Svalbard

The glacier is situated on central Spitsbergen. It has an area of 242 km^2, and the length of its main streamline is 26 km (Figure 2). Currently, Nordenskiöldbreen is changing from a tidewater glacier into a glacier ending on land.

The approach will be two-fold:

1. GPS measurements are used to determine the flow velocity of the ice mass. In March 2006 seven GPS units have been placed on the glacier (Figure 2). The first data will be available in March 2007.
2. The meltwater production is determined from a newly developed energy/mass-balance model; mass- balance data from stakes will be used for verification/tuning of the model.

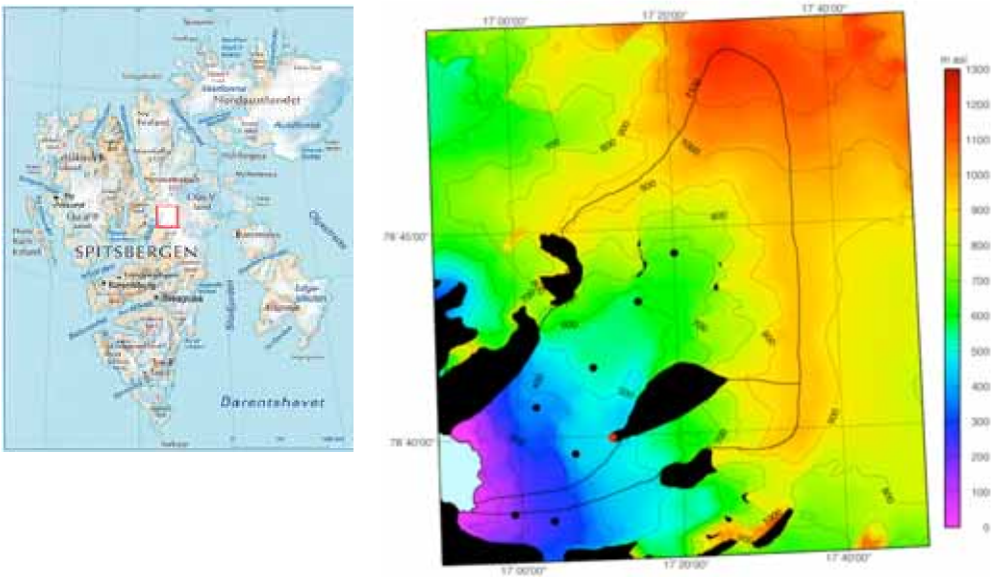

Figure 2. Left: Location of Noordenskiöldbreen on central Spitsbergen. Right: Digital Elevation Model (DEM) of Nordenskiöldbreen. A black dots represents the GPS locations, the red dot indicates the reference station.

Acknowledgements

We thank the NPI for kindly providing the Digital Elevation Model.

Snow accumulation on Austfonna, northeastern Svalbard, derived by ground-penetrating radar

Thorben Dunse[1], Thomas V. Schuler[1], Andrea Taurisano[2], Jon Ove Hagen[1], Kjetil Melvold[3], Trond Eiken[1] and Geir Moholdt[1]

[1] Department of Geosciences, University of Oslo, Norway
[2] Previously at Norwegian Polar Institute, Tromsø, Norway; now at Multiconsult AS, Tromsø, Norway
[3] Norwegian Water Recourses and Energy Directorate, Oslo, Norway

Covering an area of 8120 km², Austfonna is among the largest arctic ice caps outside Greenland. Despite the strong glaciological engagement on Svalbard during the last decades (e.g. Hagen et al., 1993, 2003) the mass balance of Austfonna and its dynamic behaviour is not yet well understood. Results from airborne laser altimetry surveys in 1996 and 2002 suggest that the ice cap is thickening in the interior, while thinning at the margins (e.g. Bamber et al., 2004). This observation is supported by a comparison of measured equilibrium line fluxes derived from satellite radar interferometry and airborne radio-echo sounding and theoretical balance fluxes, indicating that the actual mean flux across the equilibrium line is only half of the calculated balance flux (Bevan et al., 2006). Several drainage basins of Austfonna are known to have surged in the past. To what degree recent elevation changes represent a built-up towards new surge activity, and hence a change in the dynamics of the ice cap, or a climatically induced change in the accumulation and ablation pattern remains poorly constrained.

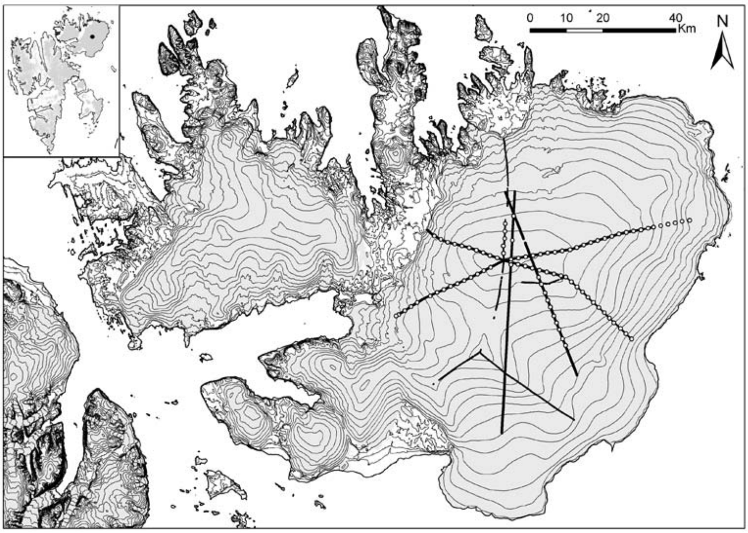

Figure 1. Location map showing the tracks of the profiles repeated in 1999, 2004, 2005 and 2006 (thick lines). The thin lines indicate profiles measured in 1999 only, while the white dots mark manual soundings of the snow thickness.

Austfonna is chosen as target glacier of both the IPY-project GLACIODYN (dynamic response of arctic glaciers to global warming) and ESA's (European Space Agency) CryoSat calibration and validation campaign. The University of Oslo and the Norwegian Polar Institute contribute to both projects with data sets collected during extensive field campaigns in spring 1998 and 99, and on an annual basis since April 2004. Activities include collection of kinematic GPS and ground-penetrating radar (GPR) data along fixed star-like transects across the ice cap (Figure 1). These data sets are supplemented by physical snow properties measurements from snow pits and shallow firn cores, a network of ablation stakes and meteorological data from two automatic weather stations.

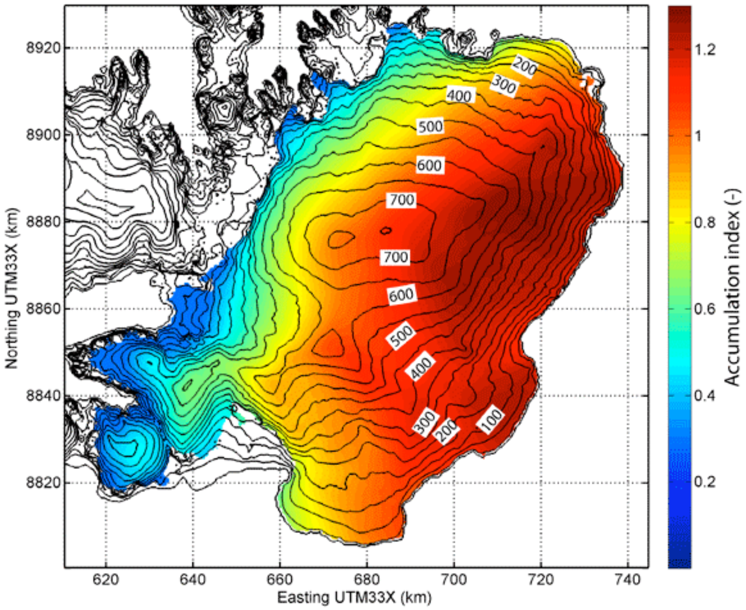

Figure 2: Accumulation index map derived from multi-regression analyses of observed snow depth (Taurisano et al., 2006). Values are dimensionless and normalized by the mean snow accumulation across the ice cap. Contour line interval of surface elevation (m a.s.l.) is 50 m.

The snow-ice transition in the ablation area produces a very distinctive GPR reflection, whereas detection of the snow-firn transition in the accumulation area can be a problematic task. Here, it is beneficial to correlate the GPR record with the manual snow depth soundings, collected at 2 km intervals along the profiles, and snow pit analyses. The simultaneous GPS measurements allow geo-coding of both manual soundings and GPR profiles and provide a record of surface elevation changes for the time span between the various surveys. Precipitation over Austfonna originates predominately from the east, off the Barents Sea. Measurements of all years show a consistent pattern in the spatial distribution of snow accumulation from highest values in the southeast of the ice cap, to lower ones in the northwest (Pinglot, 2001; Taurisano, 2006), but indicate a large interannual variability in the total amount of snow. The latter is also reflected in the kinematic GPS record, suggesting a variability of surface elevation at short time scales. GPR- and snow pit-derived accumulation rates serve as input parameters for an accumulation index map (Figure 2) and a mass balance model of Austfonna, developed at the University of Oslo by Schuler et al. (in press). A temperature-index approach is used to implement ablation. Model results indicate that the formation of superimposed ice plays an important role in the net mass balance of Austfonna.

The field work is to be continued in spring 2007 and throughout the IPY-period. Future assessments of the complete mass balance of Austfonna will encompass more thoroughly the formation of superimposed ice, as well as ablation rates and ice mass loss through calving along the east, south-easterly margin.

References

Bamber, J., W. Krabill, V. Raper, and J. Dowdeswell. 2004. Anomalous recent growth of a part of a large Arctic ice cap: Austfonna, Svalbard. Geophysical Research Letters, 31.

Hagen, J.O., O. Liestøl, E. Roland, T. Jørgensen, 1993. Glacier Atlas of Svalbard and Jan Mayen. Norsk Polarinstitutt. Meddelelser 129

Hagen, J. O., K. Melvold, J. F. Pinglot, and J.A. Dowdeswell. 2003. On the net mass balance of the glaciers and ice caps in Svalbard, Norwegian Arctic. Arctic, Antarctic, and Alpine Research, 25(2), 264-270.

Pinglot, J. F., J.O. Hagen, K. Melvold, T. Eiken and C. Vincent. 2001. A mean net accumulation pattern derived from radioactive layers and radar soundings on Austfonna, Nordaustlandet, Svalbard. Journal of Glaciology, 47, 555-566.

Schuler, T.V., E. Loe, A. Taurisano, T. Eiken T., J.O. Hagen and J. Kohler, in press. A calibrated surface mass balance model for the Austfonna ice cap, Svalbard. Annals of Glaciology, 46.

Taurisano, A., T.V. Schuler, J.O. Hagen, T. Eiken T., E. Loe, K. Melvold and J. Kohler, in press. The distribution of snow accumulation across Austfonna (Svalbard): direct measurements and modelling. Polar Research.

GLACIER MONITORING APPROACH SUGGESTED FROM ANALYSIS MASS BALANCE OBSERVATIONS

MARK DYURGEROV

INSTAAR, University of Colorado, Boulder, USA
Department of Physical Geography and Quaternary Geology, Stockholm University, Sweden

Glaciers and ice caps have experienced large decrease in surface area (*S*), acceleration in mass-balance annual rate (*b*), thus increase contribution to sea level rise (Kaser et al, 2006). Analyses of available observational results have also shown an alarming process of fast decrease in accumulation area (*Sc*). The decrease in *Sc* was found 6-10 folds as much as shrinkage of the entire glacier area (Figure 1). Climate warming has caused these changes, but faster decreases in *Sc* compare to *S* has related to glacier area distribution vs. elevation. Glacier surface area per unit elevation is much smaller in the lower parts, where glacier shows the largest shrinkage, compare to the elevation in the vicinity of the equilibrium line (*ELA*). The ratio of *Sc* to *S* (*AAR*, accumulation area ratio) tells whether change in *S*, due to dynamic response, compensate the climatically driven change of *Sc*. Results on Figure 1 show that no such compensation has observed.

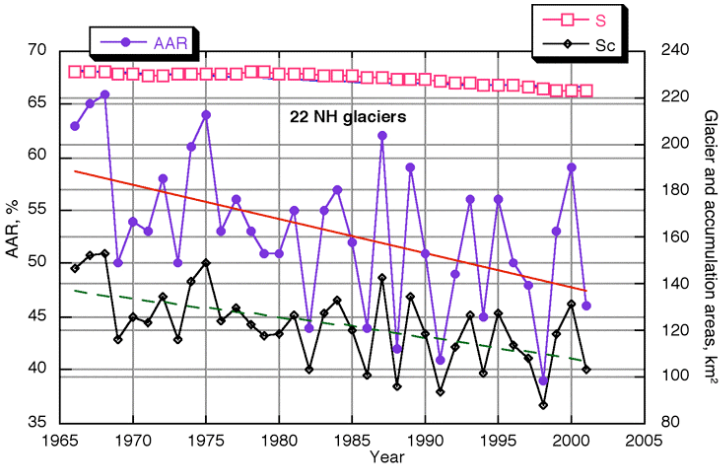

Figure 1. Change in time of glacier area (*S*), accumulation area (*Sc*) and the ratio between them for the sample of long-term continues observations on 22 glaciers. The slopes in linear regressions are: *AAR* = -0.31, *S* = -0.21, *Sc* = -0.87.

Strong empirical relationship between *AARi* and *bi* (*i* is the glacier) has always been suggested and proposed to be linear (e.g., IAHS (ICSI)-UNEP-UNESCO, 2003). The study of *AARi=f(bi)* relationships of all available observations from the dataset of 100 time series (all available from observations, see http://instaar.colorado.edu/other/occ_papers.html, and Greenland ice sheet (Box et al., 2006), have shown that the relationship may have been linear (85% in all time series), concave, convex, or not exist in few cases. *AARo* (*b*=0) were derived from these relationships of individual *AARij* and *bij* (*j* are hydrological years). These *AARo* (*b*=0) are the reference state of glaciers, or may also be called the "inventoried state" which suggests that areas of *Sc* and *S* are fixed (as these are the way these presented in any Glacier Inventories). The recent state of glaciers, compare to inventoried state is the <*AAR*>-*AARo*, where <*AAR*> averaged for the same period of time the *AARo* determined (Figure 2).

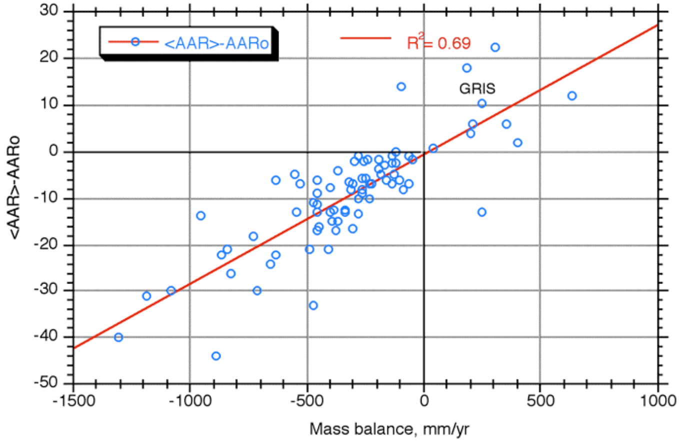

Figure 2. The difference between <*AAR*>-*AARo* in relation to averaged mass balance of bench mark glaciers (open circles) world wide, all available observational data were used and Greenland ice sheet surface mass balance and *AAR* for 1988-2004 (Box et al., 2006).

Negative deviation of <*AAR*>-*AARo* means that *Sc* is in deficit and glacier need to increase *Sc*. The largest negative values have been found for glaciers in the tropics of E.Africa and in Cordilleras of S. and N. Americas. The positive deviation mode means that *Sc* exceeds the reference state and *Sc* need to decrease. Only few glaciers have shown the positive deviation, particularly in NW Scandinavia (Figure 2). The range of deviation is between +23 and – 44%, with the average value close to -8%. This suggests that the accumulation area of glaciers (this sample, after elimination of errors, was 89 glaciers) have been in the deficit over 1961-2004. To reach the reference state glaciers need to reduce their area *S* for 8%. With existing glacier area (about 540*103 km^2, individual glaciers around Greenland and Antarctic ice sheets are not included (Kaser et al, 2006) glaciers need to decrease area for about 40*103 km^2 to restore their reference state.

Greenland Ice Sheet (GRIS) surface mass balance for the 1988-2005 period (Box et al., 2006) shows the surplus in <*AAR*>-*AARo* for about 10% (Figure 2). $<AAR_{GRIS}>-AARo_{GRIS}=f(b_{GRIS})$ belongs to the same sample as other glaciers and ice caps. This suggests the similarity in climate conditions and surface mass balance of glaciers and GRIS.

The positive mode for GRIS means that the *Sc* is in surplus, compare to the reference state. GRIS "needs" to reduce accumulation area to reach the state corresponding to the recent climate. Such statement is obvious simplification of very complex processes observed on the surface, such as increases in snow accumulation (Johannessen, et al, 2005), simultaneously increases in melt area

(Steffen et al, 2007), and the role of dynamic mass balance component (Rignot and Kanagaratnam, 2006).

Derived from observations the *<AAR>-AARo* concept can be applied to glaciers and small ice caps, as well as to GRIS surface balance estimation, everywhere the empirical relationship between change in accumulation area and surface mass balance has established.

Acknowledgements

This work was supported by NSF grant OPP-0425488, NASA NAG5-13691, and a Marie Curie International Fellowship within the 6th European Community Framework Program.

References

Box, J.E., D.H. Bromwich, B.A. Veenhuis, L-S Bai, J.C. Stroeve, J.C. Rogers, K. Steffen, T. Haran, S-H Wang, 2006. Variability of Greenland surface mass balance (1988-2004) using calibrated Polar MM5 output. 2005. J. Climate, 19 (12), 2783-2800.

Dyurgerov, M. B., 2002. Glacier Mass Balance and Regime: Data of Measurements and Analysis Occasional Paper No. 55, INSTAAR, Univ. of Colorado, 2002, available online at: http://instaar.colorado.edu/other/occ_papers.html.

IAHS (ICSI)-UNEP-UNESCO, 2003. Glacier Mass Balance Bulletin (GMB). Bulletin No 7 (2000-2001) Compiled by the World Glacier Monitoring Service. Edited by Haeberli, W., Frauenfelder, R Hoelzle, M. and Zemp, M. Zürich, 76 pp.; http://www.unzh.ch/wgms. 2003.

Johannessen, O.M., K. Khvorostovsky, M.W. Miles, L.P. Bobylev, 2005. Recent ice-sheet growth in the interior of Greenland. Science 310, 1013.

Kaser, G., J. G. Cogley, M. B. Dyurgerov, M. F. Meier, A. Ohmura, 2006. Mass balance of glaciers and ice caps: Consensus estimates for 1961-2004, Geophys. Res. Lett., 33, L19501, doi: 10.1029/2006GL027511.

Rignot, E., and P. Kanagaratnam, 2006. Changes in the velocity structure of the Greenland Ice Sheet, Science, 311, 986-990.

Steffen, K., R. Thomas, E. Rignot, G. Cogley, M. Dyurgerov, S. Raper, P. Huybrechts, E. Hanna, 2007. Cryospheric Contributions to Sea-level Rise and Variability, In: Understanding Sea-level Rise and Variability" (Ed. J. Church, P.Woodworth, Thorkild Aarup, S. Wilson) (Blackwell Publishing, in press).

AN INVESTIGATION OF THE CORRELATION BETWEEN CHANGING SNOWCOVER AND THE NET MASS BALANCE OF STORGLACIÄREN, NORTHERN SWEDEN

ELERI EVANS[1], RICHARD ESSERY[1] AND RICHARD LUCAS[2]

[1] Center for Glaciology, Institute of Geography and Earth Sciences, University of Wales, Aberystwyth, UK
[2] Department of Quaternary Science, Institute of Geography and Earth Sciences, University of Wales, Aberystwyth,UK

Introduction

The spatial and temporal variability of seasonal snowcover has important implications for the net mass balance of alpine glaciers. The seasonal snowline is a visible indicator of the complex interactions between the fluctuating precipitation and ambient temperature regimes, and the local topography. This study examines the relationship between changing snowcover distribution and the net mass balance of Storglaciären, Northern Sweden. This is done by modelling the seasonal snow cover and correlating this to field observations of the glacier's net mass balance.

Methods

Using a snow-wedge climate model based on that of Fitzharris and Garr (1995) snow accumulation and ablation was simulated using local and Norwegian (Kråkmo) meteorological data. The accuracy of the model outputs was tested by comparison with snowlines delineated from classified aerial photographs as well as ASTER and Landsat 7 ETM+ satellite imagery. The images were classified into the dominant landcover types; snow, ice and non-snow/ice.

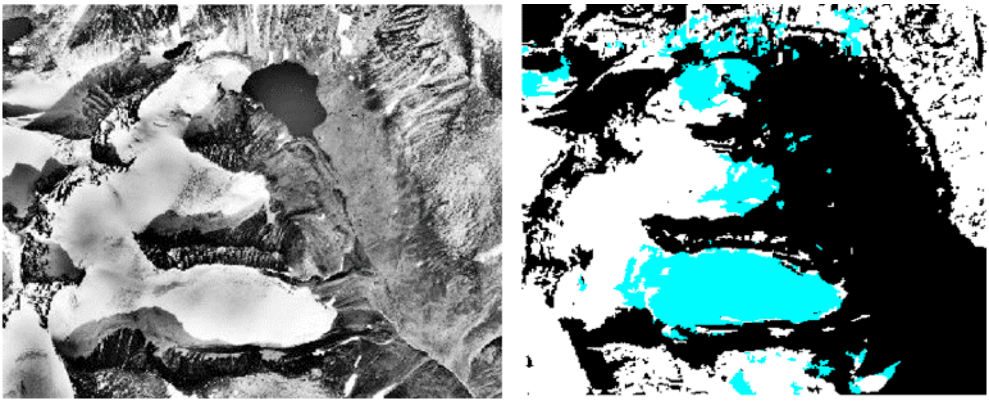

Figure 1. Original 9/9/1999 aerial photograph with corresponding classification.

Results

The classified images produced a map of snowcover, as seen in Figure 1. The elevation of the snowline on the glacier surface was extracted by overlaying the classified images onto a DEM. These elevations were then compared to the elevation bands where the model simulated snow to be present. Where they differed an error in the model assumptions was highlighted.

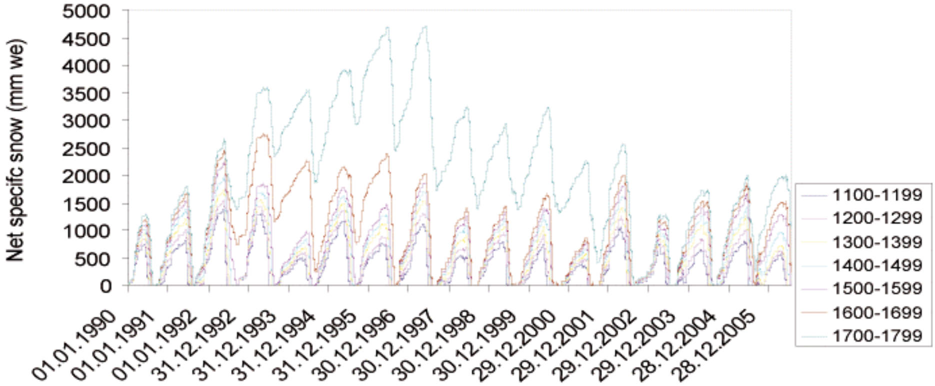

Figure 2. Net specific snow accumulation (mm) for each of the elevation bands for the years modelled using a DDF of 8.0 mm ºC^{-1} d^{-1}and T$_h$ 1.0 ºC.

The model that was run using Kråkmo precipitation, a degree-day factor of 8.0 mm ºC^{-1} d^{-1} and the threshold temperature set to 1.0 ºC, produced results which best fitted the observed Storglaciären net mass balances. The total seasonal snow fluctuated throughout the study period, but some trends were evident. Snow accumulation was greatest at the highest elevations, and ablation was greatest at the lowest elevations, as seen in Figure 2. The total seasonal snow at the highest elevations decreased throughout the study period. After 2002 the model suggests that no snow is being carried over to the next season (Figure 3). These results are correlated to the rising ELA over the study period and the observed negative mass balances from 2001 onwards. The model results therefore indicate that there is a strong correlation between the changing snowcover distribution and the net mass balance of Storglaciären.

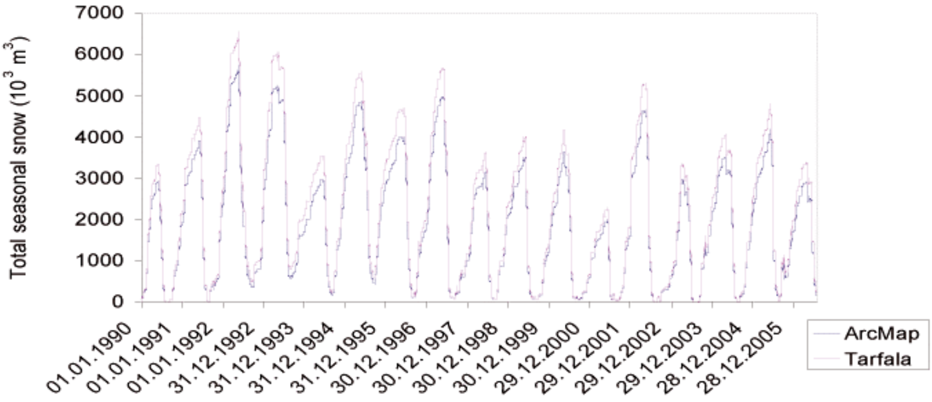

Figure 3. Total seasonal snow (10^3 m^3) for each year using a DDF of 8.0 mm ºC^{-1} d^{-1} and T$_h$ 1.0 ºC.

The model is however, subject to errors resulting from inaccuracies within the temperature and precipitation data used as well as from the parameters involved such as the degree-day factor of melt. These results may be simulating greater ablation than what actually occurs at Storglaciären as the degree-day factor is set very high in order to compensate for the high precipitation values. However, the small difference between the modelled and observed winter balances indicates that this model has applicability for modelling the winter balance of glaciers, and not just total seasonal snow within a catchment. Including a degree-day factor that fluctuates throughout the year in accordance with the season would provide a more accurate simulation of snow cover, as would including topographic variability within the glacierised catchment. Using precipitation values that are more representative of the Tarfala valley, though these may be hard to obtain, would also enhance the accuracy of the model.

Acknowledgements

This work was carried out as a partial requirement for the MSc in Glaciology at the University of Wales, Aberystwyth. I wish to thank my supervisors; Richard Essery and Richard Lucas, as well as Ninis Rosqvist, Peter Jansson and Henrick Törnberg from Stockholm University for the opportunity to study in arctic Sweden and Ian Brown for the provision of the Landsat 7 image.

References

Fitzharris, B. B. and Garr, C. E. 1995. Simulation of past variability in seasonal snow in the Southern Alps, New Zealand. *Annals of Glaciology*, **21**, 377-382.

Structure of Amundsenisen, Spitsbergen, from ground based radio echo sounding

Piotr Glowacki[1], Evgeny Vasilenko[2], Yury Macheret[3], Andrey Glazovsky[3], John Moore[4], Jon Ove Hagen[5] and Francisco Navarro[6]

[1] Institute of Geophysics, Polish Academy of Sciences, Warsaw, Poland
[2] Institute «Akadempribor», National Academy of Uzbekistan, Tashent, Uzbekistan
[3] Institute of Geography, Russian Academy of Sciences, Moscow, Russia
[4] Arctic Centre, University of Lapland, Rovaniemi, Finland
[5] Department of Geosciences, Section of Physical Geography, Faculty of Mathematics and Natural Sciences, University of Oslo, Norway
[6] Departamento de Matematica Aplicada, ETSI de Telecomunicacion, Universidad Politecnica de Madrid, Spain

Amundsenisen is the large ice plateau, 80 km^2 in area, located in Southern Spitsbergen. Data of ground-based radio-echo sounding in 2004 and 2006 show that Amundsenisen occupies a large depression between surrounding mountain ridges and strongly controlled by geological structure. Its ice volume is c. 27.1 km^3 and the maximum measured thickness is 631 m (Figure 1).

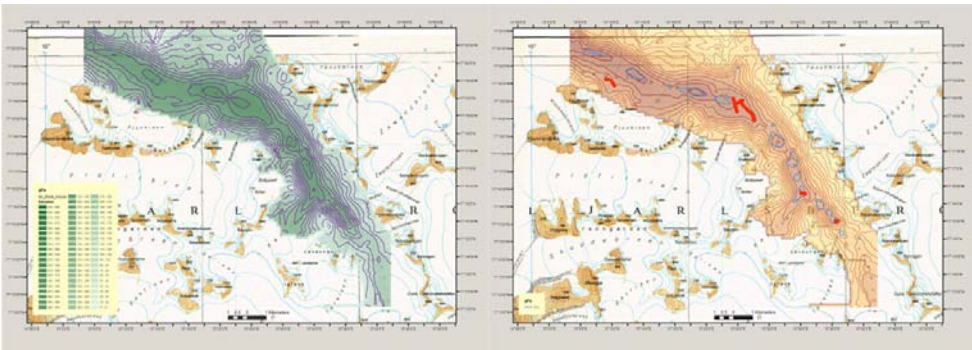

Figure 1. Amundsenissen RES results. (Left) ice thickness map. (Right) bedrock topography map. Red lines show sections of radar profiles with "flat" bed pattern. Blue contours show the areas with hydraulic potential minimums

The ice plateau consists mainly of temperate ice, which at some places, mainly near nunataks and in the upper part of its outlet glaciers, is covered by a cold ice layer up to 250 m thick, i.e. shows polythermal structure. Internal reflecting layers at depths down to 80 m and deeper are detected at many radar profiles. They can be related to discontinuities or water-impermeable horizons in the snow-firn sequence. Reflections from "flat" bedrock are recorded at depths more than 500 m at four places in the central part of the plateau and in the upper part of outlet Høgstebreen (Figure 1). The largest "flat" bedrock section is 450 m long (Figure 2).

These reflections are similar to radar reflections from subice lakes detected at many places of the Antarctic ice sheet. Judging by reflecting properties (character of fluctuation and power of reflected signals) and estimations of the hydraulic potential field, the sections of “flat” bed might be interpreted as reflections from near-bottom water bodies.

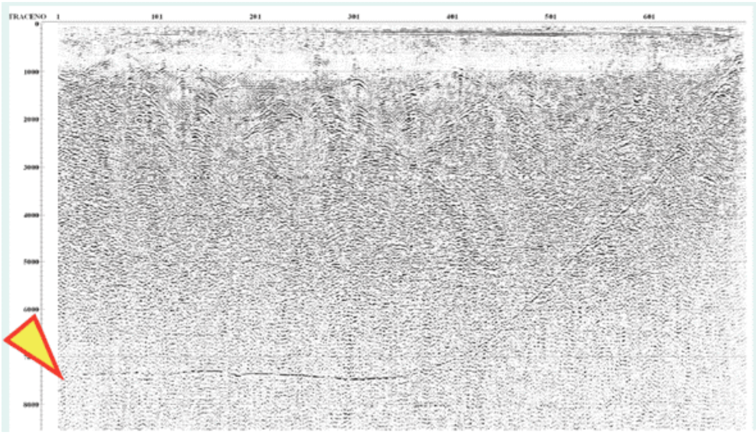

Figure 2. RES profile with “flat” bed section (X- axis shows trace numbers, Y-axis shows two-way travel time in ns)

MASS BALANCE ASSESSMENT OF WERENSKIOLDBREEN (SW SPITSBERGEN) ON THE BASIS OF METEOROLOGICAL AND CARTOGRAPHICAL DATA

MARIUSZ GRABIEC, TOMASZ BUDZIK

Faculty of Earth Sciences, University of Silesia, Sosnowiec, Poland.

Changes in geometry of glaciers are a resultant of two variables: mass balance and dynamics of glacial movement. The systematic study of dynamics and mass balance of Svalbard glaciers has been conducted on a limited number of glaciers for a few decades. Therefore, only an extrapolation of results in space and time could give a comprehensive picture of mass balance status of the Svalbard glaciers.

This work describes the method and results of assessing the Werenskioldbreen mass balance on the basis of data from weather stations located on the western coast of Svalbard. There was also an attempt made to verify the estimation by comparing changes in the glacier geometry in the period 1958 -1990.

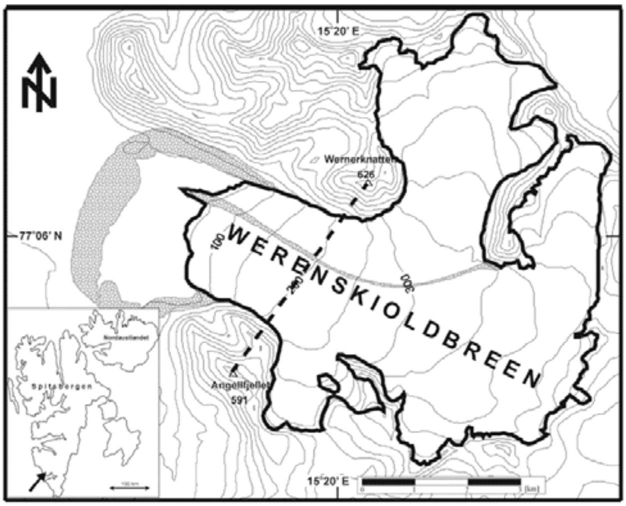

Figure 1. Location map of Werenskioldbreen.

Werenskioldbreen is located in Wedel Jarlsberg Land (SW Svalbard). It is a valley-type glacier terminating on the land (Figure 1). The surface area of the glacier is about 28 km^2 and the length c. 7 km. Folding of medial moraine shows that glacier surge took place in some past. Dynamics of glacier movement is relatively small and amounts to several centimeters per day (Baranowski, 1978).

Glacier mass balance can be expressed as follows:

$$bn = bw + bs \quad (1)$$

where: bn - net balance, bw - winter balance, bs - summer balance (mm w.e.).

The winter balance was calculated on the basis of accumulation algorithm suggested by Grabiec (2005):

$$bw_{(l,h_i)} = \left(B_{h_0} L_c\right) + \left(B_{h_0} L_c \frac{\left(h_i - h_0\right)}{100} \tau\right) \tag{2}$$

where: $bw_{(l,hi)}$ - snow accumulation (mm w.e.) on a glacier situated at a distance l from the open water at a point located at a height of h_i; B_{h0} - winter accumulation (mm w.e.) at a reference station at altitude h_0; L_c - location coefficient; τ - accumulation gradient relative accumulation increase per 100 m (%).

The winter accumulation at the selected reference station (B_{h0}) was calculated by:

$$B_{h_0} = KP_{h_0} \tag{3}$$

where: P_{h0} - winter (October to May) precipitation (mm) at a reference station at altitude h_0; K - efficient accumulation correction coefficient.

The efficient accumulation correction coefficient K calculates seasonal accumulation rates from the total winter precipitation. The value of K is affected by two factors: error in precipitation measurements, which increases K, and the effect of rain, which decreases K. If only winter precipitation data with no distinction of types is available, K is assumed to be equal to 1.1 (Førland and Hanssen-Bauer, 2000).

The location coefficient L_c describes the relation between the sum of winter precipitation at a site located at a given distance from the open water and precipitation at a particular station (Grabiec 2005). Within this work sums of winter precipitation from Isfjord Radio (1912-1975), Svalbard Lufthavn (1976-1978, 1982) and Hornsund (1979-2005) were used.

The value of sea-level accumulation obtained using the formula (3) is converted into accumulation at a given altitude of measurement point, according to the applied accumulation gradient τ. In this paper the coefficient τ equal to 0.6, as suggested by Grabiec (2005), has been applied.

The summer balance was defined on the basis of its relation with the PDD (positive degree-day) sum in the summer period:

$$bs = a \sum PDD \tag{4}$$

where: ΣPDD - sum of positive degree-day in the summer months (VI-IX) in glacier forefield, a - ablation coefficient per 1 PDD.

The set of *ΣPDD* was obtained from monthly averages of temperature in the Wereskioldbreen forefield. The averages in question were created through correlation with data from the weather stations of Hornsund and Isfjord Radio. Temperature data relates only to the glacier forefield. There is a lack of temperature data in the elevation profile. Thus the relation between elevation and ablation efficiency of one 1 PDD (a - mm w.e/1 PDD) has been applied to reconstruct the ablation on Wereskioldbreen:

$$a = -0.007h + 5.0121 \tag{5}$$

where h stands for elevation (m) above the sea level

The results of Werenskioldbreen mass balance (net balance, winter balance, summer balance) assessment in 1913 - 2005 have been put together in Figure 2. The negative mass balance predominated in discussed period. The positive budget of glacier mass occurred only in several seasons in late 1950-ties and 1960-ties, mainly due to significant winter balance.

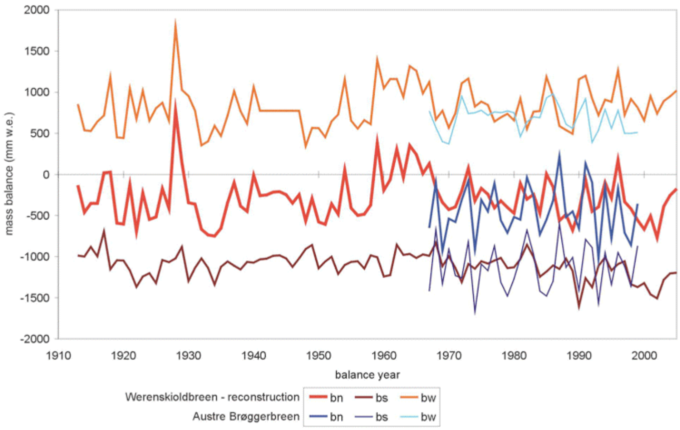

Figure 2. Reconstruction of Werenskioldbreen mass balance (1913 - 2005) and observed mass balance of Austre Brøggerbreen (1967-1999)

The estimated mass balance for Werenskioldbreen has been compared with observed balance data from Austre Brøggerbreen (NW Spitsbergen) in the period 1976 - 1999 (Mass balance data from Arctic Glaciers 2002) (Figure 2). Net balance as well as winter and summer balance for both glaciers are similar despite distinct location of the objects. The courses of winter balance in analyzed period were particularly close each other.

Figure 3 shows observed and estimated balance data in selected measurement seasons. The results obtained from those two methods are not far from each other. The average error of the estimated mass balance was noted in range 31 (1994) - 600 (2001) mm w.e., for summer balance: 89 (1999) - 275 (2001) mm w.e., however for winter balance: 41 (2000) - 325 (2001) mm w.e..

Correctness of mass balance assessment underwent verification in the frontal part of the glacier limited by the glacier range from 1990 and a profile of Angellfjellet-Wernerknatten (Figure 1). This verification consists in putting together changes in glacier thickness between 1958 and 1990 obtained from comparing digital elevation models (DEM's) for the discussed period and applying results of mass balance assessment. The following cartographical materials were in use:

- Werenskioldbreen Glacier. Frontal zone. Medial zone on a scale of 1:5000 made in 1957-1959 on the basis of field survey (Lipert, 1961).
- Werenskioldbreen and surrounding areas. Orthophotomap on a scale of 1:25000 processed on the basis of aerial photographs from 1990 (Jania et. al, 2002).

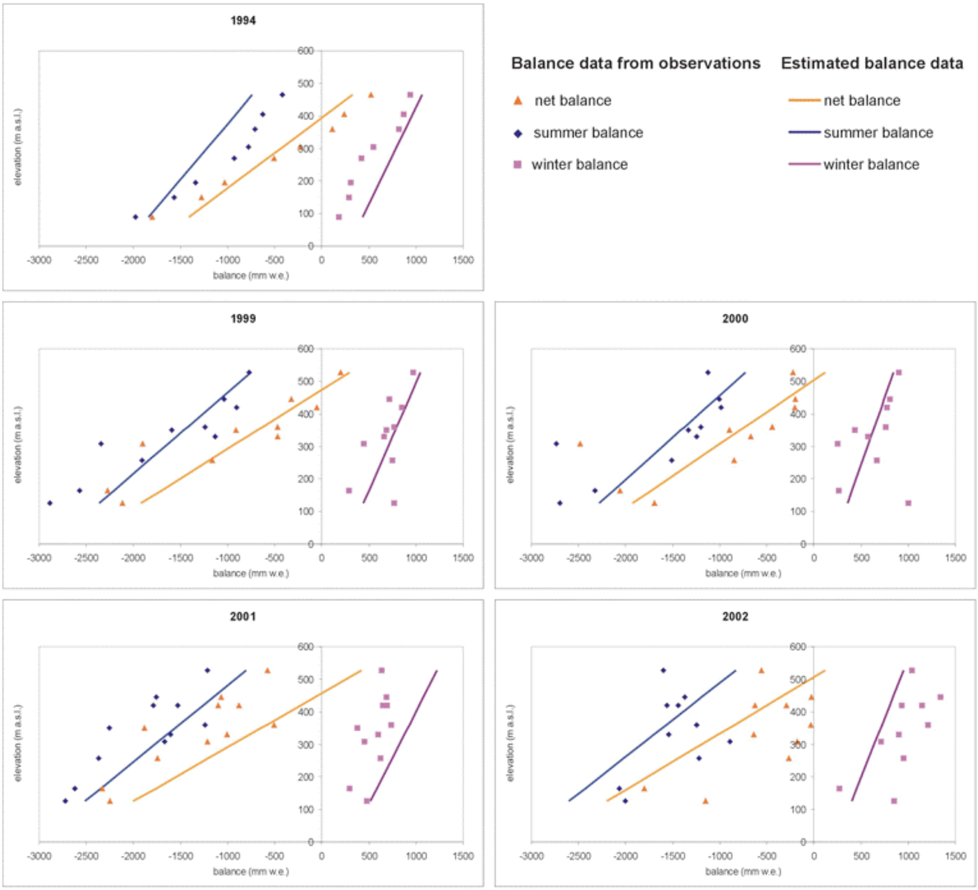

Figure 3. Estimated and observed mass balance of Werenskioldbreen (Jania, 1994; Institute of Geophysics Polish Academy of Sciences - unpublished data).

Change of thickness (in meters) within a balance year (dH) at a given point of the glacier corresponds with:

$$dH = \frac{bn}{\rho} + EV \qquad (6)$$

Where: EV - vertical component of glacier movement (in the ablation zone directed upwards in meters); ρ - ice density (in the ablation zone taken as 900 kg/m^3), firn and snow density (in the accumulation zone).

Change in thickness of glacier front calculated by the cartographical method and by estimation of mass balance amounts generally to 1.226 m over 32 years that gives 0.038 m annually (Table 1) which is very low.

Conclusions

- The procedure presented above allows for reconstruction of mass balance of small and medium size Spitsbergen glaciers.

- This method assumes that the mass balance value is constant at the same elevation.
- Local conditions determining mass balance elements are then not taken into consideration.
- A precise glacier dynamics model add to presented assessment could give more accurate results of glacier geometry changes.

Table 1. Average change in thickness of frontal part of Werenskioldbreen in the years 1958 -1990.

methods	average thinning of glacier front	
	1958 -1990	meters per 1 year
(1) cartographical method	28.746	0.898
(2) mass balance – ice dynamics method	27.520	0.860
Difference (1) – (2)	1.226	0.038

Acknowledgements

Authors would like to thank the Institute of Geophysics of the Polish Academy of Sciences and the Norwegian Meteorological Institute for granting the access to meteorological data and mass balance data. We also would like to express our thanks to dr. Leszek Kolondra for making DEM of the glacier available.

References

Baranowski, S. 1978. Subpolarne lodowce Spitsbergenu na tle klimatu tego regionu. SW Spitsbergen. Acta Univ. Wratisl. 393, Studia Geogr. 31, Wroclaw, pp. 157.

Førland, E.J. and I. Hanssen-Bauer. 2000. Increased Precipitation in the Norwegian Arctic: True or False? Climatic Change, 46, 485 - 509.

Grabiec, M. 2005. An estimation of snow accumulation on Svalbard glaciers on the basis of standard weather-station observations. Annals of Glaciology vol. 42, 269 - 276

Jania J. 1994. Field investigations during glaciological expeditions to Spitsbergen in the period 1992 - 1994 (interim report). Uniwersytet Slaski, Katowice, pp. 40.

Jania J., Kolondra L., Aas H.F. (ed.) 2002. Werenskioldbreen and surrounding areas. Spitsbergen, Svalbard, Norway. Ortophotomap 1:25 000. Uniwersytet Slaski, Katowice, Polska, Norsk Polarinstitutt, Tromsø, Norge.

Lipert C. 1961. Lodowiec Werenskioldbreen. Strefa czolowa. Strefa srodkowa 1 : 5 000. Wojskowa Sluzba Topograficzna

Mass balance data from Arctic Glaciers 2002. http://www.phys.uu.nl

Climate change response of three ice caps in Iceland

Sverrir Guðmundsson[1], Helgi Björnsson[1], Guðfinna Aðalgeirsdóttir[3], Tómas Jóhannesson[2], Finnur Pálsson[1] and Oddur Sigurðsson[4]

[1] Institute of Earth Sciences, University of Iceland, Reykjavík, Iceland
[2] Icelandic Meteorological Office, Reykjavík, Iceland
[3] Department of Geography, University of Wales Swansea, Swansea, UK
[4] Hydrological Service, National Energy Authority, Reykjavík, Iceland

Introduction

The surface and bed topography of Vatnajökull, Hofsjökull and Langjökull ice caps have been constructed from GPS and radio-echo surveys (Björnsson, 1986, 1988, Björnsson et al., 2006), mass balance measurements are conducted over the last 10 to 15 years, depending on the glaciers (Björnsson et al. 1998, 2002, 2006; Sigurðsson 1989-2004), and complimented with glacio-meteorological study (Björnsson et al., 2005; Guðmundsson et al., 2003, submitted). A degree-day mass balance model, using records of meteorological stations away from the glaciers, was calibrated against the observations of winter and summer balance (Jóhannesson et al., 1995, Jóhannesson, 1997) and evaluated with full energy balance observations (Guðmundsson et al., 2003; submitted). We used the mass balance model, coupled to a 2-D ice flow model (Aðalgeirsdóttir, 2003; Aðalgeirsdóttir et al., 2006), to simulate the evolution of Langjökull, Hofsjökull and the southern part of Vatnajökull over the next centuries in response to a prescribed climate change scenario for Iceland (the Nordic CE project). The volume of ice caps is predicted to decrease drastically over the next 200 yrs. Runoff will increase over the next 40-60 years and remain higher than at present until the close of the 21st century.

Location and geometry

Locations of the three glaciers are shown in Figure 1 and parameters describing the geometry in Table 1.

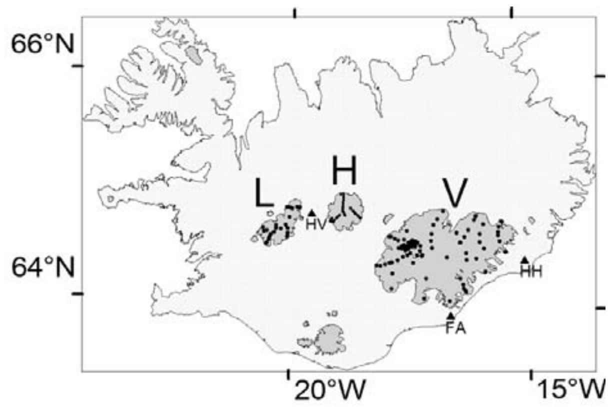

Figure 1. Langjökull (L), Hofsjökull (H) and Vatnajökull (V), sites of mass balance measurements (dots) and meteorological stations (triangles; HV: Hveravellir, FA: Fagurhólsmyri, HH: Hólar í Hornafirði).

Table 1. Characteristics of the Langjökull, Hofsjökull and Vatnajökull ice caps.

Ice cap	Area (km^2)	Volume (km^3)	Maximum ice thickness (m)	Range in elevation (m a.s.l.)
Langjökull	920	190	580	390-1450
Hofsjökull	890	200	760	600-1800
Vatnajökull	8100	3000	950	0-2100
Southern Vatnajökull	3700	3700	1280	900-2100

Observations

Daily temperature and precipitation at Hveravellir were used as an input to the mass balance models of Langjökull and Hofsjökull, and temperatures at Hólar í Hornafirði and precipitation at Fagurhólsmyri for the southern Vatnajökull (Figure 1). The mass balance models were calibrated to i) mass balance observations conducted at 22 stakes at Langjökull from 1996-2005, ii) 35 stakes on Hofsjökull from 1988 to 2005, and iii) 23 stakes on southern Vatnajökull from 1993-2005 (Figure 1), and evaluated by using full energy balance derived at several automatic weather stations operated over a decade on Vatnajökull and six years on Langjökull. DEMs of the glaciers surface and bed were constructed from GPS and radio echo surveys undertaken 1980-2000.

Mass balance modelling

The degree-day mass balance model uses a constant vertical elevation temperature lapse rate, degree-day factors that differ for snow and ice, and horizontal and vertical precipitation gradients. The parameters were calibrated to the observations by assuming a constant snow/rain threshold of 1 °C. The mass balance model describes 80% and 92% of the annual variation in the winter balance of Hofsjökull and southern Vatnajökull respectively, and 95% of the summer balance on both the glaciers. The model explains 86% of the variance in the summer balance of Langjökull but only 39% of the winter balance. Despite this, the model managed to describe 92% of the variation in the annual balance of Langjökull.

Modelled average specific net mass balance of the three ice caps 1981-2000 is close to zero; positive during the first but negative during the latter part of the time interval. Thus, the average climate of 1981-2000 was chosen as an initial reference climate for all model runs and the year 1990 as the initial year.

Coupled dynamic ice flow and mass balance model

The glaciers dynamics were described by a vertical integrated finite-difference ice flow model with shallow-ice approximation. The parameters describing the rheology of ice (Glen´s law) and Weertman type of basal sliding are the same as those determined for Hofsjökull and Vatnajökull by Aðalgeirsdóttir et al., (2006). The model neglects longitudinal stresses and surges, and excludes bed-isostatic adjustments and seasonal sliding.

Simulation of the glaciers response to the future climate scenario was initialized with stable ice geometries derived after a few hundred years spin-up with a zero mass balance input, representing the average climate condition of 1981-2000.

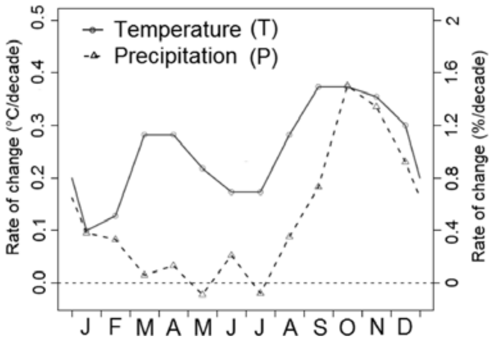

Figure 2. Average monthly temperature and precipitation change per decade between the periods 1961-1990 and 2071-2100 for the Icelandic highland according to the CE climate change scenario.

Response to a prescribed climate change scenario

A climate change scenario was defined in the Nordic CE project (Figures 2 and 3; Fenger, in press). The simulation was started from the year 1990 by using the stable ice geometries for the three glaciers and the 1981-2000 initial reference climate. Observed temperature and precipitation changes were used until 2005 and the CE scenario thereafter. The simulation predicts that Langjökull disappears within 150 years from now and the more elevated Hofsjökull and Vatnajökull almost vanish within 200 years from now (Figure 4a,b). The runoff is predicted to increase as the climate gets warmer, but peak after 40-60 years due to the reduced area of the glaciers (Figure 4c). The specific runoff rate is highest for Langjökull and lowest for Hofsjökull as expected from their elevation range (Figure 4c and Table 1).

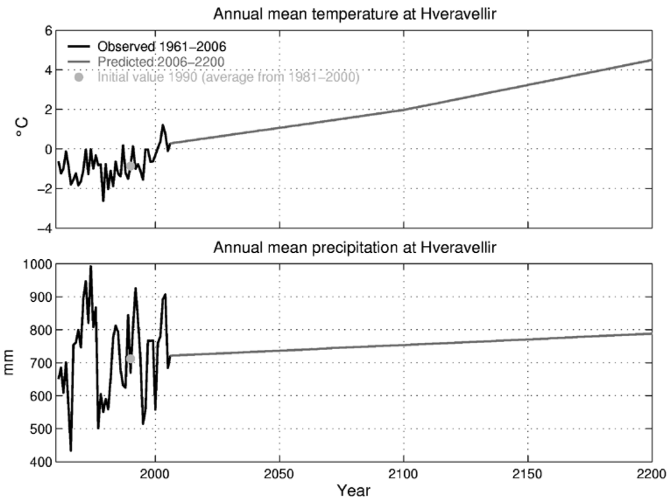

Figure 3. Observed and predicted annual mean temperature and precipitation 1961-2200 at Hveravellir.

Acknowledgement

The study of the glaciers geometry was supported by the National Power Company and the Public Roads Administration, and the mass balance by the National Power Company, Reykjavík Energy, the National Energy Authority and the EU projects TEMBA, ICEMASS and SPICE. The modelling presented was carried out during the projects Climate, Water and Energy (CWE) initiated by the directors of the Nordic Hydrological Institutes (CHIN) with funding from the Nordic Energy Research of the Nordic Council of ministers, Climate and Energy (CE), also financed by Nordic Energy Research and Veðurfar, vatn og orka (VVO) sponsored by the National Power Company and the National Energy Fund of Iceland.

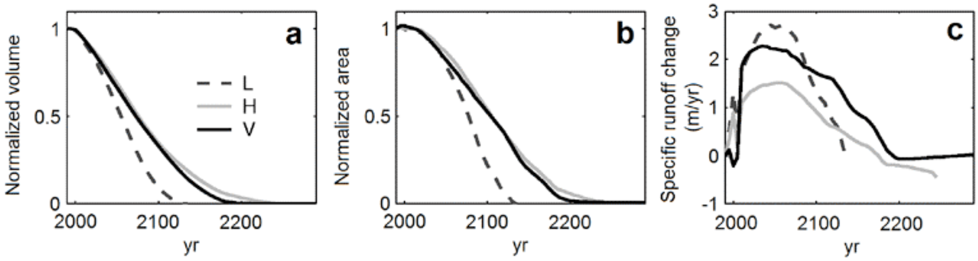

Figure 4. Change in volume (a), area (b), and specific runoff (c) of Langjökull (L), Hofsjökull (H) and Vatnajökull (V). The volumes and areas are normalized to the present-day values (Table 1). The specific runoff rate is in m yr^{-1} per the present-day glacier area.

References

Aðalgeirsdóttir G. 2003. Flow dynamics of Vatnajökull ice cap, Iceland. Mitteilung 181, Versuchsanstalt fur Wasserbau, Hydrologie und Glaziologie der ETH Zurich-Zentrum. pp. 178.

Aðalgeirsdóttir G., Jóhannesson T., Björnsson H., Pálsson F., Sigurðsson O. 2006. The response of Hofsjökull and southern Vatnajökull, Iceland, to climate change. J. Geoph. Res. 111, F03001.

Björnsson H., Pálsson F., Haraldsson H. H. 2002. Mass balance of Vatnajökull (1991-2001) and Langjökull (1996-2001), Iceland. Jökull 51, 75-78.

Björnsson H. 1986. Surface and bedrock topography of ice caps in Iceland mapped by radio echo soundings. A. Glaciol. 8, 11-18.

Björnsson H. 1988 Hydrology of ice caps in volcanic regions, 45 Societas Scientiarum Islandica, Reykjavík, pp 139.

Björnsson H., Pálsson F., Guðmundsson M. T., Haraldsson H. H. 1998. Mass balance of western and northern Vatnajökull, Iceland, 1991-1995. Jökull, 45, 35-58.

Björnsson, H., S. Gudmundsson and F. Pálsson. 2005. Glacier winds on Vatnajökull ice cap, Iceland and their relation to temperatures of its lowland environs. Ann. Glaciol., 42, pp. 291-296.

Fenger, Jes (editor). In press. Impacts of Climate Change on Renewable Energy Sources - Their Role in the Nordic Energy System. Copenhagen, Nordic Council of Ministers, 2006.

Guðmundsson S., Björnsson H., Pálsson F., Haraldsson H. H., 2003. Comparison of physical and regression models of summer ablation on ice caps in Iceland. Institute of Earth Sciences, University of Iceland, RH-20-2003. Technical report (PDF available at http://www.raunvis.hi.is/~sg/emodels.pdf, 19 April 2006).

Guðmundsson S., Björnsson H., Pálsson F., Haraldsson H. H., submitted. Energy balance and degreeday models of summer ablation on the Langjökull ice cap, SW Iceland. Submitted to J. Glaciol.,

Jóhannesson T, Sigurðsson O., Laumann T, Kennett M. 1995. Degree-day glacier mass-balance modelling with application to glacier in Iceland, Norway and Greenland, J. Glaciol. 41(138), 345-358.

Jóhannesson T. 1997.The response of two Icelandic glaciers to climate warming computed with a degree-day glacier mass-balance model coupled to a dynamic model, J. Glaciol., 43(144), 321-327.

Sigurðsson O. 1989-2004. Afkoma Hofsjökuls 1987-1988, 2002-2003 (Mass balance of Hofsjökull 1987-1988, 2002-2003), National Energy Authority. Technical reports in Icelandic.

MASS BALANCE MODELLING OF HOFSJÖKULL

TÓMAS JÓHANNESSON[1], ODDUR SIGURÐSSON[2], ÞORSTEINN ÞORSTEINSSON[2] AND REGINE HOCK[3]

[1] Icelandic Meteorological Office, Reykjavík, Iceland.
[2] National Energy Authority, Hydrological Service Division, Reykjavík, Iceland.
[3] Geophysical Institute, University of Alaska, Fairbanks, Alaska USA.

Extended abstract

The mass balance of the Hofsjökull ice cap, central Iceland, has been studied by models of different complexity, ranging from a simple ELA-based model (Jóhannesson, 1986), through traditional degree-day models (Jóhannesson and others, 1995), to degree-day models with horizontal variations in the precipitation field (Jóhannesson and others, 2006) and potential radiation included in the formulation of the melt model (Thorsteinsson and others, 2006).

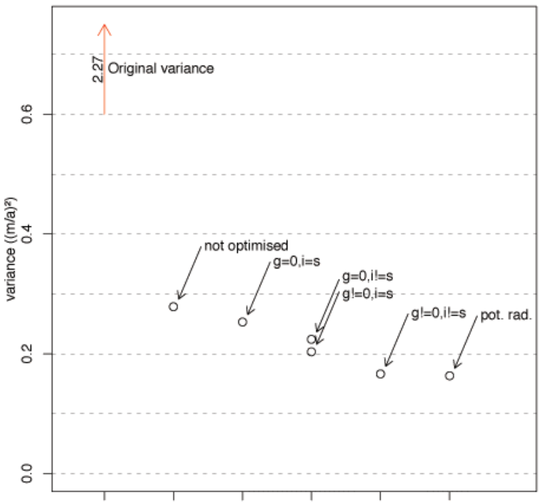

Figure 1. Residual variance of mass balance models with different specification of precipitation and melt parameters (see text for explanations). The level of detail of the models increases from left to right. The models denoted by "g=0, i!=s" and "g!=0, i=s" both introduce one additional feature compared with the model labelled "g=0, i=s" and are therefore plotted at the same location on the x-axis. The original variance is computed from the deviations of the winter and summer mass balance from the average winter or summer balance, respectively, for the whole data set. All models are run for the same mass balance data from the period 1988–2004.

The importance of the different components of the mass balance model was investigated by evaluating the performance of different model types with different specification of precipitation and melt parameters (see Jóhannesson and others, 2006, for a detailed description of the data and the models). Figure 1 shows the residual variance ordered according to increasing realism of the mass balance model. The original variance corresponds to the deviations of the winter and summer mass balance from the average winter or summer balance, respectively, for bass balance data from the period 1988–2004. All the models shown in the figure have a residual variance in the range 7–12% of the original residual variance. The first model on the left, labelled "not optimised", which has the highest residual variance, is a mass balance model applied by De Woul *et al.* (2006), to the whole of Hofsjökull in a study of the importance of the firn layer for the hydrology of the ice cap. This model includes potential radiation in the formulation of a degree-day melt model (Hock, 1999), but is without horizontal precipitation gradients. It was calibrated manually, which explains to a large extent the comparatively poor performance compared with the other models that are automatically calibrated. The next four models are different setups of the MBT degree-day model (Jóhannesson and others, 1995). The model labelled “g=0, i=s” is without horizontal precipitation gradients, and the degree-day coefficients for ice and snow are assumed to be equal. The model includes a vertical precipitation gradient as all the other models in Figure 1. This highly simplified model has a somewhat smaller residual variance than the model used by De Woul *et al.* The next two models add one additional aspect to the mass balance formulation each, the model labelled “g=0, i!=s” has different degree-day coefficients for ice and snow, and the model labelled “g!=0, i=s” has horizontal precipitation gradients. These models have 20–25% lower residual variance than the model used by De Woul *et al.* The model labelled “g!=0, i!=s” has both horizontal precipitation gradients and different degree-day coefficients for ice and snow. The model labelled “pot.rad”, which has a slightly lower residual variance than the best MBT model, is the mass balance model of Hock (1999) with potential radiation, but with horizontal precipitation gradients included, and calibrated by the same automatic calibration procedure, which was applied for the MBT model (Thorsteinsson *et al.*, 2006).

As expected, the analysis shows that the use of different degree-day coefficients for ice and snow leads to a substantial improvement in the model. The improved performance provided by a simple horizontal distribution of precipitation using linear gradients turns out to be even more important and leads to a larger reduction in the residual variance even when the degree-day coefficients for ice and snow are assumed to be equal. Using both different degree-day coefficients for ice and snow, and horizontal precipitation gradients, leads to a further decrease in the residual variance. A more complex degree-day melt model including potential radiation finally leads to a slightly lower residual variance by about 2% compared with the MBT model with both horizontal precipitation gradients and different degree-day coefficients for ice and snow, but this step is much smaller than provided by the other incremental improvements. An important step in the reduction of the residual variance appears to be careful model calibration. The main calibration of the MBT model has 6 independent parameters and the model of Hock (1999) with horizontal precipitation gradients has 7 independent parameters that need to be determined. These parameters appear to be well constrained by the measurements, which contain 1106 observations of winter and summer balance, but the best combination of the parameters can be hard to find manually.

This study underscores the importance of including horizontal precipitation variations in glacier mass balance modelling. A very simple representation of such variations using horizontal gradients appears to be equally important in terms of the residual variance as the taking into account the well known difference between the melt rate of ice and snow covered areas on this small ice cap with a simple orography compared with many glaciated mountainous regions where precipitation variations due to orographic effects may be expected to be even more pronounced.

Acknowledgements

This study was carried out as a part of the projects *Climate and Energy* (CE), funded by the Nordic Energy Research of the Nordic Council of Ministers, and *Veðurfar og orka* (VO), sponsored by the National Power Company of Iceland and the National Energy Fund of Iceland.

References

De Woul, M., R. Hock, M. Braun, Th. Thorsteinsson, T. Jóhannesson and S. Halldórsdóttir. 2006. Firn layer impact on glacial runoff - a case study at Hofsjökull, Iceland. *Hydrological Processes*, **20**, 2171–2185, doi:10.1002/hyp.6201.

Hock, R. 1999. A distributed temperature-index ice- and snowmelt model including potential direct solar radiation. *J. Glaciol.*, **45**(149), 101–111.

Jóhannesson, T. 1986. The response time of glaciers in Iceland to changes in climate. *A. Glaciol.*, **8**, 100–101.

Jóhannesson, T., O. Sigurðsson, T. Laumann, M. Kennett. 1995. Degree-day mass balance modelling with applications to glaciers in Iceland, Norway and Greenland. *J. Glaciol.*, **41**, 138, 345–358.

Jóhannesson, T., O. Sigurðsson, B. Einarsson, Th. Thorsteinsson. 2006. *Mass balance modeling of the Hofsjökull ice cap based on data from 1988–2004*. Orkustofnun, Rep. OS-2006/004.

Thorsteinsson, Th., B. E. Einarsson, T. Jóhannesson and R. Hock. 2006. *Comparison of degree-day models of the mass balance of the Hofsjökull ice cap*. Reykjavík, National Energy Authority. Rep. OS-2006/014.

NATURAL RADIOACTIVE ISOTOPES IN GLACIER STUDIES

ANTOINE KIES[1], HEINZ SURBECK[2] AND ZORNITZA TOSHEVA[1]

[1] University of Luxembourg, Luxembourg.
[2] Swiss Center of Hydrology (CHYN), University of Neuchâtel, Neuchâtel, Switzerland

Radon (^{222}Rn) is a naturally radioactive gas occurring in the decay series of Uranium 238 (^{238}U). Compared to the radon isotopes formed in the 2 other natural decay series, ^{222}Rn has by far the longest period of 3.8 d. In the following text the term radon refers to the isotope ^{222}Rn.

Radium (^{226}Ra, half life 1640 y), the immediate antecedent of radon, is found along with the parent ^{238}U in all rocks with changing concentrations. The highest concentrations are recorded in some granitic rocks and gneisses as well as in phosphatic formations and marine shales. Radon is a noble gas and as soon as it is created, if located close to grain boundaries, has the possibility to join the gaseous or liquid surroundings in contact with the hosting rocks. Soluble in water radon can be carried over longer distances during its mean life time of 5.5 days. Radon is an alpha emitter, as are some of its short-lived decay products. Based on this propriety, it is possible to measure radon concentrations in air or water continuously with a fair accuracy. Radon can be used in nature as a suitable tracer for studying short-lived phenomena.

Hydrograph separation in water catchment areas

The Laboratoire Physique des Radiations of the University of Luxembourg participated in a 3 year national research program based on the study of the interactions between different parameters in the water cycle. Small catchments in Luxembourg were selected to get information about the runoff processes before, during and after storm events (Kies, 2005).

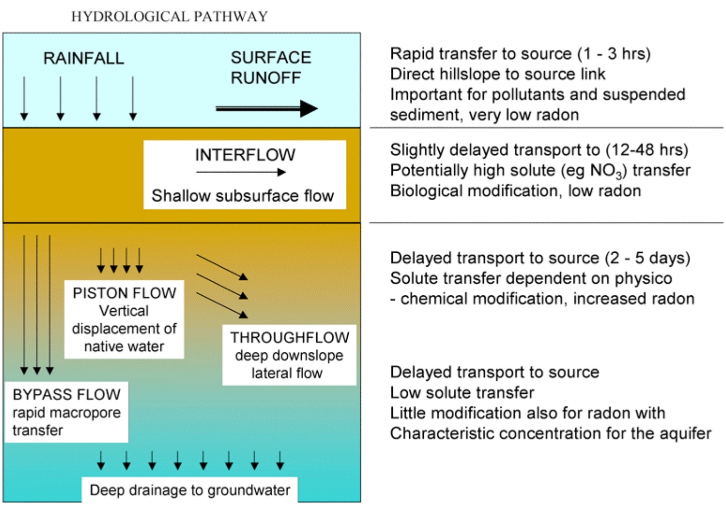

Figure 1. Hydrological pathways: the different waters may be distinguished by their radon concentrations

A classic isotope hydrograph separation is a technique that partitions the contribution of new water (event water like rain or snowmelt) and old water (pre-event water such as ground water and pore water) to a stream hydrograph. This technique is used extensively by the hydrological community to track the components of run-off and to trace water flow in unsaturated soils.

Hydrograph separations lead to a quantitatively portioning storm runoff into a stream or a river among contributions from different waters (Figure 1): superficial runoff, interflow water and groundwater (Kraemer, 1998). Environmental isotopic tracers, such as ^{222}Rn and ^{18}O are used to separate the runoff into the different components during these events. Unlike chemical tracers, isotopic tracers are relatively conservative in reactions with catchment materials; they are chemically and physically inert. Isotope hydrograph separation is based on the assumption that the isotopic composition (e.g. ^{222}Rn) of the involved runoff compartments is distinctly different and the isotopic signal within each compartment stays constant in space and time.

Hydrograph separation in glaciers

Information how water flows at the glacier bed is important in order to understand two of the major problems in glaciology: the detailed mechanisms of glacier sliding and the associated deformation of sub glacial sediments as well as the causes and mechanics of glacier surges.

In contrast to stream flow, glacier run-off has unusual features, such as large diurnal fluctuations and maximum discharge during summer. The water may be dispersed widely over the glacier bed, or concentrated in a few large channels.

The surface meltwater is the prevalent contribution to the water output in temperate glaciers. In summer water flows on the ice surface in a network of channels; much of the water enters the glacier through cracks and vertical passages. Water emerges at the terminus in more or less large channels. Understanding the flow system in and under the glacier is a major problem. This problem can be confronted in two ways: either deduction from streamflow records combined with tracer experiments or theoretical analyses.

In winter the high pressure resulting from the downward gradient of ice flow leads to the closing of channels when surface melting stops.
Two systems can carry water to the glacier bed:

1. A tunnel system that carries a large flux at low pressure in approximately the same direction as the ice flow. Dye tracing experiments in the ablation area show that water travels from the surface to terminus in a few hours at high velocities.
2. A linked-cavity system, a system of passageways whose diameter fluctuates widely along the path creating a complicated meandering network of many interconnected cavities. The wide parts are cavities on the downstream sides of the larger bedrock; the narrow parts are channels cut into the bed. Travel times are much longer than in a tunnel. Because sliding tends to keep cavities open, the sliding velocity influences their size. Conversely, the sliding velocity depends on the water pressure in the cavities.

Melt water of the glacier has negligible radon concentrations, as there exist nearly no sources of radon in the ice; without contact to rocks water will keep negligible levels. Depending on the duration of contact with radon with rocks and till at the glacier bed, melt water will be charged in radon. This radon can be measured at the resurgence if the time delay between radon charge and resurgence is not above about 4 decay periods of radon, i.e. 15 days.

Melt water carried by tunnel systems (see above system 1), even in contact with the base sediments and rocks, is expected to have low radon concentrations, as the travel time is very short. It is the water carried through a linked-cavity system in contact with rocks and till (see above system 2) that is supposed to have increased radon concentrations.

Melt water at the resurgence is a mixture from these different contributions: direct melt water, system 1 water with very low radon concentrations and system 2 melt water in contact with the bed rocks and sediments with measurable radon enrichment. Variations of radon concentrations over time, together with continuous information on conductivity and temperature, pH, dissolved oxygen and other parameters to be defined, could lead to a sort of hydrograph separation. The obtained information may be useful in the overall study of the behaviour of the glacier and have to be discussed in combination with the results from meteorological parameters, ice movement etc.

A major problem of radon is the easy degassing of radon when water is flowing in not confined aquifers. Therefore the ideal investigation location is artesian meltwater outputs. In Hornsund (Spitsbergen) measurements from meltwater were performed in September 2006 at two different glaciers: Ariebreen and the Werenskioldbreen.

At Ariebreen, meltwater could only be sampled at open outflow tunnels where, especially due to turbulent water flow, by far most of radon had degassed. Radon concentration was 0.070 +/- 0.020 Bq/l. The effective electrical conductivity of 53.3 µS/cm documented meltwater in contact with the basement.

At Werenskioldbreen, different water channels were sampled (figure 2). Most of them showed to be actually meltwater (surface water, or water not in contact with bedrock) where radon concentrations varied between 0.15 to 0.29 Bq/l, the electrical conductivity, 4.92 to 4.95 µS/cm, was low and fairly constant. The measurements performed at the largest artesian outflow at the central part of the glacier front main gave unexpected high radon concentrations of 18 to 22 Bq/l, the electrical conductivities ranged from 76.6 to 77.2 µS/cm. The conductivity measurements are similar to those reported from previous campaigns at the same time period (reference). This kind of outbursts has been interpreted as arising from the progressive accumulation of subglacier meltwater behind a cold ice dam, as no degassing occurs before the outburst. Radon is not degassed from the meltwater and the study of concentration over longer time periods should give valuable information. These measurements should be done together with at last one other parameter measured continuously. We propose to use electrical conductivity and temperature, eventually dissolved gases, turbidity and discharge.

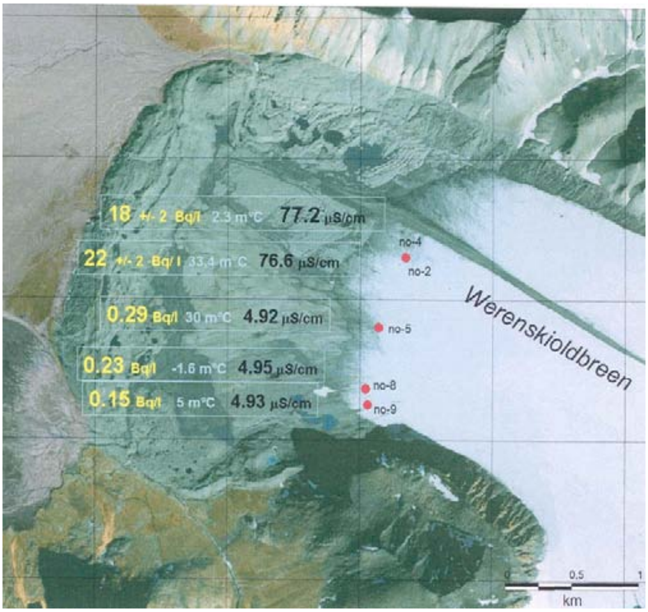

Figure 2. Location of the sampling points at Werenskioldbreen together with the measurements done on September 20th 2006.

The geochemical fingerprint of the water at the terminus of Werenskioldbreen was:
^{238}U: 8.9 +/- 0.4 mBq/l; ^{234}U: 9.9 +/- 0.4 mBq/l; ^{235}U: 0.30 +/- 0.02 mBq/l
^{232}Th: 0.6 +/- 0.02 mBq/l; ^{230}Th: 0.7 +/- 0.02 mBq/l; ^{228}Th: 1.7 +/- 0.1 mBq/l
^{226}Ra: 7.6 +/- 0.7 mBq/l; ^{210}Pb: 5.5 +/- 0.7 mBq/l; ^{210}Po: 7.3 +/- 1.8 mBq/l

Conclusion

A typical temperate or polythermal glacier may be treated as a retention basin (slow drainage) hydraulically connected with channel systems (rapid drainage) with different radioactive isotopic signatures. Major natural radionuclides and especially radon give a promising investigation method of a glacier hydrological system. Methods based on continuous measurements of radon, tested in classical hydrograph separation in water catchment areas and in karsts, will be applied in future glacier studies.

References

Kies A., Hofmann H., Tosheva Z., Hoffmann L. and Pfister L., 2005:
Using 222Rn for hydrograph separation in a micro basin (Luxembourg), Annals of Geophysics, vol. 48, 101-108.

Kraemer, T. F. and Genereux, D. P. 1998. Application of uranium- and thorium-series radionuclides in catchment hydrology studies, p. 679-722. In Kendall, C. and McDonnell, J. J.: 1998. Isotope Tracers in Catchment Hydrology, Elsevier Science B.V., Amsterdam.

Pälli Anja, Moore John C., Jania Jacek, Kolondra Leszek, Glowacki Piotr, 2002: The drainage pattern of Hansbreen and Werenskioldbreen, two polythermal glaciers in Svalbard. The Changing Physical Environment, Sixth NY-Alesund International Seminar, 8-10 October 2002, 355-371.

FRIDTJOVBREEN CHANGES IN XX CENTURY FROM REMOTE SENSING DATA

IVAN I. LAVRENTIEV

Lomonosov Moscow State University, Moscow, Russia.

Fridtjovbreen (77°50’N, 14°26’E) is a 13 km long surge-type glacier in central Spitsbergen, which flows southwards into an inlet of Van Mijenfjorden. As the majority of glaciers in this region Fridtjovbreen has been retreated since the Little Ice Age. Fridtjovbreen is one among only five glaciers in Svalbard for which two surges have been observed; at Fridtjovbreen they occurred in 1860s and ~133 years later, in the 1990s, probably between 1991 and 1997 (Murray et al., 2003). At present the glacier is up to 5 km wide but narrows to 1.5 km at the glacier terminus. Fridtjovbreen is one among the many glaciers in Svalbard identified as polythermal. Such glaciers are characterized by an upper cold ice layer overlying a temperate ice layer; strong radar internal reflections from the boundary between both layers are the most striking indicator of their polythermal character.

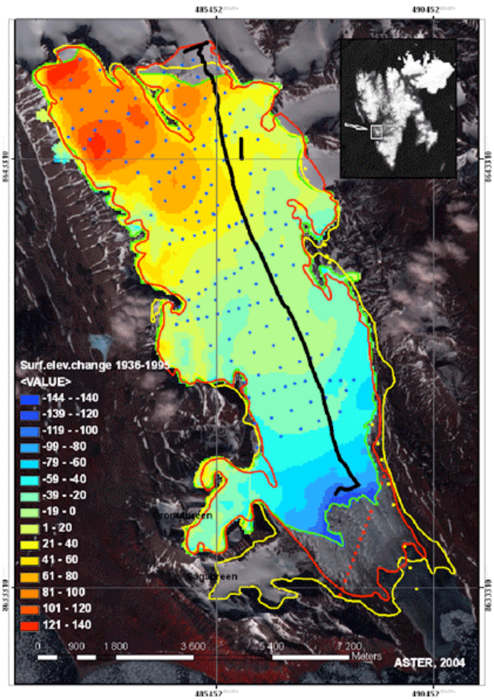

Figure 1. Map of Fridtjovbreen changes. Red, green and yellow lines shows contours of the glacier in 1936, 1995 and 2004 respectively; blue, red and yellow dots are points of RES measurements done in 1988 with 8 MHz radar, IceSat altimetry profile and points of lidar ice surface elevation measurements in 1996-2002 (Bamber et al., 2005) respectively; bold black lines is RES profiles were made in 2005 with 18 MHz radar.

This paper considers the changes in ice thickness and geometry of this glacier, as determined by comparing repeated radio-echo-sounding (RES), performed before and after its surge in the 1990s, GPS measurements and analysis of ASTER imagery and digital elevation models (DEM) of the glacier for different years before the surge, made on the base of topographic maps of Fridtjovbreen. RES measurements were made in 1988, using 8 MHz radar along the number of transversal and longitudinal profiles covering the whole glacier surface (Glazovsky et al., 1991); in 2005, using 18 MHz radar together with GPS positioning along two profiles previously measured in 1988 (at ice divide and along longitudinal profile from upper to lower part of the glacier) and along transversal profile at a distance of 2 km from the glacier calving front (Vasilenko et al., in press) (Figure 1).

Comparison of the repeated RES data shows remarkable (from -180 to +60 m) changes in ice thickness over the whole glacier area (Figure 2). The loss of ice thickness is observed in upper 8-km part of Fridtjovbreen, and it is increased in lower part of the glacier. This is typical of a surging glacier recharging its reservoir zone. Moreover, 2005 RES measurements show no internal reflected horizon (IHR) in glacier body, which had been identified in 1988. This could signify that the upper cold ice disappeared after the surging. These changes consistent with the pattern of elevation changes derived from airborne lidar data by Bamber el al. (2005) and IceSat altimetry data.

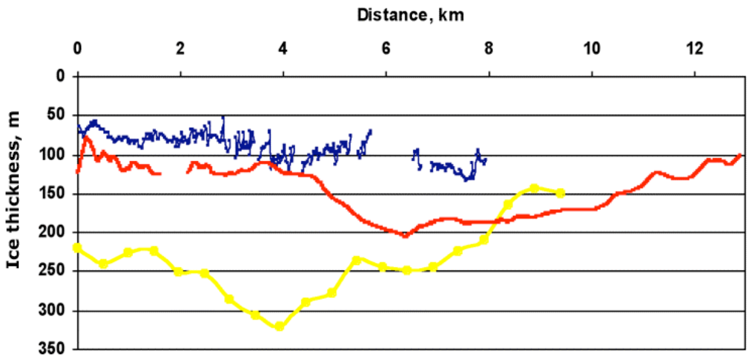

Figure 2. Ice thickness of Fridtjovbreen along a longitudinal profile. The yellow and red lines show an ice thickness in 1988 and 2005, respectively; the blue line is internal reflected horizon, which was found in 1988.

Comparison of the 1936 and 1995 DEMs shows, that Fridtjovbreen retreated up to 2200 m during this period. Changes in surface elevation with rising of surface in the upper part and reduction in central and lower part of Fridtjovbreen are shown in Figure 1**.** The glacier area was decreased up to 10 km^2 (from 55.3 km^2 to 45.3 km^2). The analysis of all data allows to calculate the volume loss in 1936-1995 as -0.97 km^3 because of the surface change and frontal retreat. Calculated mass balance was approximately - 0.33 m/y^{-1}.

Further detailed RES measurements at the whole Fridtjovbreen area are planned for spring 2007. These are expected to provide additional data to estimate the real changes in glacial geometry and hydrothermal state related with surging behaviour.

References

Bamber J.L., Krabill W., Paper V., Dowdeswell J.A., Oerlemans J. Elevation changes measured on Svalbard glaciers and ice caps from airborne lidar data. Annals of Glaciology, vol. 42, 2005, p. 202-208.

Glazovsky A.F., Konstantinova T.N.,Macheret Yu.Ya., Moskalevskiy M.Yu., Bobrova L.I., Sankina L.V. Tolshina i podledniy rel’ef lednika Fridtjof po dannim naemnoy

radiolokatsionnoy s'emki [Ice thickness and subglacial relief of Fridtjovbreen from ground-based RES studies]. Materialy glyatsiologicheskikh issledovaniy, Vol. 72, 1991, p. 161-166.
Vasilenko E.V., Glazovsky A.F., Lavrentiev I.I., Macheret Yu.Ya., Navarro F.J. Izmeneniya tolshiny i gidrotermicheskoy struktury lednika Fridtjof s 1977 po 2005 gg. [Changes in geometry and hydrothermal structure of Fridtjovbreen in 1977-2005]. Materialy glyatsiologicheskikh issledovaniy, vol. 101 (in press).
Murray T., Luckman A., Strozzi T., Nutall A.-M. The initiation of glacier surging at Fridtjovbreen, Svalbard. Annals of Glaciology, vol. 36, 2003, p. 110-116.

Preliminary results from radio-echo sounding at Ariebreen, Hornsund, Spitsbergen

F. Machío[1], J. Lapazaran[2], P. Dolnicki[3], M.Petlicki[4], P. Glowacki[4] and F. Navarro[2]

[1] Dept. Electrónica y Comunicaciones, Facultad de Ingeniería Informática, Universidad Pontificia de Salamanca, Madrid, Spain.
[2] Dept. Matemática Aplicada, ETSI de Telecomunicación, Universidad Politécnica de Madrid, Madrid, Spain.
[3] Faculty of Earth Sciences, University of Silesia, Sosnowiec, Poland.
[4] Institute of Geophysics, Polish Academy of Sciences, Warsaw, Poland.

Introduction

Ariebreen (Lat. 77º 01', Long. 15º 29') is a small valley glacier located at Hornsund, Spitsbergen (Svalbard), *ca.* 2.5 km to the west of Hornsund Polish Polar Station. The central flow line of Ariebreen follows a curved trajectory that can be approximated by three straight sections with lengths and azimuths (from glacier head to snout) 0.5 km at 42º, 0.2 km at 108º and 0.9 km at 172º, respectively.

Ariebreen area, as determined from an ortophotomap based on aerial photos taken in August 1990, was 0.52 km^2, while that determined from a satellite image (L1B ASTER) taken in August 2004 was 0.40 km^2, showing that Ariebreen has experienced a significant retreat during the recent years. Ice velocities are rather low. Summer velocities (from August to October 2006) were of the order of 1-5 cm per month in the lower and upper parts of the glacier and 15-30 cm per month in its central part. Ablation and accumulation rate measurements are underway, thus mass balance is still not determined. At the end of last ablation season (September 2006), the glacier was almost totally free of snow cover, even in the uppermost areas.

The thinning of polythermal glaciers may result in a switch to cold thermal structure under appropriate conditions. The small size of Ariebreen makes it an ideal candidate to undergo such change. Ariebreen surface is steep and is orientated to the South. Therefore it is well exposed to solar radiation and is likely sensitive to warming. The presence of a single water discharge stream makes it easy to conduct a complete hydrological investigation. Water is flowing out of this valley through a wide delta to Revdalen, where biological and geomorphological studies have been conducted for 25 years. The changes of the hydrological regime of Arieälva are expected to have an influence on Revdalen.

Ground-penetrating radar measurements

In order to determine the ice thickness and understanding the internal structure of Ariebreen we made a set of ground-penetrating radar profiles. There have been no previous radio-echo sounding measurements at Ariebreen. We made three longitudinal and three transverse profiles.

The measurements were done walking over the glacier surface using a Ramac/GPR with 200 MHz unshielded antennas, separated 0.6 m in collinear configuration, recording one trace per second, using a sampling frequency of 2012 MHz and a time window of 509 ns. This choice of time window implies that only radar returns from the uppermost 42 m of ice are recorded. The selection of the frequency and the configuration parameters was done thinking of a thin glacier where we should determine the extent and thickness of the firn layer.

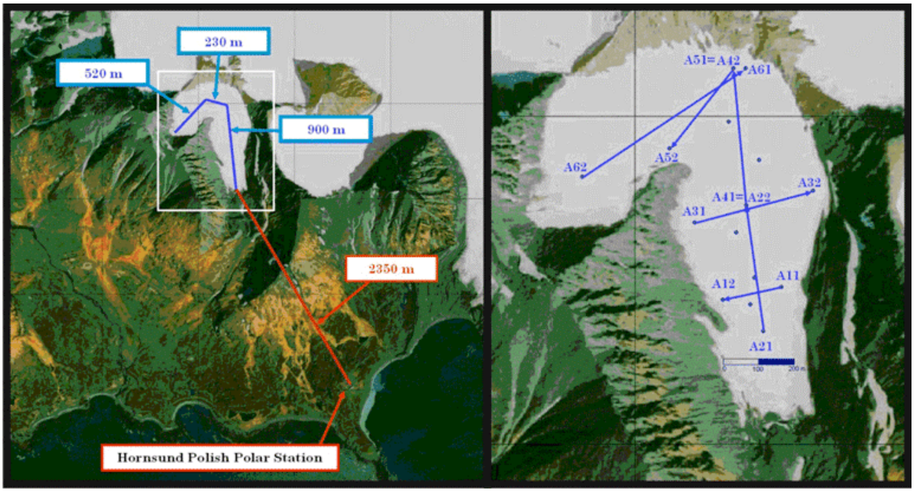

Figure 1. Location of Ariebreen in Hornsund area and schematics of the radar profiles done in August 2006.

Results and discussion

The preliminary analysis of the radar profiles shows an internal structure almost absent of endoglacial diffractions, typical of cold glaciers. This is consistent with the results from geochemical analysis. Two observations support this. First, the conductivity of water flowing out of the snout is low (6.5 μS, August 2006), similar to the conductivity of fresh snow on the glacier (*ca.* 10 μS) and much lower than the conductivity of water in Arieälva, downstream from the glacier (*ca.* 50 to 70 μS). Second, there is a very low concentration of radon in the outlet stream (September 2006). This suggests hardly any contact of the glacial water with the bedrock and therefore low subglacial drainage (Hodgkins, 1997).

The radar profiling did not reveal a firn layer, which is consistent with the absence of snow at the end of the last melting season (September 2006).

Ice thickness is typically of the order of tens of metres. The maximum depth in the transverse profile across the intermediate part of the glacier tongue is about 35 m. There is thick ice (up to 24 m) under the western lateral moraine, which covers completely the glacier surface in this area. Ice thickness larger than 40 m was detected in the northern area, where the bedrock was not reached. There might still exist a thin layer of temperate ice close to the bedrock in this part of the glacier. We expect this to be ascertained in the course of a radar survey scheduled for spring 2007.

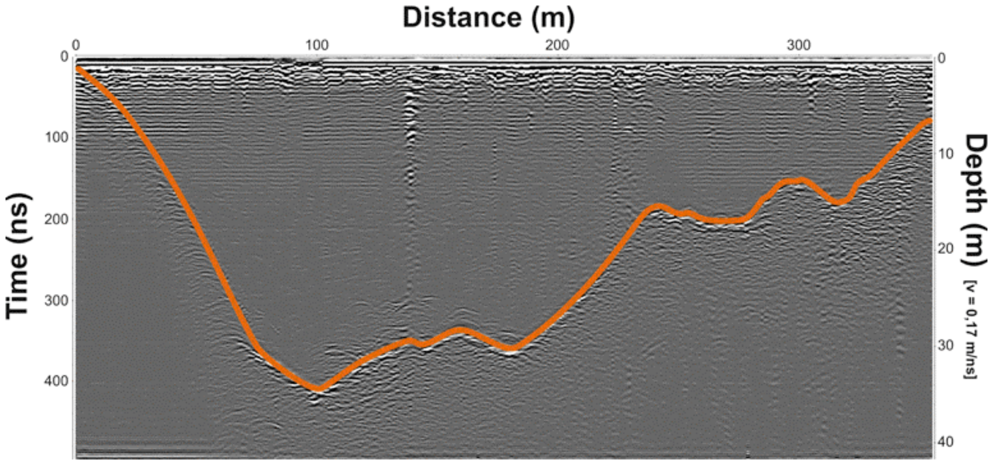

Figure 2. Profile A31-A32. The orange line represents the bedrock. Depth calculated using *v* = 0.17 m/ns.

Conclusions

- Ariebreen has recently experienced a significant retreat in a short time period: from 0.52 km^2 in August 1990 to 0.40 km^2 in August 2004.
- It shows no firn layer, which is consistent with the almost complete absence of snow at the end of the ablation season (September 06).
- Ariebreen seems to be a cold glacier. This is supported by the absence of internal reflections of radar waves throughout the full glacier, and by the evidences of absence of contact of glacial water with bedrock, deducted from the preliminary geochemical analysis.
- Only the northern part of the glacier, where the bedrock was not reached, could preserve a thin layer of temperate ice close to the bed. We hope to ascertain this during the radar survey planned for spring 2007.

References

Hodgkins, R. 1997: Glacier Hydrology in Svalbard, Norwegian High Arctic. *Quaternary Science Reviews*, Vol. **16**, 957-973

ABLATION OF HANS GLACIER (SVALBARD) ESTIMATED USING ENERGY BALANCE FROM THE AWS DATA

KRZYSZTOF MIGAŁA[1], DARIUSZ PUCZKO[2], JACEK JANIA[3] AND PIOTR GŁOWACK[2]

[1] University of Wroclaw, Institute of Geography & Regional Development, Dept. of Meteorology & Climatology
[2] Institute of Geophysics, Polish Academy of Sciences, Dept of Polar & Marine Research
[3] University of Silesia, Faculty of Earth Sciences, Chair of Geomorphology

Study area

Research was carried out on the Hans Glacier and near the Polish Polar Station of the Polish Academy of Sciences (PPS), located in South Spitsbergen, on Wedel Jarlsberg Land. Hans Glacier (Hansbreen) is a typical valley glacier, which terminates in a 50 m high cliff in the sea. It is 16 km long and on average 2.5–3 km wide. Its area is c. 56 km^2 and its thickness reaches c. 400m (Jania et al. 1996).

Methods

Meteorological measurements on the glacier, together with the ablation dynamics were carried out during three, full ablation seasons in the years 2004-2006. An AWS with Campbell CR7 was placed in the central part of ablation zone (201 m a.s.l.). Hourly values of surface ablation (sonic height ranger SR50), air temperature and humidity, wind speed and direction, total short−wave radiation, and net radiation balance including long−wave radiation were recorded. Ablation (Ae) was calculated using a formula of energy balance (after Oerlemans, 2000) and the results were compared with surface ablation (As) controlled by sonic height ranger SR50.

Results

The main results including a participation of latent heat are summarized in Table1 and Figure 1.

Table 1. Ablation of Hans Glacier in the years 2004-2006.

	2004	2005	2006
duration (days)	86	97	102
PDD (Σ T >°C)	212,5	218,5	180,5
Total ablation			
As (Σ cm)	271,9	244,8	256,6
Ae (Σ cm w.e.)	146,3	101,8	93,2
A, total by glacier stakes (Σ cm w.e.)	148,0	119,0	94,0
evaporation (cm w.e.)	0,38	0,34	0,72
water income by condensation (cm w.e.)	1,6	1,05	0,86
contribution of melting by heat of condensation (cm w.e.)	12,0	7,8	6,4
Daily rate (cm d^{-1})			
avg As	3,2	2,5	2,5
avg Ae	1,7	1,71	0,9
max As	19,3	7,8	12,7
max Ae	4,5	2,9	2,3

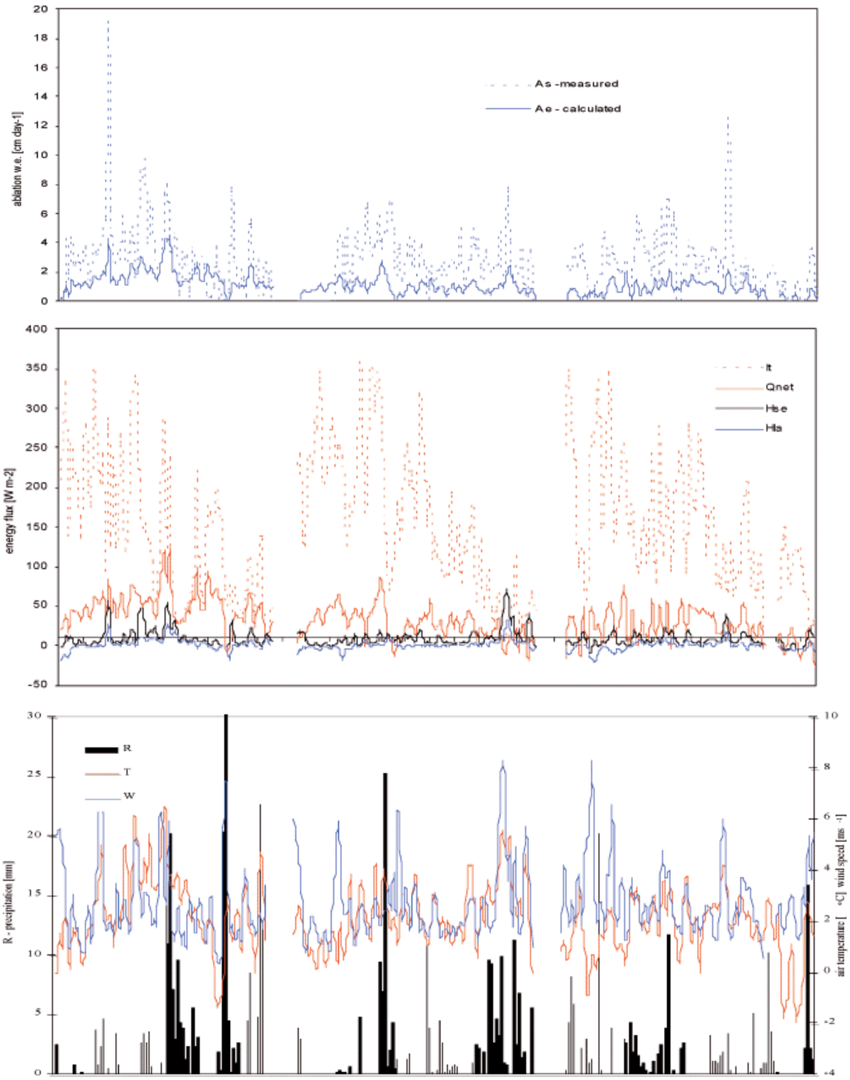

Figure 1. (a) daily ablation, (b) components of energy balance (It – shortwave total radiation, Qnet – net radiation, Hse – sensible heat flux, Hla – latent heat flux) and (c) air temperature (T), wind speed (W) , precipitation (R) in the years 2004, 2005 and 2006.

Statistical analysis showed a significant correlation between ablation and air temperature on AWS (especially maximum daily temperature) and mean daily wind velocity (Table 2 and 3). Also, the relationship with air temperature recorded at the PPS is significant. The influence of radiation balance and precipitation on the average seasonal ablation is less important; however, these values are quite significant in episodes of an extreme nature. The weak correlation between ablation and net radiation displays the considerable role of other contributions to the ablation energy balance, i.e. turbulent sensible and latent heat flux. Their influence is indirectly shown by the clear correlation between temperature and air temperature as well as wind velocity, which can be explained by detailed structure of energy balance. In the case of precipitation as a result of advection melting, the amount of heat proportional to the mass of rain precipitation and supplied to snow should be taken into account.

Table 2. Statistical relationship between daily values of surface ablation (As) and some meteorological parameters.

Parameter	Pearson's correlation coefficient (R)
air temperature (at AWS)	0,60
air humidity (at AWS)	0,04
vapour pressure (at AWS)	0,49
wind speed (at AWS)	0,38
mean intensity of total radiation (at AWS)	0,12
mean of net radiation (at AWS)	0,27
sensible heat flux (at AWS)	0,64
latent heat flux of evaporation / condensation (at AWS)	0,56
sum of precipitation (at PPS)	0,17

Table 3. Statistical relationship between daily values of ablation (Ae) calculated from a formula of energy balance and some meteorological parameters.

Parameter	Pearson's correlation coefficient (R)
air temperature (at AWS)	0,58
air humidity (at AWS)	-0,01
vapour pressure (at AWS)	0,45
wind speed (at AWS)	0,20
mean intensity of total radiation (at AWS)	0,27
mean of net radiation (at AWS)	0,84

A correct evaluation of the ablation rate is often problematic because of the paucity of meteorological measurements on a glacier. Therefore, an evaluation can be based on the model, which includes totals of positive daily air temperatures (Krenke and Khodakov 1966; Braithwaite 1995, Migała et al. 2006). The use of cumulative values for the whole ablation season (daily ablation and totals of positive air temperature) gives satisfactory results, even if only data from the PPS are included. Good correlations enable to construct the polynomial formulas:

$$A = -0{,}0002 * (\Sigma\ T_{max}AWS)^2 + 0{,}4791 * \Sigma\ T_{max}AWS + 2{,}1723, \text{ with } R = 0{,}99$$
$$A = -0{,}0002 * (\Sigma\ T_{max}PPS)^2 + 0{,}3873 * \Sigma\ T_{max}PPS - 0{,}2698, \text{ with } R = 0{,}99$$

where:
A – water equivalent of ablation (cm w.e.], $T_{max}AWS$ and $T_{max}PPS$ – daily maximum of air temperature in Polish Polar Station (PPS) and on the Hans Glacier (AWS).

The comparison of mean values for the glacier (ablation measured by stakes) with the data calculated for the zone of 200 – 220 m a.s.l.) leads to the conclusion that the monitored zone represent general weather conditions responsible for the ablation processes on the Hans Glacier (Figure 2).

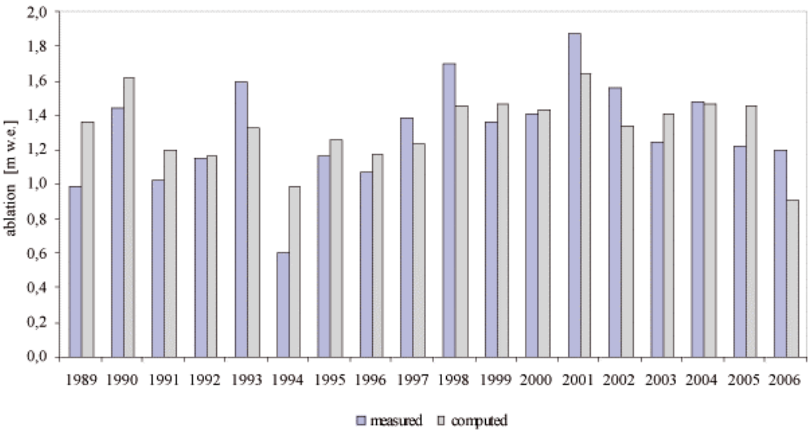

Figure 2. Mean water equivalent of ablation of the glacier (measured by all stakes) and calculated for the zone of 200-220 m a.s.l. for the years 1989 – 2006.

Conclusions

Both statistical significance of air temperature and high contribution of heat of condensation in melting (7-8%) indicate the importance of the air mass advections concerned with local / regional character of climate and its impact on the glaciological processes. The results confirm also, that air temperature is a satisfactory parameter to study interannual variability of ablation. The results indicate that zone of 220-220 m a.s.l. represents general weather conditions responsible for melting processes on the Hans Glacier.

Acknowledgements

Studies were supported by the grant of the Ministry of Science and Higher Education (No PBZ – KBN-108/P04/2004). Assistance of the crew of the Polish Polar Station, Hornsund is greatly appreciated and with special regards for colleagues from 28th, 29th and 30th expeditions.

References

Braithwaite R.J. 1995. Positive degree−day factors for ablation on the Greenland ice sheet studiedby energy−balance modeling. Journal of Glaciology 41 (137): 153–160.

Jania J., Mochnacki D., Gądek B.,1996. The thermal structure of Hansbreen, a tidewater glacier in southern Spitsbergen, Svalbard. Polar Research 15 (1): 53–66.

Krenke A.N., Khodakov V.G. 1966. O svyasi povercknostnogo tayaniya lednikov s temperaturoy vozdukha (On the relationship between melt of glaciers and air temperature). Materialy Glyatsiologicheskikh Issledovaniy 12: 153–163 (in Russian).

Migała K., Piwowar B.A., Puczko D., 2006, A meteorological study of the ablation process on Hans Glacier, SW Spitsbergen, Polish Polar research, 27, 3: 243 – 258.

A NEW DEM OVER AUSTFONNA ICE CAP FROM SAR INTERFEROMETRY, ICESAT ALTIMETRY AND GPS GROUND PROFILES

Geir Moholdt[1], Trond Eiken[1], Jon Ove Hagen[1], Andreas Kääb[1], Even Loe[1], Thomas V. Schuler[1], and Andrea Taurisano[2]

[1] Department of Geosciences, University of Oslo, Norway.
[2] Previously at Norwegian Polar Institute, Tromsø, Norway; now at Multiconsult AS, Tromsø, Norway

Introduction

Most digital elevation models (DEM) on land are made from stereo photogrammetry. Large glaciers and ice caps, however, are difficult to map accurately because of poor contrast in aerial photos. DEMs of Antarctica and Greenland have been made primarily from satellite altimetry. This technique is often not appropriate for smaller ice caps with sloping surfaces and rugged marginal zones.

The most extensive elevation dataset covering Austfonna is from the 1983 airborne radio echo sounding (RES) campaign carried out by the Norwegian Polar Institute (NP) and Scott Polar Research Institute (SPRI) (Dowdeswell et al., 1986). These data were used by NP to improve their maps and DEMs. Since that, others have attempted to make DEMs over Austfonna based on SAR-interferometry (Unwin and Wingham, 1997) and shape-from shading (Bingham and Rees, 1999). In lack of more recent ground control points, both of these DEMs were tied to the RES profiles of 1983.

Ground GPS-profiles and ICESat's laser altimeter reveal elevation differences of up to +/- 40 m with regards to previous DEMs. The deviations are systematically distributed indicating thickening in the interior and thinning towards the margins. This is a typical pattern for surge type glaciers, which many of Austfonna's drainage basins are known to be. The build-up trend is confirmed by airborne laser altimetry in 1996 and 2002 (Bamber et al., 2004), ice flux studies from SAR-Interferometry (Bevan et al., in press) and from GPS ground profiles (Eiken et al., 1997) between 1999 and 2006. A new DEM will be a useful tool for future studies of geometric change, and for the ongoing research that culminate in the IPY GLACIODYN project.

Method

This work aims to construct a more up to date DEM by combining the good spatial coverage of SAR-interferometry with accurate, but sparsely distributed surface elevations from ICESat's laser altimeter and GPS ground profiles. Recent elevations from ICESat and GPS are used as tie-points for a DEM derived from differential SAR interferometry. In this process, the topographic phase is isolated from the displacement phase by subtracting two interferograms formed by two pairs of coherent repeat-pass SAR scenes (Kwok and Fahnestock, 1996).

Because of rapid coherence loss and the long repeat time of present SAR-satellites, it is necessary to use SAR-scenes from the ice phases of ERS1 in 1992/94 (3 day repeat) or the tandem phase of ERS1/ERS2 in 1996 (1 day repeat). Thus, we have to assume that the small scale shape of the basins have been more or less stable from that time until today. Possible surge-like activity during this period (e.g. Dowdeswell et al., 1999) has to be considered carefully.

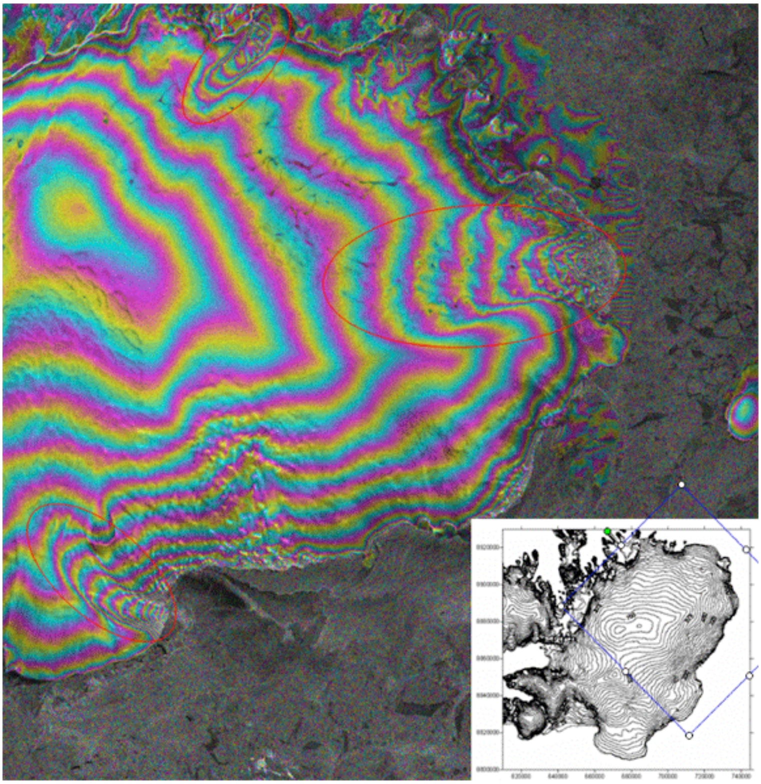

Figure 1. Interferogram of eastern Austfonna generated from ERS1/ERS2 tandem SAR scenes from 7/8 November 1995. Inset is the SAR image frame plotted on a contour map of Austfonna. The fringe pattern corresponds fairly well to the topography except from a few units of pronounced glacier flow (marked in red).

Processing is carried out in the Gamma Remote Sensing software. We use a 4 pass approach that consists of the following steps:

- Offset estimation between SLC image pairs (Img.$_1$ vs. Img.$_2$, and Img.$_3$ vs. Img.$_4$)
- Baseline estimation from precise Delft orbit data
- Generation of multilook interferograms (Int.$_{1,2}$ and Int.$_{3,4}$)
- Removal of the “flat earth” phase trend from the interferograms (Figure 1)
- Filtering and phase unwrapping of the interferograms
- Coregistration of the interferograms to same geometry
- Topographic phase isolation by interferogram subtraction (Int.$_{topo}$ = Int.$_{1,2}$ – Int.$_{3,4}$)

- Geocoding and baseline refinement using gound control points from ICESat and GPS
- Phase-to-height transformation and resampling into a DEM

A new glacier outline digitized from Landsat imagery will serve as the outer boundary of the DEM. The quality of the DEM will be validated by comparing DEM elevations with independent datasets obtained from ICESat and GPS ground profiles.

References

Bamber, J., W. Krabill, V. Raper and J. Dowdeswell. 2004. Anomalous recent growth of a part of a large Arctic ice cap: Austfonna, Svalbard. *Geophys. Res. Lett.*, 31, L12402.

Bevan, S., A. Luckman and T. Murray. In press. Positive mass balance during the late 20th century on Austfonna, Svalbard revealed using satellite radar interferometry. Annals of Glaciology, 46.

Bingham, A. W., and W. G. Rees. 1999. Construction of a high-resolution DEM of an Arctic ice cap using shape-from-shading. *Int. J. Remote Sensing,* 20, 3231-3242.

Dowdeswell, J. A., D.J. Drewry, A. P. R. Cooper, M. R. Gorman, O. Liestøl and O. Orheim. 1986. Digital mapping of Nordaustlandet ice caps from airborne geophysical investigations. *Annals of Glaciology, 8, 51-58.*

Dowdeswell, J. A., B. Unwin, A. M. Nuttal and D. J. Wingham. 1999. Velocity structure, flow instability and mass flux on a large Arctic ice cap from satellite radar interferometry. *Earth Planet. Sci. Lett.,* 8, 51-58.

Eiken, T., J.O. Hagen and K. Melvold. 1997. Kinematic survey of geometry changes on Svalbard glaciers. *Annals of Glaciology*, 24, 157-163.

Kwok, R. and M. A. Fahnestock. 1996. Ice sheet motion and topography from radar interferometry. *IEEE Transactions on Geoscience and Remote Sensing,* 34:1, 189-200.

Unwin, B. V. and D. J. Wingham. 1997. Topography and dynamics of austfonna, Svalbard, from SAR interferometry. *Annals of Glaciology,* 24, 403-408.

GLACIER-CLIMATE INTERACTIONS IN ARCTIC ALASKA

MATT NOLAN AND JASON GECK

University of Alaska Fairbanks, Fairbanks, Alaska, USA.

Due to the lack of long-term climate measurements throughout arctic Alaska, we are using glaciers and climate reanalysis models as proxies to understand recent climate trends here.

Our primary glacier study area is McCall Glacier, in the eastern Brooks Range. Here we have field data dating back nearly 50 years. Analysis of mass balance trends shows that the annual equilibrium line has been steadily rising over this time period, and in some recent years there has been no surface accumulation at all with substantial loss of firn. This long-term negative mass balance has led to significant volume loss, with the rate of loss increasing in time.

We have only just begun a project to measure volume change of all arctic glaciers here from roughly the 1950s to present, by differencing digital elevation models. Results thus far show that volume loss is widespread, though we do not yet have enough information to determine whether spatial variations in rate exist. Mean glacier elevations decrease substantial towards the west, from highs of over 2000 m near McCall Glacier to less than 1500 m in the west, indicating that there are substantial climate differences here.

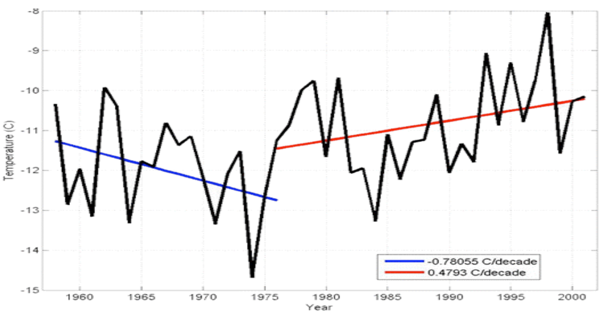

Figure 1. Analysis of ERA40 mean annual air temperatures (MAAT) at McCall Glacier. A) MAAT at McCall Glacier. Note the large jump in temperatures around 1976.

We looked at ERA40 surface variables to assess whether any trends in air temperature were observed there. We found that while air temperatures in general have increased in the Arctic between 1958 and 2001, that the general year-to-year trend for Alaska was cooling, except after 1976 in the arctic region. Around 1976, air temperatures in Alaska jumped by over 5 degrees over a several year period, compared to only about 2 degrees for the entire 1958-2001 record. The explanation for the sudden jump seems to come from an increase in strength of the Aleutian low pressure systems at this time, which brings warm air up across Alaska from the south. From these analyses, it would seem that decadal-scale shifts in weather patterns have a stronger influence on Alaskan air temperatures than does the long-term trend due to global warming. Further, Arctic Alaska responds differently than the rest of the state. Given that these results are based on model output and not real station data, caution is required when applying them to the real world. Comparisons with real station data are ongoing.

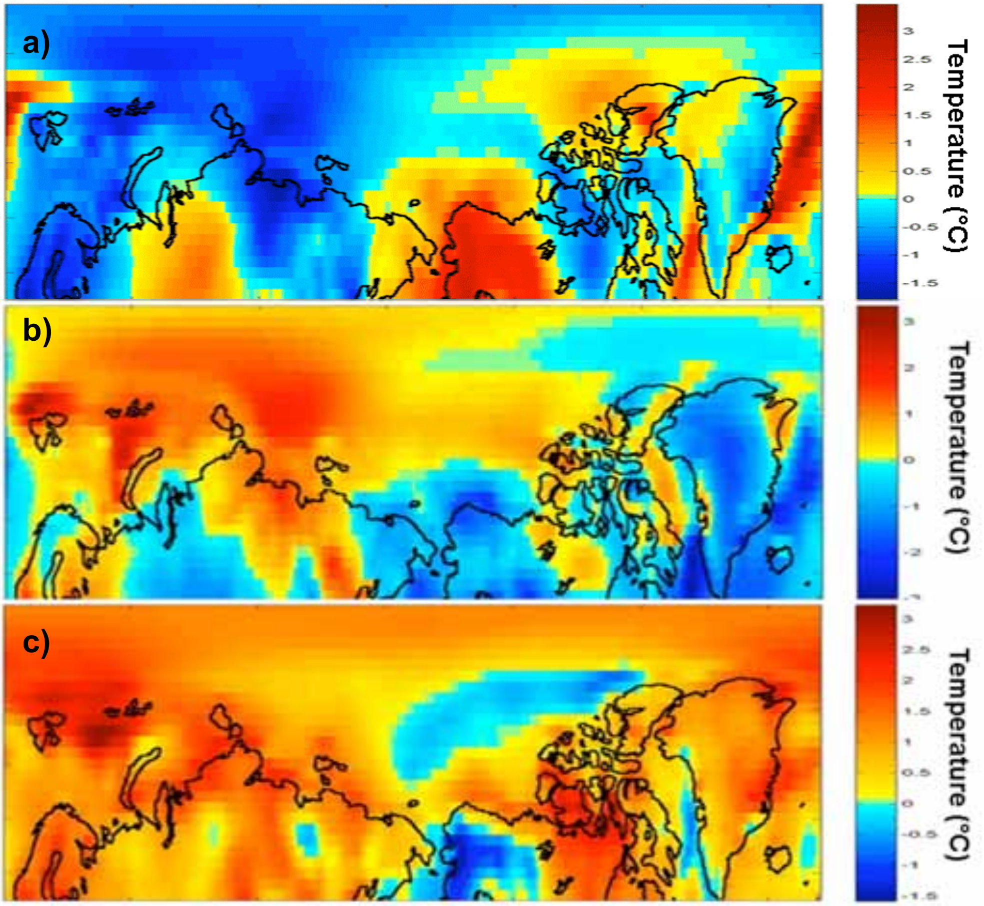

Figure 2. Analysis of ERA40 mean annual air temperatures (MAAT, in °C). a) The difference in MAAT trend lines before and after 1976 (as in Figure 1) for all nodes north of 60N. Note that Alaska stands out as being strongly affected by temperature at this time. The change in Greenland is a trend-line artifact due to an earlier warming in the late 1960s. b) The trend MAAT from 1958-1976. Note that all of Alaska cooled during this period. c) The trend in MAAT from 1976-2001. Note that most of Alaska continued to cool during this period, except for the arctic region.

SIMULATION OF THE TURBULENT FLUXES AT SUMMIT, GREENLAND

FRIEDRICH OBLEITNER[1], NICOLAS J. CULLEN[2] AND KONRAD STEFFEN[3]

[1] Institute for Meteorology and Geophysics, University of Innsbruck, Innsbruck, Austria.
[2] Department of Geography, University of Otago, Dunedin, New Zealand.
[3] Cooperative Institute for Research in Environmental Sciences, University of Colorado, Boulder, USA.

Introduction

The interpretation of geophysical data from ice core records largely depends on establishing a quantitative understanding of the structure of the surface boundary layer at the site. Energy balance exchanges play an essential role in this context, linking regional scale atmospheric flow with the near surface snow layers. Recent measurements at the summit of the Greenland ice sheet (72.58N, 34.46W, 3202m asl.) revealed that during summer the turbulent fluxes of sensible and latent heat are frequently directed away from the surface. Similar characteristics have been reported by Obleitner (1995), Albert and Hawley (2000), Box and Steffen (2001) and Schelander et al. (2003). Moreover, there are strong indications that the feature may be common in the interior Antarctic plateau as well (Van As et al., 2005; Argentini et al., 2005). These findings raised important questions about the persistence and structure of the stably stratified surface layer in the interior of the Greenland ice sheet, as well as the underlying snow pack. In this paper we verify the seasonal evolution of the heat and vapour fluxes using a numerical snow model.

Data

A well supported infrastructure at Summit, Greenland has enabled extended meteorologically oriented field experiments to be conducted at this site. One of the exiting outcomes of these experiments was the finding of frequently unstable atmospheric conditions during summer. The evidence is based on independent data from profile measurements, direct flux measurements and atmospheric soundings. Notably, Cullen (2003) has documented a good agreement of turbulent fluxes calculated from turbulence measurements and profile data using different parameterizations, respectively. In this paper we use data collected between July 2000 and July 2001. The data collection and instrumentation is thoroughly described by Cullen and Steffen (2001) and Cullen et al. 2007.

Net radiation is the basic input to the surface energy balance. On average, sensible heat flux accounts for 63% of the radiative losses, while latent heat and conductive fluxes are small but also directed to the surface (Table 1). Unstable atmospheric conditions (negative sensible heat fluxes) occur from May to August, when net radiation is positive. There is an associated prevalence of heat loss due to sublimation from the surface and conduction into the deeper layers of the snow pack. The residual quantifies diverse uncertainties due to measurement and parameterisation problems (Cullen, 2003).

Table 1. Mean monthly energy balance components (Wm^{-2}) measured at the Greenland summit. Positive values denote a gain to the surface.

	JUL	AUG	SEP	OCT	NOV	DEC	JAN	FEB	MAR	APR	MAY	JUN	YEAR
Net radiation	15.2	8.3	-1.9	-18.6	-17.7	-20.0	-20.8	-22.2	-13.3	-2.0	6.6	15.1	-5.9
Sensible heat flux	-7.9	-5.1	2.0	7.4	10.2	12.1	12.2	12.5	6.5	2.0	-1.5	-6.3	3.7
Latent heat flux	-2.5	-2.0	-0.2	2.7	2.9	1.9	2.4	2.2	2.1	1.7	-0.7	-1.6	0.8
Conduction	-2.2	-1.2	0.5	3.5	2.8	3.0	2.1	2.6	3.1	0.7	-0.5	-1.6	1.1
Residual	2.6	-0.1	0.4	-4.9	-1.8	-3.1	-4.2	-4.8	-1.6	2.4	3.9	5.6	-0.5

Simulations

The available measurement data provide a solid basis for associated model studies. The numerical snow model SNTHERM (Jordan, 1991) is used to simulate the seasonal evolution of the near surface snow layers and their interaction with the atmosphere aloft. From a methodological point of view this modelling study benefits from high quality input and validating data as well as from the homogeneous measurement and dry snow conditions. The model is driven by mean hourly meteorological parameters and initialized using snow temperature and density profiles derived from snow pit measurements. The model is set up using a temperature and wind dependent parameterization for fresh snow density (Jordan, 1991), while heat conductivity and absorbed solar radiation are parameterized according to Sturm et al., (1997) and Meirold-Mautner (2004), respectively. The model's parameterization of the turbulent heat fluxes is based on Andreas (1987) and Högstrom (1988), respectively. The simulations are verified by hourly snow temperature profiles down to 10m below the surface, snow pit data in June 2001 and continuous summer time eddy correlation measurements of the turbulent heat fluxes.

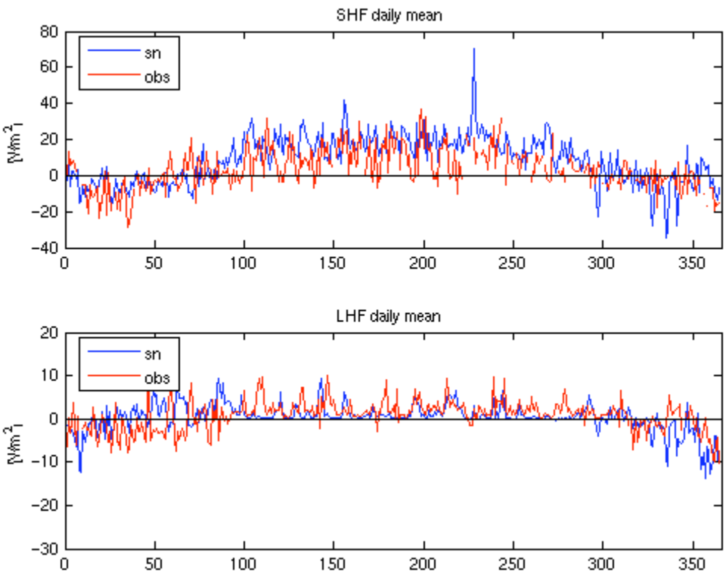

Figure 1. Daily means of measured (eddy correlation) and simulated (Sntherm) fluxes of sensible (a) and latent heat (b). Positive values denote a gain to the surface.

The model results confirm that net radiation is positive during summer (June to August). Most of the inherent amount of energy is absorbed within a relatively shallow snow layer. Heat conduction into the deeper layers is not able to effectively redistribute this energy surplus. Therefore, the energy surplus is directed away from the surface via the sensible and latent heat fluxes. Figure 1 demonstrates the skill of the model to reproduce the seasonal evolution of the directly measured turbulent heat fluxes. The overall negative sensible heat flux is responsible for the frequently unstable surface layer that is observed in summer. The negative latent heat fluxes result in mass loss through sublimation during summer. In contrast, net radiation is negative during polar night conditions, which is mainly compensated by turbulent fluxes directed towards the surface. This results in an overall stably stratified atmosphere and positive turbulent fluxes, which is normally associated with polar ice sheet surfaces.

Summary

Recent year-round meteorological experiments at Summit, Greenland, which is near the top of the ice sheet, revealed a striking reversal of the sign of the turbulent fluxes of sensible and latent heat. Notably, there is the occurrence of frequently unstable atmospheric conditions during summer (May to August). A one-dimensional snow model has been used to simulate the processes within the near surface snow pack. The simulations are verified by independent measurements of snow surface temperature, vertical profiles of snow temperature and density. A comparison of calculated and directly measured turbulent fluxes demonstrates the high skill of the model. Consideration of the inherent processes indicates that the development of unstable atmospheric stratification during summer is strongly related to the low effective conductivity of the near surface snow layers. This limits the ability of the snow to redistribute the radiation energy surplus, which is absorbed within a relatively shallow layer. This is compensated by sensible and latent heat fluxes directed away from the surface.
The seasonal changes of the stratification of the atmosphere must have important consequences on the development of katabatic flow at Summit and its surrounding regions, as well as on the transfer of atmospheric chemical species at the snow/air interface. A more detailed analysis of the snow modeling results will contribute to a better understanding of these issues.

References

Albert, M.R. and Hawley, R.L., 2000. Seasonal differences in surface energy exchange and accumulation at Summit, Greenland., Ann. Glaciol. 31, 387-390.

Andreas E., 1987: A theory for the scalar roughness and the scalar transfer coefficients over snow and sea ice, Boundary-Layer Meteorol., 38, 150-184.

Argentini S., A. Viola, A. M. Sempreviva and I. Petenko, 2005: Summer boundary-layer height at the plateau site of Dome'C, Antarctica, Boundary-Layer Meteorology 115, 3, 409-422.

Box, J.E. and K. Steffen, 2001: Sublimation estimates for the Greenland ice sheet using automated weather station observations, J. Geophys. Res., 106(D24), 33965-33982.

Cullen, N.J, and K. Steffen, 2001: Unstable near-surface boundary conditions in summer on top of the Greenland ice sheet, Geoph. Res. Letters, 28 (23), 4491-4494, 2001.

Cullen N.J, 2003: Characterisation of the Atmospheric boundary layer at summit, Greenland, PhD, Univ. Boulder, USA, 146pp.

Cullen, N.J., Steffen, K., and Blanken, P.D. 2007: Nonstationarity of turbulent heat fluxes at Summit, Greenland. Boundary-Layer Meteorol., 122, 439-455, doi: 10.1007/s10546-006-9112-2.
Högström U.: 1988: Non-Dimensional Wind and Temperature Profiles in the Atmospheric Surface Layer: A Re-Evaluation, Boundary- Layer Meteorol. 42, 55-78.
Jordan R., 1991: A one-dimensional temperature model for a snowcover, CRELL Spec. Rep., 91-116.
Maurold-Meitner I., 2004: A physical snow radiation model, PhD, Innsbruck Univ., 122pp.
Obleitner F. and Olesen O. 1995: An evaluation of the energy budget at the summit of the Greenland ice cap, in: Mass balance and related topics of the Greenland Ice Sheet, Open File Series 95/5, Geological Survey of Greenland, 33-43.
Schelander, P., Ohmura, A., Calanca, P., 2003: Seasonal variability of the boundary layer structure at
Summit, Greenland. JSM16/O4A/C31-003, IUGG, Sapporo, Japan.
Sturm M., Holmgren J., König M, and Morris K., 1997: The thermal conductivity of seasonal snow, Journal of Glaciol., 43, 143, 26-41.
Van As, D., Van den Broeke, M. R., Van de Wal, R. S. W., and Reijmer, C. H.: 2005, The summer surface energy balance of the high Antarctic plateau, Boundary-Layer Meteorol. 115, 289-317.

THE IMPACT OF VOLCANIC AND GEOTHERMAL ACTIVITY ON THE MASS BALANCE OF VATNAJÖKULL

FINNUR PÁLSSON, SVERRIR GUÐMUNDSSON, AND HELGI BJÖRNSSON

Institute of Earth Sciences, University of Iceland, Reykjavík, ICELAND

Introduction

About 60 % of glaciers in Iceland are underlain by an active volcanic zone (Figure 1). Ice is continuously melted at a few subglacial geothermal areas (Figure 2) and occasionally during short-lived eruptions. In about 4 % of the area of Vatnajökull ice cap (8100 km^2) geothermal activity eternally affects the ice flow and basal drainage of meltwater. During the period 1992 to 2005, more than 90% of the ablation within these areas was basal melting while less than 10% of the melting took place during two volcanic eruptions (1996 and 1998). Volcanic eruptions in the entire volcanic zone have permanently amplified the glacier surface ablation through the dispersal of tephra over the glaciers, maintaining albedo as low as 0.1 in the ablation areas; rarely they insulate the glacier and prevent melting. Increased net short-wave radiation considerably increased the summer melting after the two most recent eruptions in Vatnajökull (in 1997 and 1999). Looking at the entire Vatnajökull ice cap over the period 1992 to 2005 basal melting comprised only 3% of the total ablation.

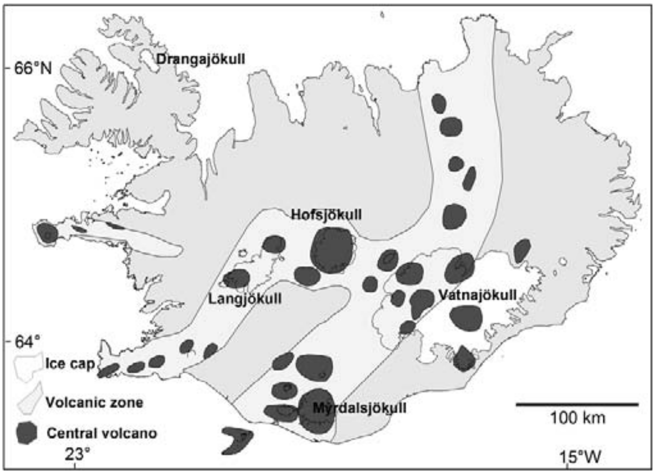

Figure 1. Map of Iceland.

Melting at subglacial geothermal areas

Ice is continuously melted at the glacier bed creating permanent depressions in the glacier surface that reveal hydrothermal activity (Figure 2; Björnsson, 1988). The surface depressions tend to be gradually reduced by inflow of ice. The meltwater may be trapped in a lake at the bed due to relatively low basal fluid potential under the depression. High overburden pressure at the rim around the depression seals the lake.

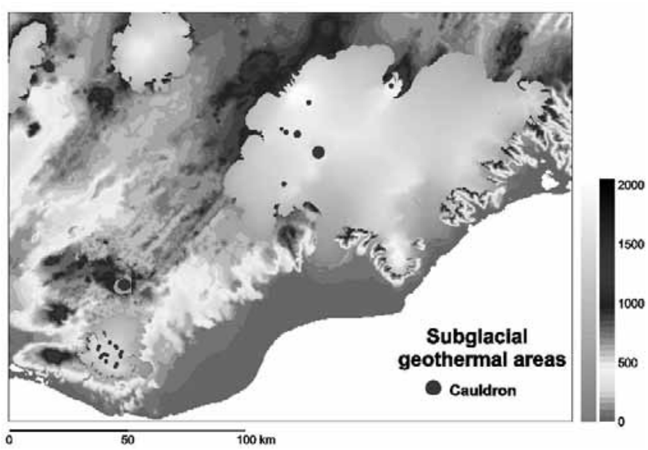

Figure 2. Subglacial geothermal areas.

Melting in subglacial eruptions

There are several active volcanic systems beneath Vatnajökull ice cap (Figure 3). Research of the tephra layers cropping out of the ice in the glacier ablation zone yields a minimum of 86 eruptions the past 800 years (Larsen et al., 1998). The Grímsvötn caldera and vicinity is the most active eruption site, and has erupted 8 times the past 100 years. In 1938 and 1996 eruption´s in Gjálp north of Grímsvötn melted 3-4 km3, but recent eruptions within the Grímsvötn caldera have melted about 0.1 km^3 or less (Björnsson, 1988; Björnsson et al., 1993; Guðmundsson et al., 2004). Small subglacial eruptions may not melt through the ice, and are therefore not seen in the tephrochronical record. On average we estimate eruptions melting 0.05 km^3a^{-1}.

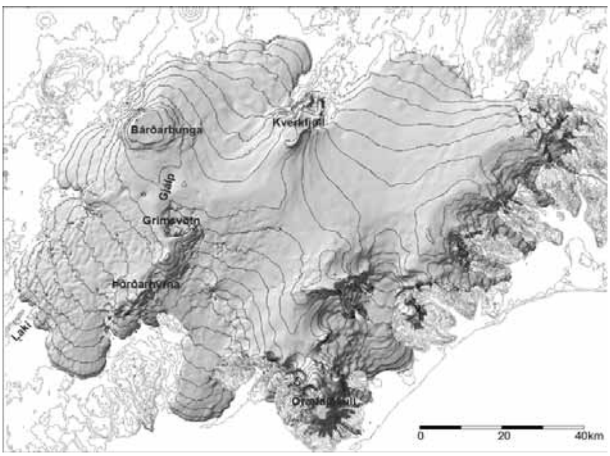

Figure 3. Location of subglacial volcanoes.

Enhanced melting due to volcanic tephra and dust

Volcanic ash is spread aerially over large areas. Depending on wind direction during eruption, Vatnajökull may be partially or totally covered with volcanic ash from eruptions within or outside the glacier. In the ablation zone most of the particles will wash off in the next melting season. In the accumulation area the tephra cover gets buried and turns up again few hundred years later in the ablation zone.

Mass balance for the outlets of Vatnajökull has been monitored since 1991-92 (Björnsson et al., 1998; 2003), and automatic weather station (AWS) have been operated since 1996 for surface full energy balance estimation (Figure 4; Guðmundsson et al., 2006). The AWS and mass balance data has been used for spatial modelling of the surface energy balance and melting. The energy contribution from short wave radiation is on average about 70-80%, long wave radiation contribution is small and turbulent heat fluxes contribute about 20-30%.

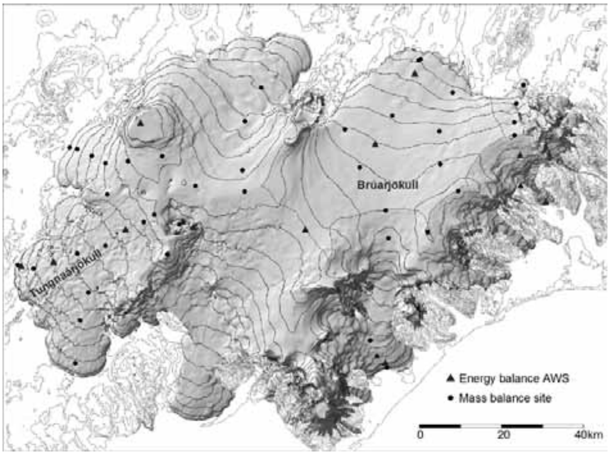

Figure 4. Mass and energy balance observation sites.

Volcanic debris cropping out in the ablation zone lowers the albedo considerably. Values as low as 0.1 are measured, whereas typical values of albedo for pure ice are about 0.4. For evaluating the impact of low albedo we run spatial energy balance models for the outlet glaciers Brúarjökull and Tungnaárjökull (Figure 4; Guðmundsson et al., 2006) for different assumed minimum values of albedo (Figures 5 and 6). Changing the dirty ablation zone to pure ice results in about 13% less total ablation (up to about 20-25% in the ablation zone). The low albedo in the ablation zone highly affects the long term mass balance of Vatnajökull (Figure 6). Clean ice would result in Brúarjökull being in a long term mass equilibrium instead of fast shrinkage.

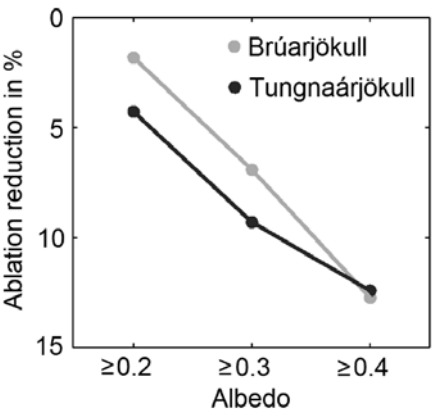

Figure 5. Ablation reduction with increased albedo for ice, relative to observed.

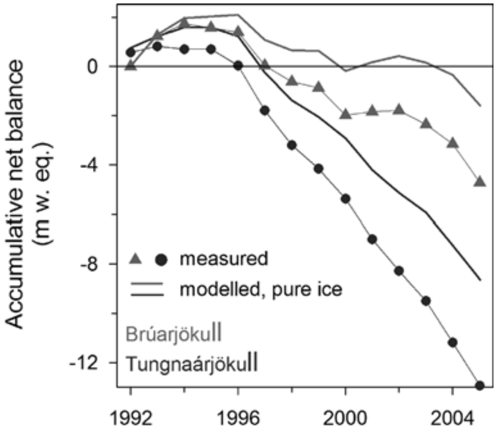

Figure 6. Measured mass balance, compared to that resulting from surface energy balance models when assuming clean ice surface in the ablation zone.

Concluding discussion

The short term effect of volcanic activity on the mass balance of glaciers are direct melting in subglacial eruptions, melting during cooling of a volcanic edifice and one or a few seasons of increased melt due to exposed volcanic ash. This may control the mass balance in close vicinity of the volcano for a few years, but has little effect on the long term mass balance of the ice cap (Table 1).

The long term effects are basal melting in geothermal areas, and enhanced melting in the ablation zone where volcanic ash layers crop out of the ice and increase absorption of short wave radiation. In drainage basins presently containing geothermal areas 90% of the ablation is due to basal melting. The enhanced melting due to volcanic ash is in the order of 10% of the total melting (Table 1) and has significant impact on the mass balance of the ice cap.

Despite geothermal and volcanic influence on Vatnajökull the mass balance reflects meteorological conditions (Table 1), and the ice cap can be used as a laboratory for study of climate variations.

Table 1. Melting rates of Vatnajökull late 20th century.

	Surface ablation km^3a^{-1}	Geothermal systems km^3a^{-1}	Volcanic eruptions km^3a^{-1}
Vatnajökull			
8200 km^2	20	0.5	0.05
3100 km^2	(3)*		
Geothermal areas			
200 km^2	0.5	0.5	0.05

* Contribution from volcanic ash reducing the albedo

Acknowledgement

We acknowledge the support of the National Power Company of Iceland, European Union (Framework V, projects TEMBA, ICE-MASS and SPICE), the Public Roads Administration, Rannís, Iceland University Research Fund and Iceland Glaciological Society for help in field work.

References

Björnsson H., 1988. Hydrology of ice caps in volcanic regions. Societas scientarium Islandica.

Björnsson H., Guðmundsson M.T., 1993. Variations in the thermal output of the subglacial Grímsvötn caldera, Iceland. Geophysical research letters, 20.

Björnsson, H., F. Pálsson, M.T. Gudmundsson and H.H. Haraldsson, 1998. Mass balance of western and northern Vatnajökull, Iceland, 1991-1995. Jökull, 45, pp. 35-58.

Björnsson, H, F. Pálsson and H.H. Haraldsson. 2003. Mass balance of Vatnajökull (1991-2001) and Langjökull (1996-2001), Iceland. Jökull, 53, pp. 75-78.

Guðmundsson M.T., Sigmundsson F., Björnsson H. and Högnadóttir Th., 2004. The 1996 eruption of Gjálp, Vatnajökull ice cap, Iceland: efficiency of heat transform, ice deformation and subglacial water pressure. Bulletin of Volcanology, 66.

Guðmundsson S., Björnsson H., Pálsson F. and Haraldsson H.H., 2006. Energy balance of Brúarjökull and circumstances leading to the August 2004 floods in the river Jökla, N-Vatnajökull. Jökull 55.

Larsen G., Guðmundsson M.T., Björnsson H., 1998. Eight centuries of periodic volcanism at the center of the Iceland hotspot revealed by glacier tephrostratigraphy. Geology.

Zóphóníasson S., 2002. Rennsli í Skaftárhlaupum 1955-2002. National Energy Authority report.

VARIATIONS IN MASS BALANCE AND SNOW AND FIRN DENSITIES ALONG A TRANSECT IN THE PERCOLATION ZONE OF THE GREENLAND ICE SHEET

VICKI PARRY[1], PETE NIENOW[1], DOUG MAIR[2] AND JULIAN SCOTT[3]

[1] School of Geosciences, University of Edinburgh, UK.
[2] School of Geosciences, University of Aberdeen, UK.
[3] British Antarctic Survey, Cambridge, UK.

Accurate elevation changes over large areas of the polar ice sheets can be measured using satellite radar altimetry from which mass balance can be derived. However, in the percolation zone seasonal changes in snowpack density ensure that limited changes in surface elevation may not reflect significant changes in mass. Meltwater generated at the surface refreezes at depth in the snowpack/firn causing a redistribution of mass through densification. A decrease in elevation may be caused by surface melt, percolation and refreezing, but with no mass loss (Braithwaite and others, 1994). Similarly there may be positive accumulation in the form of rain or solid precipitation over the summer, which subsequently melts and percolates into the underlying snowpack before refreezing, thus causing an increase in snowpack density and mass, but little change in surface elevation. Determining the influence of summer densification on accurate geodetic mass balance measurements is limited in the percolation zone of ice sheets by inadequate data to constrain the extent, intensity and processes of meltwater refreezing (Pfeffer and others, 1991).

In 2004 and 2006 the densification associated with meltwater percolation and refreezing was measured in Greenland's percolation zone along a 57 km transect. The main field site was located at point T5 (69^{o} 51N, 47^{o} 15W) on the EGIG line (Expedition Glaciologique International au Groenland). In 2004 measurements were taken at T5, and ~10 km towards the ice sheet margin and interior at T4 and T6 respectively. In 2006 this transect was increased in length starting at T1, and continuing for 57 km to T7, with measurements at ~10 km intervals at T1, T2, T3, T4, T5, T6 and T7. In 2004 there were two field campaigns, the first pre melt in spring, and the second post melt in the autumn. In 2006 there was one pre melt spring trip.

Density measurements were taken from individual stratigraphic layers (identified by visual distinctiveness or hardness) in shallow cores and snowpits at each site. In spring 2004, snowpit measurements were taken from the pre melt snowpack to the previous year's end-of-summer melt surface. This was an easily identifiable continuous icy layer at the base of the winter snowpack. A shallow core of ~2 m was also retrieved from the base of the snowpit, so densities of the end-of-summer 2003 snowpack could be measured. The post melt 2004 snowpack densities were measured in autumn snowpits down to the end-of-summer 2003 layer (a mass balance stake was emplaced in the spring to ensure the same reference horizon was used). In 2006, the density of stratigraphic layers in the winter snowpack was measured in snowpits dug to the end-of-summer 2005 surface layer. A shallow core was also retrieved from the base of the snowpit providing density measurements of the end-of-summer (post-melt) 2005 snowpack.

Density measurements from T1 to T7 in spring 2006, prior to melt, reveal no significant variation in mean snowpack density along the transect (Figure 1), with a correlation coefficient -0.21 (at significance level 0.5%). In order to investigate the effect of meltwater percolation and refreezing on mean snowpack density, the density of the top 1 m of each shallow core retrieved from below the end-of-summer 2005 surface was determined. This reveals a significant change (at 1% significance level) in ‘firn’ density along the transect with average values decreasing by 20% from T1 (0.55 g cm^{-3}) to T7 (0.44 g cm^{-3}) with a correlation coefficient of -0.86 (Figure 1).

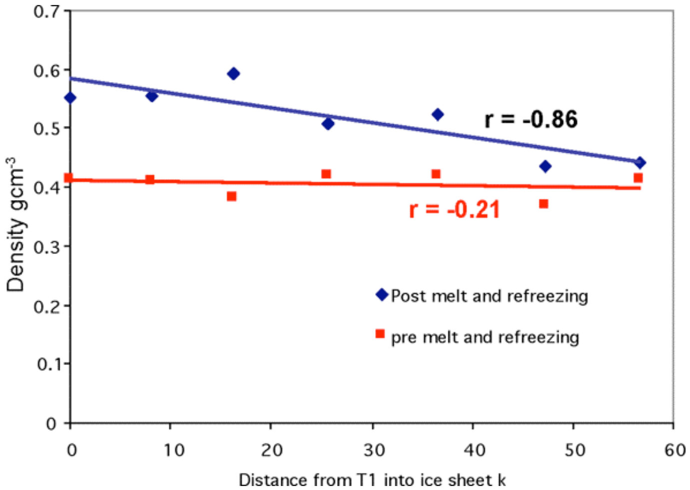

Figure 1. Average snowpit densities from spring 2006 show pre melt and refreezing there is no change in average density associated with distance into ice sheet. Average densities from 1 m firn core retrieved from the base of the snowpits show meltwater percolation and refreezing in summer 2005 causes a decrease in density with distance into the ice sheet.

Similar trends in density are observed in the measurements made along the shorter transect between T4 and T6 in 2004. The end-of-summer 2003 average snowpack densities were found from the first 1 m of firn cores retrieved from the base of spring 2004 snowpits. The average density decreases towards the ice sheet interior with a correlation coefficient of -0.98 (0.1% significance). The end-of-summer 2004 average snowpit densities, found in autumn 2004 snowpits, also decreased with distance up-ice sheet (r=-1.00, significance 0.1%)

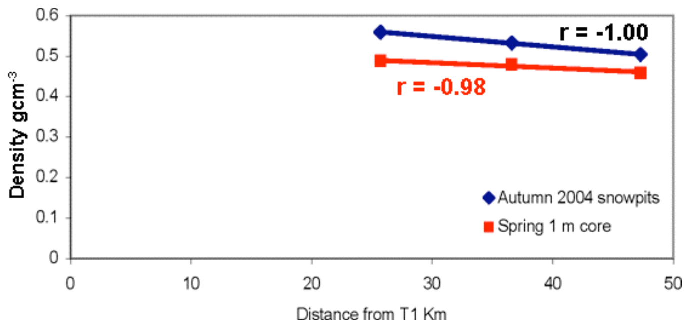

Figure 2. Average densities from the autumn snowpits in 2004, which have been affected by melt in summer 2004, and 1 m core from spring 2004 which have been affected by melt in summer 2003 both show decreasing density into the ice sheet from T4 to T6.

Our results demonstrate, over three different melt seasons, the densification of the snowpack associated with meltwater percolation and refreezing decreases with distance into the ice sheet. Prior to melt, there is no significant change in density associated with location. The densification of the snowpack is important for mass balance measurements based on elevation changes. Results from 2004 show that at T5 the elevation before melt to after melt increased by 5%. This corresponded to an accumulation increase of 31%, which was not reflected in the elevation change due to snowpack densification of 26% (Parry and others, in press) Clearly, if accurate estimates of mass balance are to be obtained from elevation change measurements, spatial variations in these densification processes must be determined, since the densification gradients in Greenland's percolation zone can be steep when average end-of-summer snowpack density can decrease by 20% over a 57 km transect

References

Braithwaite, R., M. Laternser, W. Pfeffer. 1994. Variations of near-surface firn density in the lower accumulation area of the Greenland ice sheet, Patkitsoq, West Greenland. J. Glaciol., 40(136), 477-485.

Parry, V., P. Nienow, D. Mair, J. Scott, B. Hubbard, K. Steffen, D. Wingham. 2007. Investigations of meltwater refreezing and density variations in the snowpack and firn within the percolation zone of the Greenland Ice Sheet. Ann. Glaciol. 46. in press.

Pfeffer, W., M. Meier, and T. Illangasekare. 1991. Retention of Greenland runoff by refreezing: Implications for projected future sea level change. J Geophys. Res. 96(C12), 22,117-22,124.

A NEW GLACIER INVENTORY FOR THE SVARTISEN AREA (NORWAY) FROM LANDSAT ETM+: METHODOLOGICAL CHALLENGES AND FIRST RESULTS

FRANK PAUL[1], LISS MARIE ANDREASSEN[2,3]

[1] Department of Geography, University of Zurich, Zurich, Switzerland.
[2] Norwegian Water Resources and Energy Directorate, Oslo, Norway.
[3] Department of Geosciences, University of Oslo, Norway.

Glacier changes in Norway showed a considerable regional variability in recent decades. From strongly advancing glaciers with a more westerly exposition and near to the coast, to constantly retreating glaciers in dryer regions and more away from the coast. Although a large number of direct mass balance and length change measurements reveal a good overview of the regional variability, today's overall state of Norwegian glaciers is not well known. Indeed, the last glacier inventory for northern Scandinavia is based on aerial photography from the 1960s and 1970s (1980s for southern Norway) and the information only exists in form of point data (coordinates with attributes) and printed maps. In order to get an overview of their present state, the Norwegian Water Resources and Energy Directorate (NVE) has decided to create a new glacier inventory from Landsat TM/ETM+ data within the framework of the project Global Land Ice Measurements from Space (GLIMS). This approach will also provide digital glacier outlines, that are a mandatory prerequisite for any change assessment related to glacier area. The new inventory is based on the latest Landsat TM/ETM+ data that can be used for glacier mapping with respect to snow conditions and cloud cover. The glacier mapping has started in the Jotunheimen region and is here presented for the Svartisen region using the Landsat ETM+ scene 199-13 from 7. September 1999 (Figure 1).

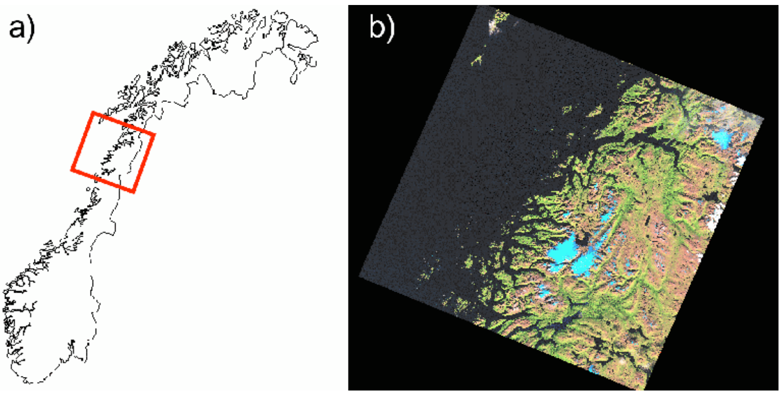

Figure 1. a) Location of the Landsat scene in Norway (red rectangle). b) The ETM+ scene 199-13 with bands 543 as RGB showing glaciers in bright blue-green and clouds in white.

Some glaciers to the border of Sweden are covered by thick clouds, the Blåmansisen ice cap in the north is covered by high (optical thin) cirrus clouds. The techniques for automated glacier mapping from thresholded ratio images and the following GIS-based data processing are well established and straight forward. For this scene we use a band 3/5 ratio image with a threshold of 2.6 and an additional threshold in band 1 to improve the classification accuracy in regions of cast shadow. Apart from a few regions with thicker debris cover (moraines) and turbid lakes everything is well mapped, even the glaciers in cast shadow under thin clouds (Figure 2a). Glacier outlines from 1985 of the Blåmannsisen ice cap are superimposed in Figure 2a and show little overall change of the ice cap size between 1985 and 1999. Some glacier snouts show small advances or retreats but most termini are unchanged, indicating an ice cap size that is in balance with current climatic conditions. However, assessment of changes with respect to individual glacier units is not straight forward. The digitally available hydrologic catchments which are based on recent digital elevation models (DEMs) are not compatible with the ice divides used for the 1970s inventory as the latter are partly based on military maps from the 1940s with a much lesser topographic accuracy (Figure 2b). As a consequence, we have chosen to generate two inventories from the 1999 satellite scene: One for the change assessment using the divides of the original inventory and one for the GLIMS database with the DEM-based ice divides.

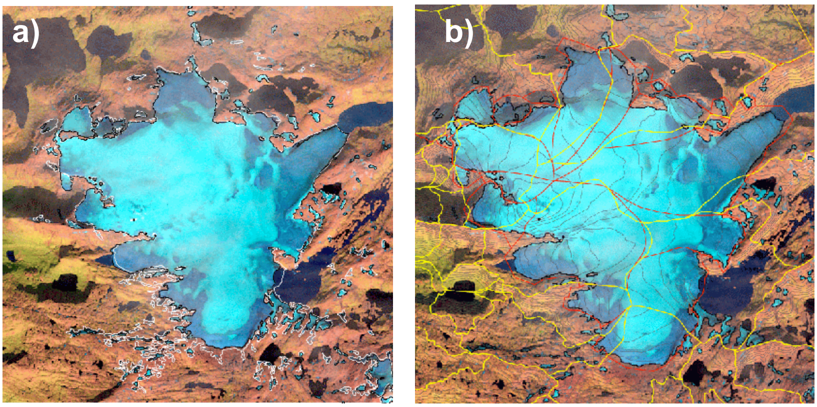

Figure 2. a) Glacier outlines from Blåmannsisen in 1999 as mapped with ETM+ (black) and from Statens kartverk (white) in 1985. b) Approximate ice divides from the former glacier inventory (red) and hydrologic divides derived from a DEM (yellow), with elevation contour lines in grey.

Another challenge for glacier mapping in this region is related to seasonal snow cover that hides possible glaciers or their perimeter. While manual delineation might help to exclude such regions for larger valley and mountain glaciers, it fails for most of the small snow patches without any bare ice visible (Figure 3a). The associated area changes are often random in such cases and should not be used as a climatic signal. As a general rule, we will exclude everything that is doubtful (e.g. without an entry in the former inventory) and exclude obvious snow patches where possible. A third challenge is related to the number of glaciers that have been identified in the previous inventory. Several ice masses that could clearly be identified as glaciers (i.e. showing bare ice) have no identification code (Figure 3b). As we would like to include them in the new inventory we have another reason to generate two inventories from the 1999 satellite scene: One for the change assessment and one for the GLIMS database.

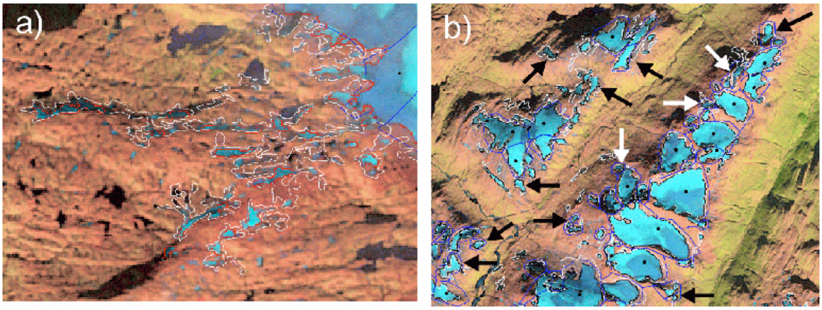

Figure 3. a) Snow fields near Blåmansisen that could hide glacier ice or not. b) Glaciers without an identification code (black dot) in the former inventory are marked by arrows.

The comparison with the former glacier outlines reveal interesting changes for the southern part of the scene. While we observe small advances to little retreat for the Vestisen ice cap, we found for the Ostisen complex (it is not really an ice cap) many individual small glaciers that increased in size while the large valley glaciers display strong terminus retreats (Figure 4). Most often these advancing and retreating glaciers are located side-by side and we assume that individual response times could be involved in this behaviour. However, some glaciers near the glaciation limit have also disappeared completely. Our analysis confirms, that only changes that are assessed for a large sample of glaciers provide a reliable estimate of ongoing cryospheric changes and that special care has to be taken for correct glacier delineation (ice divides, seasonal snow) as the artificial glacier changes due to different basins are several times larger than the real changes. We hope that the new digital inventory will provide a solid baseline for future studies of glacier change or mass balance in this region.

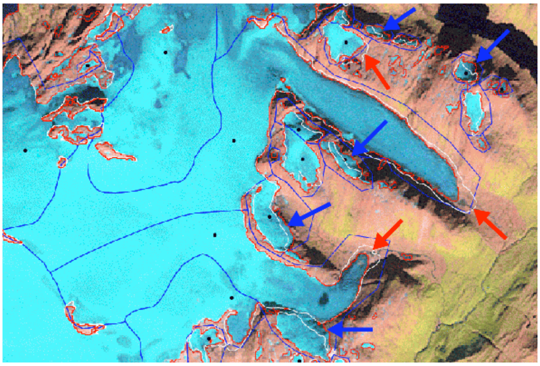

Figure 4. Glacier change (blue arrows: advance, red arrows: retreat) for a part of Ostisen with glacier basins (blue), glacier outlines from ETM+ in 1999 (red) and from Statens kartverk in 1968 (white)..

Acknowledgement

The project is supported by the Norwegian Space Centre as part of the project Cryorisk. Jon Endre Hausberg (NVE/University of Oslo) tested the quality of the orthorectified scene delievered by Norsk Satelittdataarkiv. F. Paul wishes to thank R. Engeset (NVE) for the invitation to Oslo and the possibility to perform this study.

A STUDY OF δ^{18}O AND TEMPERATURE GRADIENTS AND THEIR TRENDS AND RELATIONS OVER THE ICE FIELD LOMONOSOVFONNA, SVALBARD, DURING THE LAST CENTURY

VEIJO POHJOLA[1], BJÖRN SJÖGREN[1], TÕNU MARTMA[2], ELISABETH ISAKSSON[3], JACK KOHLER[3], KARIN TÖRNBLOM[1] AND RODERICK S.W. VAN DE WAL[4]

[1] Department of Earth Sciences, Uppsala University, Uppsala, Sweden.
[2] Institute of Geology, Tallinn University of Technology, Tallinn, Estonia
[3] Norwegian Polar Institute, Tromsø, Norway.
[4] Institute of Marine and Atmospheric Research, University of Utrecht, The Netherlands

δ^{18}O is a well established proxy for ambient temperatures, and is used to reveal past temperature records from paleo-archives, such as ice core records. One problem with the δ^{18}O / temperature (δ^{18}O/T) relation is that atmospherical processes complicates the δ^{18}O/T relation. We used δ^{18}O from seven ice cores drilled 1997 on the ice field Lomonosovfonna, Spitsbergen (Figure 1) together with T records from neighboring coastal stations, and from the ERA-40 dataset to investigate temporal and spatial gradients of δ^{18}O and T, to calculate the δ^{18}O/T relationship over central Spitsbergen.

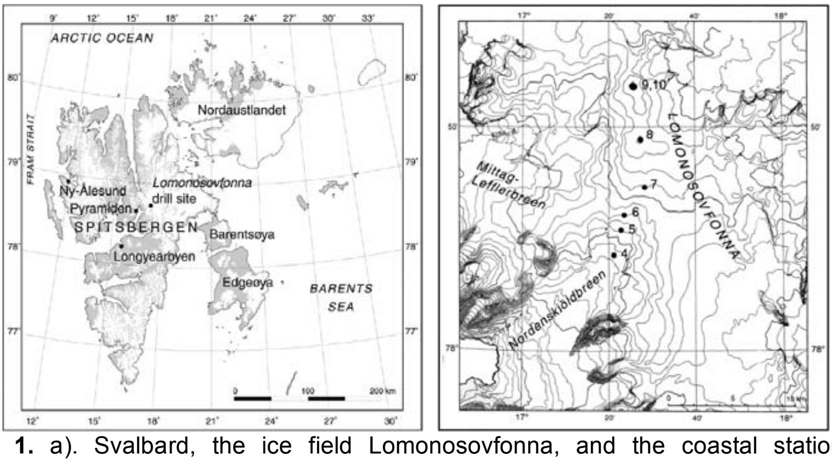

Figure 1. a). Svalbard, the ice field Lomonosovfonna, and the coastal stations. b). Lomonosovfonna, Nordenskiöldbreen and the positions of the ice cores drilled 1997, referred to as cores 97:4-10 in the text.

We found that δ^{18}O and T lapse rates are approximately -0.6 ‰ 100 m^{-1} and -0.4 °C 100 m^{-1} respectively, giving a $\partial\delta^{18}O / \partial T(z) \sim 1.5$ ‰ °C^{-1} (Table 1).

The temporal gradients of annual averages suggested $\partial\delta^{18}O/\partial T(t) \sim 1$ ‰ °C^{-1}. We finally conclude that neither the ice core, nor the temperature records show any statistical redundant signs of Arctic warming in the Barents region during the 1925-1996 period, all available records on the contrary show a cooling over the last decades of the 20th century (Figure 2).

Table 1. $\partial T/\partial z$ is regressed from the ERA-40 monthly average record. $\partial \delta^{18}O/\partial z$ is regressed between all cores (97:10-97:4). The uncertainty is calculated for P = 0.05.

Time period	$\partial T/\partial z$ (ºC 100 m^{-1}) 1000 – 775 hPa	$\partial \delta^{18}O/\partial z$ (‰ 100 m^{-1}) all cores	$\partial \delta^{18}O/\partial T$ (‰ ºC $^{-1}$) (median)
Last snowfall	-0.36[1]	-0.78 ± 0.54	~2
Last winter	-0.42 ± 0.09[2]	-0.30 ± 0.96	0.7
1994-1996	-0.44 ± 0.04	-0.65 ± 0.72	1.5
1992-1996	-0.43 ± 0.03	-0.69 ± 0.26[3]	1.6

1. Defined as April 1997.
2. Defined as November 1996 - April 1997.
3. Only cores 97:6 - 97:10.

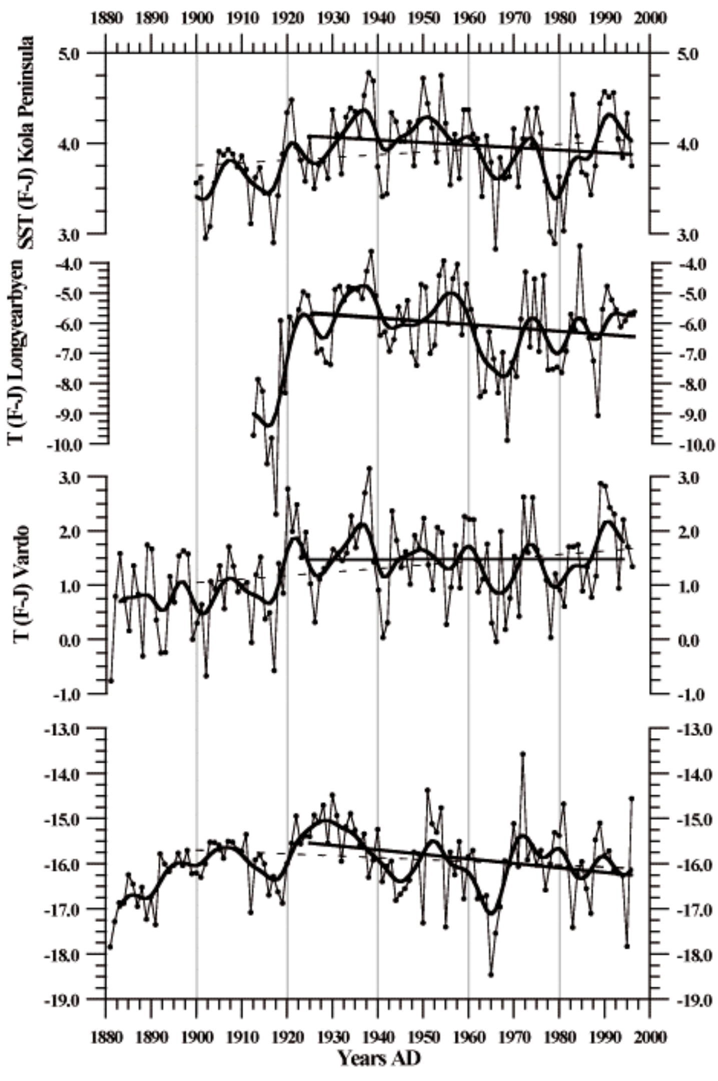

Figure 2. The time series of annual average (Feb-Jan) 1.5 m temperatures of Longyearbyen and Vardø (http://www.unaami.noaa.gov/analyses/sat/), and the sea surface temperatures off Kola Peninsula (Bochkov Yu.A. 2005. Large-scale variations in water temperature along the "Kola meridian" section and their forecasting. 100 years of oceanographic observations along the Kola Section in the Barents Sea. Papers of the international symposium. - Murmansk, PINRO: 201-216) compared to the annual average $\delta^{18}O$ from the Lomonosovfonna 97:10 ice core. Each year is marked by a symbol. The thicker curve is smoothed using a Gauss filer (σ =2).

GLACIER VOLUME PROJECTIONS: FLOWLINE MODELLING VS VOLUME-AREA SCALING

VALENTINA RADIĆ[1], REGINE HOCK[2] AND JOHANNES OERLEMANS[3]

[1] Department of Physical Geography and Quaternary Geology, Stockholm University, Stockholm, Sweden
[2] Department of Earth Sciences, Uppsala University, Uppsala, Sweden
[3] Institute for Marine and Atmospheric Research Utrecht, University of Utrecht, Utrecht, The Netherlands

Purpose

Volume-area scaling provides a practical alternative to ice-flow modelling to account for glacier size changes when modelling future glacier evolutions, however, uncertainties remain as to the validity of the approach under non-steady conditions. The main objectives of this work were: (1) to determine and compare the volume-area relationships for steady-state and non-steady-state conditions in order to test the validity of the power law relationship for non-steady-state conditions, and (2) to compare volume projections derived from volume-area scaling with those derived from ice-flow modelling.

Methodology

Using the 1-D ice-flow (flowline) model by Oerlemans (1997) we generated a set of 37 synthetic steady-state glaciers of different sizes, with uniform width lying on uniform slope ($tg\alpha$ =0.1), and then modelled volume evolutions for the subset of 24 synthetic glaciers responding to the climate warming and cooling as prescribed by negative and positive mass balance perturbations, respectively, on a century time scale.

Results and conclusions

Scaling exponent γ =1.56 in the volume-area relationship obtained from the 37 synthetic steady-state glaciers differed from γ =1.375 derived theoretically by Bahr and others (1997) and from the exponents (γ =[1.80, 2.90]) derived for each of 24 investigated glaciers under non-steady-state conditions. Exponents γ were generally larger for negative mass balance perturbations (warming scenarios) than for positive perturbations (cooling scenarios) and γ tended to decrease with increasing initial glacier size. However, the range of differences in scaling exponent by up to 86% is shown to make negligible differences, less than 6%, in 100-year volume changes derived from the scaling approach (Figure 1a).

Volume projections on a century time-scale differed within the range of 12%-23% of initial volume from the flow model results depending on the method by which the area-averaged net mass balance is calculated, i.e. whether or not volume-area scaling is applied and area changes obtained from volume-area scaling are included ('conventional' mass balance) or excluded ('reference surface mass balance') in the mass balance computations (Figure 1b). The most sophisticated method accounting for area-changes and considering these in the mass-balance

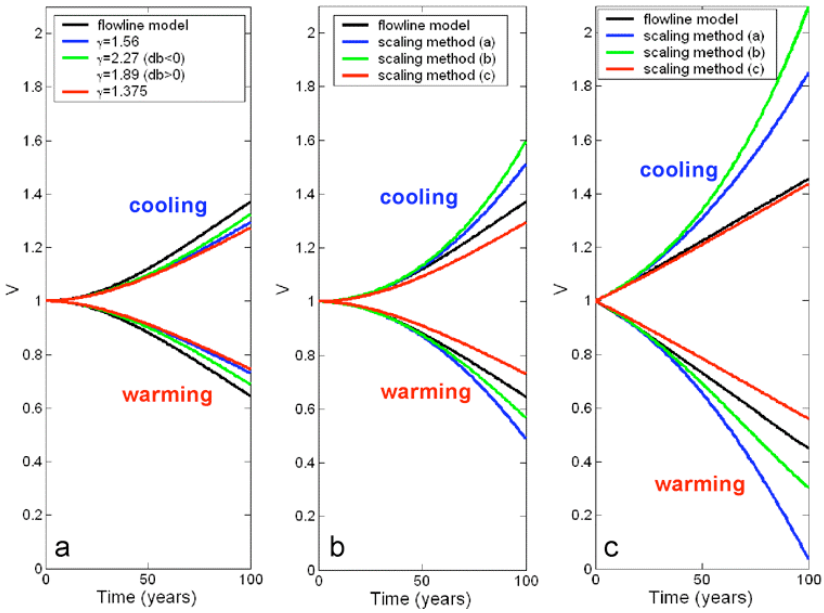

Figure 1. Normalized volume evolutions of the largest synthetic glacier responding to the mass balance perturbation of *db(0)* =+0.015 ma^{-1} ('cooling scenario') and *db(0)* =-0.015 ma^{-1} ('warming scenario'). In figure (a) volume evolutions are derived from scaling method (c) using three different scaling exponents: γ =1.56 derived from our 37 synthetic steady-state glaciers, γ =2.27 (1.89) derived from the transient response to warming (cooling) of this synthetic glacier, and γ =1.375 derived theoretically by Bahr and others (1997). In figure (b) and (c) the three methods correspond to three different ways of calculating area-averaged net mass balance and volume changes: the 'reference-surface' mass balance without volume-area scaling (method a), the 'reference surface' mass balance with scaling (method b) and the 'conventional' mass balance with scaling (method c). Scaling exponent γ =1.56 is used in the volume-area relationship. In figure (b) the synthetic glacier is initially in steady state, in figure (c) the glacier is in non-steady state prior to the mass balance perturbation.

computations resulted in the smallest differences (up to 12%) in projected volume changes over 100 years. This method best agreed with the projections by the ice flow model when the glaciers are initially in non-steady state (Figure 1c) or when the climate is assumed to stabilize after a period of perturbation (Figure 2). In fact, the method is capable of simulating the glacier approaching a new steady state by simulating the feedback between area-averaged mass balance and glacier geometry/elevation changes resulting from retreat or advance of the glacier. This feedback is captured by excluding area from or adding area to the lowest part of the glacier. In contrast, neglect of volume-area scaling and neglect of area-changes in the mass balance computations fails to simulate this feedback and the approach to a new steady state. Further details can be found in Radić et al (in press).

Although based on a set of synthetic glaciers of highly simplified geometry, our results are promising for use of volume-area scaling in glacier volume projections provided that the mass balance-elevation feedback is captured by considering area-changes in the mass balance computations.

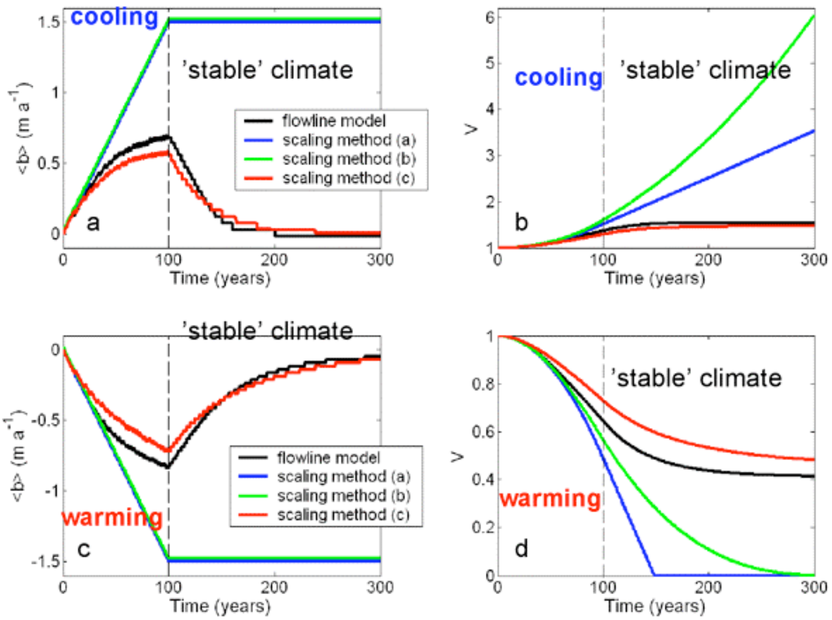

Figure 2. Evolution of area-averaged mass balance (a, c) and normalized glacier volume (b, d) derived from the flowline model and from the scaling methods. Initial perturbation is $db(0)=0.015$ m a^{-1} (cooling scenario) and $db(0)=-0.015$ m a^{-1} (warming scenario). Scaling methods (a) and (b) are based on 'reference surface' mass balances and scaling method (c) is based on 'conventional' mass balances as also in the flowline model.

References

Bahr, D. B., M. F. Meier, and S. D. Peckham. 1997. The physical basis of glacier volume-area scaling. J. Geophys. Res., 102(B9), 20355-20362.

Oerlemans, J. 1997. A flowline model for Nigardsbreen, Norway: projection of future glacier length based on dynamical calibration with the historic record. Ann. Glaciol., 24, 382-389.

Radić V., Hock R. and Oerlemans J. Volume-area scaling vs flowline modelling in glacier volume projections, accepted by Ann. Glaciol., 46.

MODELLING THE 21ST CENTURY MASS BALANCE OF SVALBARD GLACIERS USING ERA-40 REANALYSIS AND GENERAL CIRCULATION MODELS

CAMERON RYE, IAN WILLIS AND NEIL ARNOLD

Scott Polar Research Institute, University of Cambridge, Cambridge, UK.

Summary
A research proposal is presented for modelling the spatial and temporal variations in mass balance across glaciated regions in Svalbard. A model driven using the ERA-40 reanalysis data set will be developed for the Kongsfjorden region of northwest Spitsbergen, Svalbard, and validated against available mass balance observations. Statistically downscaled climate scenarios from 17 general circulation models (GCMs) will be used to investigate the response of the area to climate change. Preliminary results are presented for Midre Lovénbreen, a small valley glacier in the Kongsfjorden region. The ERA-40 data used to drive the mass balance model is validated against observations from a surface weather station near the glacier and 21st century projections of temperature and precipitation from five GCMs are downscaled.

Introduction
The Arctic climate is currently warming at a faster rate than observed elsewhere on the planet and projections from GCMs suggest that this trend will continue for at least the next century. With glaciers and ice caps covering 36 600 km^2, Svalbard is one of the largest glaciated areas in the Arctic. The archipelago is thought to be particularly sensitive to climate change due to its location at the northern limit of the warm North Atlantic drift and is therefore expected to make a disproportionate contribution to sea level rise in the coming century. While there have been a number of investigations undertaken on Svalbard glaciers and ice caps, mass balance measurements have only been made for 0.5% of the total glaciated area. The aim of this project is to develop a numerical model to simulate the spatial and temporal variations in mass balance across glaciated regions in Svalbard. The model will be used to investigate the climatic sensitivity of large glaciated areas as well as their contribution to sea level rise under climate change scenarios.

Proposed methodology
The mass balance model will be based on the distributed energy balance model used by Arnold et al. (1996) and subsequently developed by Brock et al. (2000a,b) and Arnold et al. (2005). The model solves the hourly surface energy balance for each grid cell of a digital elevation model (DEM) by taking account of: (1) the net short-wave radiation; (2) the net long-wave radiation; and (3) the sensible and latent heat fluxes. Additionally, the model also calculates the energy flux from the surface into the body of the glacier. An accumulation routine will be added to the model, as well as a simple calving routine where required. In the first instance only the static mass balance will be considered.

The model will initially be developed for Midre Lovénbreen, a small (6 km^2) valley glacier in the Kongsfjord region of northwest Spitsbergen, Svalbard. The model will be run using a 20 m DEM of the glacier (Arnold et al., 2006) and driven using the ERA-40 reanalysis data set for the period 1970-2000. The results will be validated using mass balance measurements made by the Norwegian Polar Institute (Hagen et al., 2003). The ERA-40 data set will also be validated for the study site by investigating the correlation with observations from a surface weather station located on the glacier snout. Once the model has been tested for Midre Lovénbreen it will then be applied to the surrounding Kongsfjord region using a 100 m DEM and validated using available mass balance observations.

Forcing the model with statistically downscaled outputs from 17 GCMs will derive projected mass balance time series for the 21st century. The downscaling methodology will be based on that used by Radić and Hock (2006). The GCM data will be downscaled to the ERA-40 grid and then corrected locally for each grid cell of the DEM by simple linear regression.

Preliminary results

To validate ERA-40 for the study site, correlation coefficients were calculated between observations from the surface weather station and 9 ERA-40 grid cells that cover the Kongsfjord region. Monthly and seasonal correlations were calculated for the period 1970-2000. Correlations greater than 0.98 were found for monthly temperatures. However, seasonally the correlations were lower during the summer (0.669 - 0.735) compared with the winter (0.862 - 0.949), spring (0.914 - 0.940) and autumn (0.952 - 0.988). The monthly correlations for precipitation were between 0.596 and 0.712, while seasonal correlations were found to be lower during the winter (0.464 - 0.660) compared to the spring (0.588 - 0.700), summer (0.670 - 0.720) and autumn (0.586 - 0.670). The monthly results for relative humidity (0.454 - 0.572) and wind speed (0.393 - 0.444) were lower than both temperature and precipitation, as were the seasonal correlations.

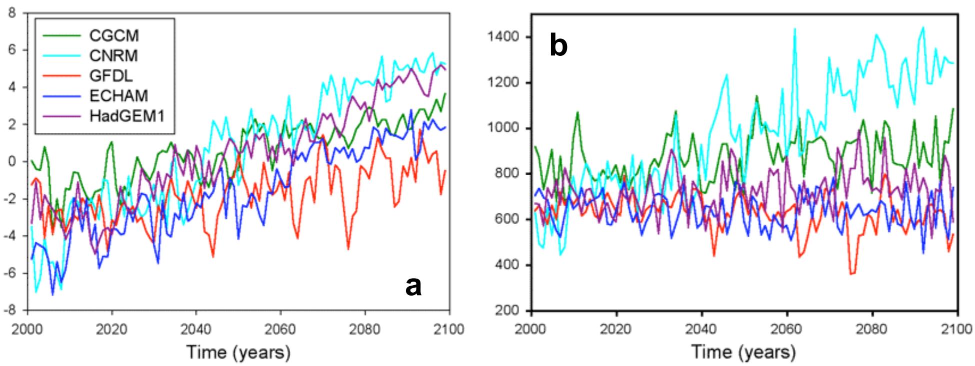

Figure 1. Statistically downscaled temperature (a) and precipitation (b) scenarios for Midre Lovénbreen for the 21st century.

The downscaling methodology was tested for Midre Lovénbreen using a sample of five GCMs (Figure 1). Downscaling relationships were derived using observed data for the period 1970-2000 and then applied to the IPCC A2 simulation for each

GCM. The models predict that the mean annual air temperature of the glacier will increase by between 4.8 and 9.9ºC between the periods 1970-2000 and 2070-2100, while mean annual precipitation is predicted to change between -50 and +597 mm.

Conclusions

The preliminary validation of ERA-40 provides encouraging results, although further work is required to investigate the reasons behind the lower temperature correlations during the summer and the overall lower correlations for precipitation, particularly during the winter. The energy balance model being used has a relatively low sensitivity to both relative humidity and wind speed. Therefore the lower correlations for these variables should not have a significant impact on the modelled mass balance.

Temperature and precipitation have been successfully downscaled for the study site. Future work will now involve downscaling other climate variables required by the model, including relative humidity, wind speed, cloud cover, and solar radiation. Long-term aims of the project include applying the same methodology to glaciated regions in Iceland and extending model simulations back to the mid 19th century.

References

Arnold, N.S., W.G. Rees, A.J. Hodson, and J. Kohler, (2006) Topographic controls on the surface energy balance of a high Arctic valley glacier, J. Geophys Res. 111 (F2): Art. No. F02011, doi:10.1029/2005JF000426.

Arnold, N. (2005), Investigating the sensitivity of glacier mass balance/elevation profiles to changing meteorological conditions: Model experiments for Haut Glacier d'Arolla, Valais, Switzerland, Arct. Antarct. Alpine Res., 37(2), 139–145.

Arnold, N., I. C. Willis, M. J. Sharp, K. S. Richards, and W. J. Lawson (1996), A distributed surface energy balance model for a small valley glacier: I. Development and testing for Haut Glacier d'Arolla, Valais, Switzerland, J. Glaciol., 42(140), 77– 89.

Brock, B. W., I. C. Willis, M. J. Sharp, and N. S. Arnold (2000a), Modelling seasonal and spatial variations in the surface energy balance of Haut Glacier d'Arolla, Switzerland, Ann. Glaciol., 31, 53–62.

Brock, B. W., I. C. Willis, and M. J. Sharp (2000b), Measurement and parameterisation of albedo variations at Haut Glacier d'Arolla, Switzerland, J. Glaciol., 46(155), 675–688.

Hagen, J. O., K. Melvold, J. Kohler, and J.-G. Winther (2003), Glaciers in Svalbard: Mass balance, runoff and freshwater flux, Polar Res., 22(2), 145– 159.

Radić, V. and Hock, R. (2006), Modeling future glacier mass balance and volume changes using ERA-40 reanalysis and climate models: A sensitivity study at Storglaciären, Sweden, J. Geophys. Res, 111 (F3): Art. No. F03003.

GROUND CONTROL FOR MODELLING GLACIER CHANGES IN "HORNSUNDET"

ALEKSEY I. SHAROV AND ROLAND WACK

Institute of Digital Image Processing, Joanneum Research, Graz, Austria

You will not find the name Hornsundet in existing maps. This invented toponym refers to a hypothetical sub-glacial strait between Torell and Sörkapp lands in South Spitsbergen, Norwegian High Arctic. A relatively low and flat ice isthmus formed by Hornbreen and Hambergbreen tidewater glaciers is currently bridging the two lands. In the narrowest part, the ice bridge is 7.5 km wide, approx. 1.5 km long and 130 m high (2006). Our previous remote sensing studies using spaceborne radar interferograms, optical imagery and altimetry data revealed essential changes in the extent, elevation and mechanics of the Hornbreen - Hambergbreen (H - H) glacier system, and provided some evidence for short-term vertical motions of the ice bridge (Sharov 2006). Yet several unresolved questions remained concerning the character and causes of these changes and motions, which could not be answered in the lab.

In early spring 2006, we visited the Polish Polar Station in Hornsund, South Spitsbergen, and conducted ground control surveys in the H - H study area using two snowmobiles, Novatel DL4 GPS receivers, a Riegl LPM-2K pulse laser rangefinder mounted on the Leica TCRA1103 theodolite, and a tilt meter. Apart from the acquisition of reliable basic control and ground truth data for the generation of glacier elevation and evolution models, we performed a series of field observations in order

- to determine present glacier extent and to obtain representative quantitative measurements of glacier changes in the H – H study area in linear, aerial and volumetric terms for the past 20 years, and to compare them with long-term records available for neighboring glaciers;
- to measure glacier velocities at several specific points and to reliably interpret ERS-1/2 (C-band) and JERS-1 (L-band) radar interferograms of the ice bridge;
- to validate the transferential approach (Sharov and Etzold, 2005) to measuring frontal velocities of tidewater glaciers based on the interferometric analysis of the displacement of fast sea ice pushed away from the shore by the moving glacier;
- to estimate the impact of tides on glacier motion and fast ice displacements;
- to forecast potential changes of the H – H glacier system in the nearest future.

Steady and cold (-10 to -19°C) weather conditions enabled us to perform uninterrupted and extensive topographic and tachometric surveys in the H – H study area in the period 26 March – 03 April, 2006. Present elevations of the ice bridge were surveyed by 3-D kinematic DGPS profiling in relation to two reference stations (point Nos. 6 and 7) placed close to Icingfjellet in the north and Ostrogradskifjella in the south of the study area as had already been done by (Pälli et al., 2003). The locations of reference stations were well observable in the field and identifiable in available topographic maps and spaceborne imagery. Our topographic measurements were carried out along 5 radial and 5 circumferential profiles with a total length of 80 km and the centre point lying in the mid of the H - H ice isthmus. In each profile, the distance between neighbouring records was approx. 100 m. The maximum distance from measured points to the nearest reference station did not exceed 9 km, and the rms elevation difference checked at cross-points was ± 3 dm. The glacier elevations obtained were referred to the WGS84 geodetic datum established by long-term continuous GPS records at the Polish Polar Station, which is thirty km away from the ice-bridge area. In the field, we determined the present positions of glacier termini and recognized that the calving face of Hornbreen retreated by 1 km compared to its position in the ASTER image of August 2004.

Moreover, we performed threefold high-precision DGPS measurements in a static mode at 10 target points homogeneously distributed over the ice isthmus and at 5 characteristic points on the fast sea ice surface within 1 km from the glacier front. The receiving antennas were reliably mounted on large snow screws made of plastic and screwed into the glacier surface at each target point. The relative accuracy of the 3-D coordinates measured over 15 target points with 0.5 and 2-day intervals was characterized by the rms difference of ± 3 mm. The results were used for the quantitative estimation of glacier motion, tidal effects and corresponding displacement of the fast sea ice in the study area. The resultant displacement vectors were decomposed in horizontal and vertical terms. Their daily projections are specified in Table 1. For the sake of reliable interpretation, the motion vectors were overlaid on the spaceborne SAR interferograms taken by JERS-1 and ERS-1/2 satellites in the cold seasons of 1994 and 1995/96 respectively. One example is given in Figure 1 representing horizontal components of the glacier motion (in red) and the fast sea ice displacement (in blue) at the end of March 2006.

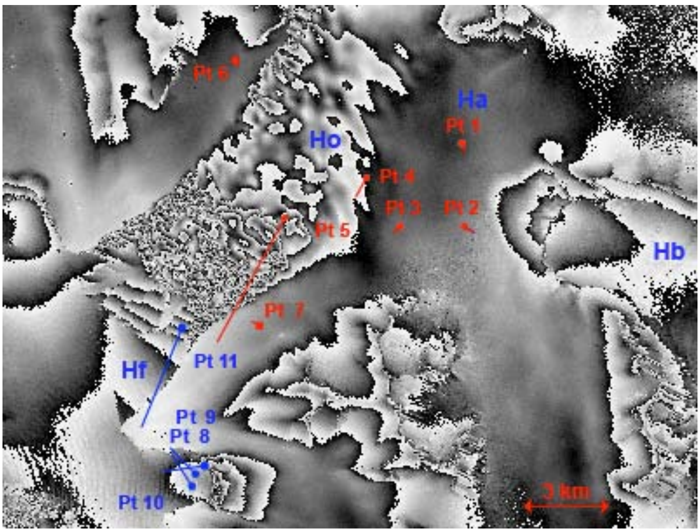

Figure 1. ERS-1/2-SAR interferogram (April 09/10, 1996, ☾) of the H – H study area (Ha - Hambergbreen, Hb – Hambergbukta, Hf – Hornfjord, Ho – Hornbreen) with target points and horizontal terms of ice flow in March 27-31, 2006 (●)

Table 1. Daily displacement of target points in March 2006.

Point No.	Displacement, cm		Azimuth, °	Location
	horizontal	vertical		
1	0.3	- 1.9	170,5	glacier surface
2	1.1	- 0.5	111.8	glacier surface
3	0.5	+ 0.3	234.2	glacier surface
4	4.8	- 0.2	214.4	glacier surface
5	40.9	- 0.8	206.6	glacier surface
6	0.1	+ 0.1	173.1	ref on dead ice
7	0.2	- 0.0	301.8	ref on dead ice
8	10.7	- 120.3	322.1	fast sea ice
9	11.9	- 114.9	254.1	fast sea ice
10	11.1	- 102.7	335.0	fast sea ice
11	31.5	- 80.2	207.2	fast sea ice

Concerted measurements of the glacier motion and fast sea ice displacements revealed that when small differences in water level occur, the fast sea ice displacement remains collinear with glacier motion vectors. The displacement vanishes with the distance from the glacier front. At 500 meters from the glacier front, the sea ice displacement was approx. 80 % of the value measured at the glacier front. During spring tides reaching 1.5 m (http://www.math.uio.no/tidepred/), the sea ice displacement vectors may rotate by as much as ± 45° depending on the tide phase (ebb or flood) and point location. The interferometric velocities at the target points 8 - 10 (approx. 7 cm/day) and 11 (approx. 33 cm/day) corresponded well with those measured in the field (Table 1). The validity of our transferential approach to estimating glacier velocities in winter by measuring the fast sea ice displacement in single tide-coordinated SAR interferograms was thus confirmed. Frontal glacier velocities were additionally measured from two different positions on the ice-free coast with a known baseline using the “theolaser” and conventional geodetic techniques of forward intersection and tachymetry. The frontal heights of the study glaciers above the sea ice level were determined by measuring vertical angles and slant distances to glacial fronts with subsequent trigonometric calculations. The results obtained were in good agreement with those obtained by concurrent DGPS surveys. Heavy equipment, high energy consumption and the lack of ice- and snow-free tracts of land for installing the instrument, however, hampered the extensive use of the tachymetric technique in the study area.

The maximum amplitude of vertical displacements of the fast sea ice was given as 1.2 m, while vertical motions in frontal parts of the study glaciers reached 1.5 – 2.0 cm (Figure 2). The vertical motions of fast sea ice and tidewater glaciers were nearly synchronous and semidiurnal in character. The glacier front reached its highest position approx. 1 hour later (at approx. 5:00 and 17:00 UTC) and stayed in the lowest position (at approx. 11:00 and 23:00 UTC) somewhat longer than the sea ice. This can be explained by different inertial properties and correspondingly different reactions of the glacier and the fast ice to tidal effects. Independent geodetic measurements in the frontal part of Hansbreen, another tidewater glacier lying closer to the Polish station, provided very similar results and verified the representative character of our observations. It is worth noting that the calm weather and consistently high atmospheric pressure during the whole campaign lowered the tide amplitude compared to its predicted value and diminished the difference between the water levels recorded at the same time on consecutive days. Vertical displacements of the target points lying in the nearly horizontal (glacier slope less than 0.5°) middle part of the H - H ice bridge ranged from 0.5 cm to 2 cm and could not be explained by the inherent glacial flow since the horizontal displacement of these points was very small. DGPS measurements at the reference stations showed that the effect of snow densification could be neglected. Hence, we supposed that, apart from measuring inaccuracies, the horizontal displacement of all target points was a result of glacier flow and that their vertical displacements were mostly caused by tides and, probably, basal melting.

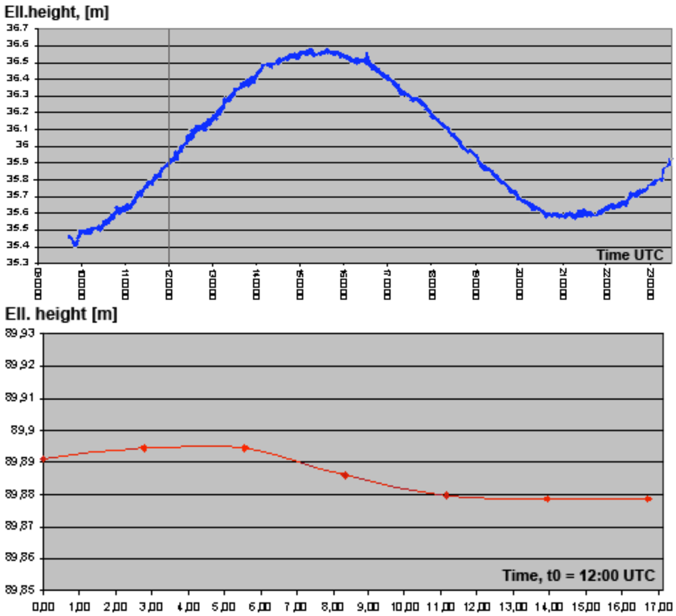

Figure 2. Semidiurnal vertical motions of the fast sea ice (blue) and tidewater glacier margin (red).

After completion of the field campaign we received 10 sheets of Polish topographic maps of the study region issued in 1987 at 1:25 000 scale (10-m contour interval). Together with 3 sheets of Norwegian 1:100 000 topographic maps (50-m contour interval) published in the 1990s, these were used for generating a basic elevation model representing the glacier state in the 1960s. In addition, we also used British and Polish hydrographic charts showing water depths in Hambergbukta, Hornsund and Brepollen in order to estimate the thickness of the submerged part of grounded tidewater glaciers. The basic glacier elevation model with 50 m posting was upgraded in a manner similar to that used in (Sharov and Etzold 2005) using the results of the field campaign, available INSAR models and the ICESat-GLAS altimetry data obtained in 2003 – 2005, and assuming a homogeneous character of glacier elevation changes in the past decades. Finally a glacier evolution / change model was calculated by differentiation between the basic model and the upgraded one.

In the evolution model, the area of significant lowering of the H - H glacier surface appears in the form of a ∧ - shaped stripe comprising target points 1 through 5, which was previously detected in several SAR interferograms and interpreted as “motion feature” (Sharov, 2006). Within this stripe the lowering rate amounts to 2 and even 3 m/year, which is twice that observed at similar elevations on neighbouring tidewater glaciers, such as Storbreen, Svalisbreen and Mendeleevbreen. The surface lowering decelerates in the areas where small tributaries, e.g. Mikaelbreen, Professorbreen or Tatianapasset, merge with the main glacier. Local vertical movements of the glacier surface indicate that rapid thinning results in relatively large parts of the H - H system being afloat, at least transiently, at high tides. These observations provide a good verification for the assumption about the existence of two overdeepened glacier valleys joined together between Hornsund and Hambergbukta. The high lowering rate of Sykorabreen, a former tributary of Hambergbreen, allows the conclusion to be drawn that this glacier also has an over-deepened basin.

Glacier changes in linear, areal and volumetric terms were represented both qualitatively and quantitatively in the form of 3 image-line maps at 1:50 000 and 1:100 000 scales, which can be downloaded from http://dib.joanneum.at/integral/ (cd results). Some values of changes in the H – H glacier system for the past 40 years are given in Table 2. They allow the conclusion to be drawn that glacier retreat in south Svalbard has accelerated compared with previous periods of observation. Two new proposed toponyms are contained in our maps, i.e. Joanneumbukta and Polarisodden (both around 76°59’N and 16°37’E), which reflect real geographic findings, acknowledge the support provided by our sponsors and have yet to be confirmed by the Norwegian Polar Institute. The field campaign was carried out in the framework of the EC FP6 Contract No. SST3-CT-2003-502845 INTEGRAL. Our deepest gratitude is due to our Polish colleagues for their hospitality and invaluable assistance before, during and after the field campaign.

Table 2. H - H glacier changes, 1960s - 2000s

Change parameter	Glacier			
	Hornbreen	Hamberg.	Svalisbr.	Sykorabr.
Front position, km	- 4.2	- 4.2	- 2.3	- 0.4
Ice coast length, km	- 0.9	- 1.6	- 0.1	+ 2.3
Glacier area, km²	-13.5	- 9.0	- 3.3	- 0.9
Ice volume f. retreat, km³	- 1.1	- 1.1	- 0.3	- 0.1
Ice volume f. lowering km³	- 2.3	- 0.4	- 0.7	- 2.6

References

Pälli A., et al., 2003: Glacier changes in southern Spitsbergen, Svalbard, 1901-2000. Annals Glac., 37, 219-225.

Sharov A.I. and S.Etzold, 2005: Upgrading Interferometric Models of European Tidewater Glaciers with Altimetry Data. Proc. of the 1st International CRYOSAT Workshop, ESA ESRIN, Frascati, Italy, 8 - 10 March, 2005 (accessible at http://dib.joanneum.at/integral/ cd publications).

Sharov A.I., 2006: Exegesis of interferometric and altimetric observations in South Spitsbergen. In: H.Oerlemans (Ed.) “The Mass Budget of Arctic Glaciers”. IASC, IMAU, Utrecht, p. 88-93.

Ablation and outflow from Kaffiøyra glaciers in 1996-2006, Svalbard

Ireneusz Sobota

Department of Cryology and Polar Research, Institute of Geography, N. Copernicus University, Poland

Ablation of glaciers

The study of ablation of the Kaffiøyra glaciers refers to Waldemarbreen, Irenebreen and Elisebreen. The study of the summer balance of Waldemarbreen was based on direct field measurements conducted from 1996 to 2006. The study of the summer balance of Irenebreen was carried out between 2001 and 2006. In 2005 the study of ablation of Elisebreen began. These researches are continued (Sobota, 2004, 2005). The measurements of surface ablation were made every 5-7 days from July to September each year. All ablation poles were drilled 10 m deep with a steam driven Heucke Ice Drill (Heucke, 1999). Snow, firn and ice ablation were converted into water equivalent (w.e.).

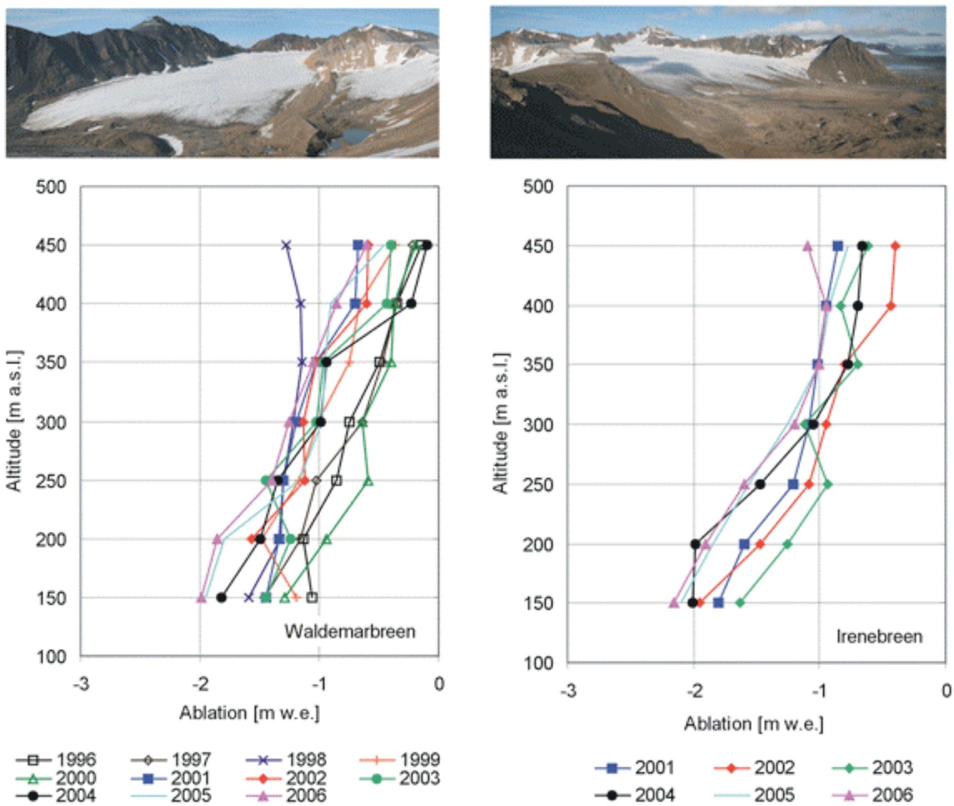

Figure 1. Ablation of Waldemarbreen and Irenebreen as a function of elevation.

Time changeability of ablation of Waldemarbreen and Irenebreen at various latitudes was significantly diverse. The greatest changeability was observed in the lowest parts of glacier. With the growing altitude the fluctuations decrease. There is a large difference in ablation intensity between the frontal part of the glacier and its accumulation part. This is mainly connected with the diverse weather conditions in these parts of glacier. The parts of glacier which are located high are influenced by lower air temperatures and thus ablation there are either much less intense or non-existent. The lowest part of glacier, however, is often located in the zone of much warmer air masses, and thus ablation are much more intensive there. Very often the altitude-related ablation is also influenced by local conditions of a given glacier, such as the slope aspect, its exposition, surrounding mountain slopes, the amount of morainic material on the glacier and the system of supraglacial streams. As far as Waldemarbreen is concerned, the highest ablation level throughout the studied period was found at the altitude of up to 250 m asl. Above that level ablation decreases. A similar situation was recorded on Irenebreen (Figure 1).

Spatial diversity of ablation of Waldemarbreen was larger compared to Irenebreen. It was mainly caused by weather conditions in the individual parts of glacier, as well as by the relief. Waldemarbreen is strongly inclined not only in its frontal part but also towards the medial moraine. Such a situation means a larger area of glacier has southern exposition; additionally, the system of supraglacial streams develops and the amount of the morainic material on the glacier's surface increases. As a result, ablation in this part of the glacier intensifies. Spatial differentiation of ablation on Irenebreen also shows some regularity. The most intensive ablation was recorded in the northern part of the frontal section of glacier, while the least intensive was recorded on the accumulation field. Lower values of ablation intensity were also recorded in the south-central part of glacier. It is located at the foot of the mountains which means sunrays are blocked there. Such a situation influences the intensity of ablation.

In 2006 there were also measurements of ablation of Elisebreen undertaken. Spatial diversity of ablation of this glacier shows clearly that the largest values were reached in the front part; they decreased towards the accumulation field, where snow cover was found throughout the entire summer season. The size of ablation in the frontal part of glacier (about 3 m of w.e.) was much higher than those of both Waldemarbreen and Irenebreen. This mainly resulted from the fact that the altitude of this part of glacier is lower.

Both Waldemarbreen's area and the altitude difference between the accumulation zone and the ablation area are relatively small. Nevertheless, spatial variation of ablation is observed. That variation is caused by local conditions such as hypsometry, solar exposition, slope as well as density and the course of supraglacial streams (Sobota, 1999, 2000, 2005). In all years the highest ablation values were observed at altitudes below 250 m a.s.l., as well as at the foot of the medial moraine.

The most negative mean summer balance of Waldemarbreen was –1.20 m w.e. in 1998 and –1.30 m w.e. in 2006, while the least negative was –0.63 m w.e. in 2000. The average summer balance of Waldemarbreen amounted to –1.04 m w.e. for the period of 1996-2006. In the years 1996-2006 the cumulated total ablation of Waldemarbreen was about –11.48 m w.e.. The average summer balance of Irenebreen amounted to –1.24 m w.e. for the period of 1996-2006. In the years 1996-2006 the cumulated total ablation of Irenebreen was about –7.40 m w.e.. In 2006 the summer balance of Elisebreen was –1.35 m w.e. Such large negative values during that period resulted from a very early beginning of the ablation season.

Outflow from glaciers

Catchment basins of six rivers can be distinguished on Kaffiøyra plain. They include Waldemar River, Irene River, Elise River, Eivind River, Andreas River and Oliver River. They all have similar (elongated) shape, although they have different areas, relief, lithology and the level of glaciation. The catchment basin of Waldemar River is the smallest; its area covers 4.4 km^2, 62% out of which is taken by Waldemarbreen. The measurement site was located at the point where the river enters the outwash plain, about 500 m from the glacier frontal part. The length of Waldemar River from that place is about 1 kilometer (Sobota, 2005). The catchment basin of River Irene takes up about 7.95 km^2, 54% of which is taken by Irenebreen. Measurement points were located in three river beds where the river enters the outwash plain; the distance to the front of glacier was about 1 km. The length of the river from that place is about 1.4 km.

The largest intensity of the discharge corresponded with the period of highest ablation level. The closest correlation was visible when a few-day values were analyzed. Additionally, there were periods when increased intensity of discharge was recorded later than the maximum of ablation. This mainly resulted from temporary retention of melted snow in the form of slush, large patches of which were found on glaciers. Consequently, high and low water stages were observed. The factor which caused this was, most of all, melting of slush, especially after intense rainfall. Water retention in the form of slush was larger than water discharge in the period preceding a high water stage. Other high water stages were caused by intensive rainfall. Low water stages were mainly caused by a drop in temperature and lack of precipitation. At the end of the ablation season ice phenomena are observed on Waldemar River and Irene River. As the indicator of irregularity of discharge shows, Waldemar River has distinctly higher changeability of discharges than Irene River. Mean discharge of Waldemar River from 1996 to 2006 was 1.21 m^3s^{-1}, while in 2006 1.08 m^3s^{-1}.

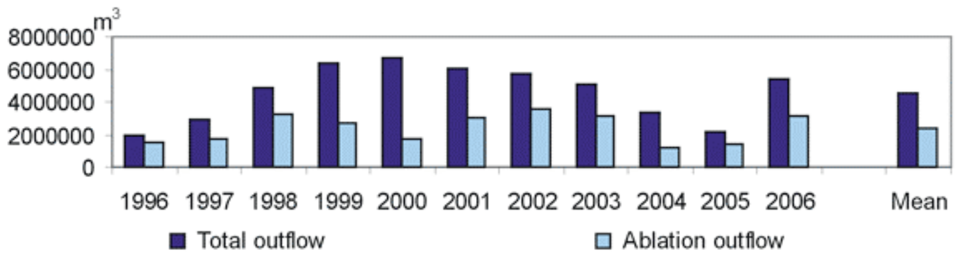

Figure 2. Outflow from Waldemarbreen in 1996-2006.

In order to measure water stages and water temperatures at 5-minute intervals the HOBO logger was used. This enabled the author to estimate the discharge rate, both daily and mean for the entire summer season.

The mean outflow from Waldemarbreen between 1996 and 2006 was 4,578,641 m^3s^{-1} of water, which was carried away by Waldemar River. The share of ablation within the outflow was, on average, 56% (Figure 2). The remaining part was made up by rainfall, outflow from the ice covers as well as other local sources of water (inter-glacier outflow, melting of snow from the mountain slopes). Despite the length of the measurements, thus, the share of ablation in the total outflow of both River Waldemar and River Irene during individual seasons is similar.

References

Heucke, E., 1999. A light portable stream-driven ice drill suitable for drilling holes in ice and firn. Geografiska Annaler , 81 A (4): 603-609.

Sobota, I., 1999. Ablation of the Waldemar Glacier in the summer seasons 1996, 1997 and 1998. Polish Polar Studies, XXVI: 257-274.

Sobota, I., 2000. Ablation and discharge of the Waldemar Glacier, north-western Spitsbergen, in summer 1998. Polish Polar Research, 21(1): 3-18.

Sobota, I., 2004. Bilans masy lodowca (1996-2003) Waldemara i lodowca Ireny (2002-2003). Polish Polar Studies, XXX: 345-355.

Sobota, I., 2005. Zarys hydrografii Kaffiøyry. The outline of Kaffiøyra hydrography. Kaffiøyra. Zarys środowiska geograficznego Kaffiøyry (NW Spitsbergen), 13-16.

MASS BALANCE MONITORING OF KAFFIØYRA GLACIERS, SVALBARD

IRENEUSZ SOBOTA

Department of Cryology and Polar Research, Institute of Geography, N. Copernicus University, Poland

Mass balance monitoring of Kaffiøyra glaciers refer to two groups of methods. First were glaciological methods. These methods include summer balance, winter balance and outflow from glaciers. Direct glaciological investigations of the glacier mass balance are not always possible. Therefore, an attempt to assess the mass balance of glaciers through indirect methods was undertaken. These methods were divided into three major groups: climatic, hydrologic and geodetic. These studies refer to the Waldemarbreen, Irenebreen and Elisebreen. The data on the structure of the mass balance of Waldemarbreen were based on the direct field measurements conducted from 1996 to 2006 (Sobota, 1999, 2000, 2004, 2005, Grześ and Sobota, 2000). The studies of the mass balance of Irenebreen were taken between 2001 and 2006. In 2005 the studies of the mass balance of Elisebreen began. These investigations are continued. At the same time geodetic and cartographic measurements were carried out (Lankauf, 2002, Bartkowiak et al., 2004).

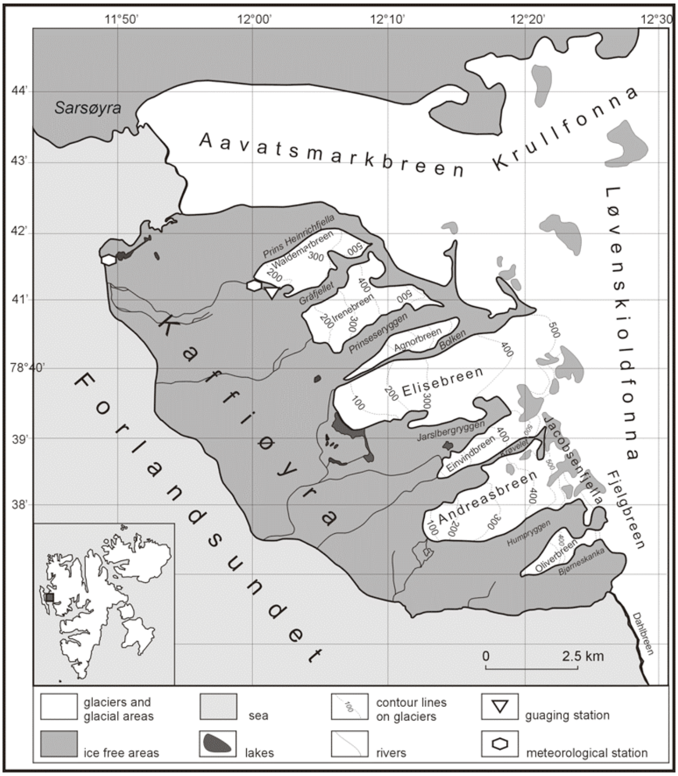

Figure 1. Location map of Kaffiøyra glaciers.

Glaciers are located in the northern part of the Oscar II Land, Kaffiøyra, north-western Spitsbergen. Waldemarbreen is about 3.5 km long and has an area of 2.6 km^2. The ice originates in one cirque and flows from an elevation of more than 500 m to the present terminus at 130 m a.s.l.. Irenebreen, a valley glacier located to the south of Waldemarbreen, flows down towards the Kaffiøyra plain. The area of Irenebreen amounts to 4.2 km^2. Elisebreen area is 11.9 km^2. Its length is about 7 km, while its width is up to 1.8 km. To the north the glacier borders Agnorbreen which is often treated as part of Elisebreen (Figure 1).

In order to estimate the mass balance of Kaffiøyra glaciers the method of direct measurements was used. It was based on a set of ablation poles completed with the studies of the snow cover in the snow profiles. This method belongs to the most precise and most often used (Østrem and Brugman, 1991; Kaser et al.; 2003, Hubbard and Glasser, 2005). Twenty-two poles were placed on Waldemarbreen; Irenebreen and Elisebreen had ten poles installed each. All the ablation poles were drilled 10 m deep with a steam driven Heucke Ice Drill (Heucke, 1999). Snow, firn and ice ablation were converted into water equivalent (w.e.).

The studies of winter mass balance mainly referred to the estimation of the size of the snow accumulation on glaciers, as well as its selected properties. Soundings of the snow depth on both Waldemarbreen and Irenebreen were carried out in about 150 measurement points. Location of the measurement points was based on both geodesic and the GPS measurements. The measurements also were made in the selected snow profiles in accordance with the International Commission on Snow and Ice (ICSI) standards.

The studies on the summer and winter balance enabled the author to estimate the net mass balance of the studied glaciers in the analysed period.

Time changeability of ablation processes of Waldemarbreen and Irenebreen at various latitudes was significantly diverse. The greatest changeability was observed in the lowest parts of glacier. With the growing altitude the fluctuations decrease.

Spatial distribution of winter snow accumulation on Waldemarbreen shows some regularity. The largest accumulation is found in the accumulation part and at the foot of the mountain slopes. The smallest accumulation, however, is observed in the front part of glacier up to the altitude of 220 m and at the foot of the medial moraine. In the case of Irenebreen snow accumulation increases significantly from the front part of glacier towards the accumulation fields. In 2005 and 2006 measurements of snow accumulation on Elisebreen were taken as well.

The lowest snow accumulation on Waldemarbreen was recorded in 2000; it amounted to 0.32 m w.e. on average. The highest snow accumulation of 0.75 m w.e. was recorded in 1996. From 1996 to 2006 the mean snow accumulation on Waldemarbreen was 0.47 m w.e. From 2002 to 2006 the mean snow accumulation value for Irenebreen was 0.52 m w.e. In 2005 the snow accumulation for Elisebreen was 0.59 m w.e., while in 2006 it was 0.63 m w.e. These values are similar to those estimated for other studied Svalbard glaciers.

Mass balances of glaciers based on a network of poles are burdened with measuring errors. They result from reading errors of the poles, as well as from the influence of the morphological conditions of a given glacier, which often make field-readings difficult. Additionally, mass balance estimations are influenced by a complicated process of glacier feeding and its outflow. As numerous papers indicate, a standard measuring error can be calculated: its value is similar for most glaciers. It was also found out that the direct measurements of mass balance of Waldemarbreen, Irenebreen and Elisebreen are burdened with a small error. This mainly results from reading errors of the measurement ablation poles. Errors connected with the inner accumulation, condensation and evaporation do not play a significant role in estimating the size of glacier's mass balance. The error of the annual mass balance for Waldemarbreen, Irenebreen and Elisebreen, based on various methods and formulas used by various authors, as well as on direct field measurements, was estimated at about ± 0.10-0.20 m w.e.

Spatial diversity of mass balance of Waldemarbreen, Irenebreen and Elisebreen is mainly influenced by the weather conditions in a specific part of glacier and by local morphological conditions. The areas of the glaciers may be generally divided into the part of the negative mass balance and the part of the positive mass balance. In the case of Waldemarbreen the year 1998 was exceptional, as the entire glacier showed negative mass balance. Irenebreen shows more positive mass balance in its both accumulation parts. The accumulation part of Elisebreen also shows positive mass balance. This results from the fact that they both are located at higher altitude than Waldemarbreen.

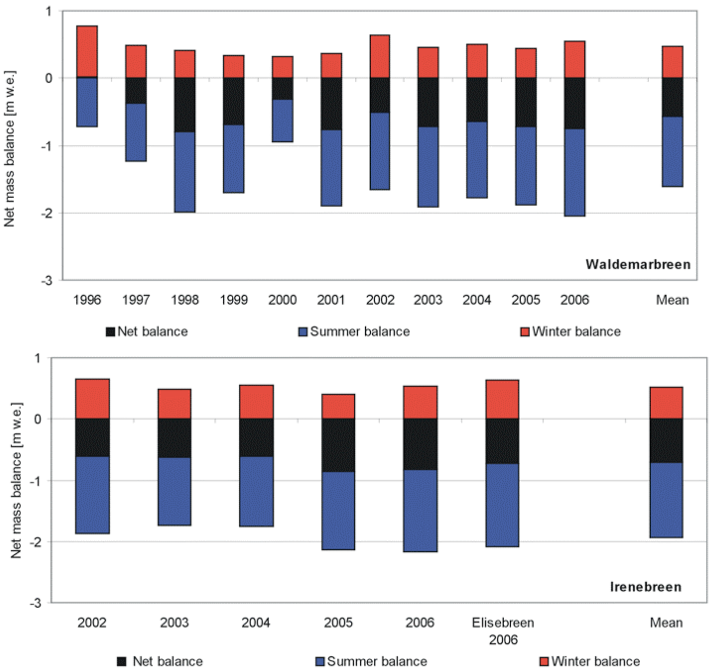

Figure 2. Winter, summer, and net balances for Kaffiøyra glaciers (Waldemarbreen, Irenebreen and Elisebreen).

The results of the mass balance structure of Kaffiøyra glaciers are shown on figure 2. The average mass balance of Waldemarbreen amounted to –0.57 m w.e. in 1996-2006. Between 2002 and 2006 the mean annual mass balance of Irenebreen was –0.71 m w.e. In 2006 the mass balance of Elisebreen was –0.73 m w.e., and was similar to other glaciers of the region, even though its winter mass balance was larger. In this case the important factor was the low altitude of the frontal part of the glacier which results in intensive ablation.

Mean annual net mass balance of Kaffiøyra glaciers (Waldemarbreen and Irenebreen) is close to other Svalbard glaciers of similar size. These glaciers have negative long-term mass balance.

The mass balance record on Waldemarbreen, Svalbard, is especially important because it is one of the few long-term mass balance records on Svalbard.

References

Bartkowiak, Z., Lankau,f K.R., Sobota, I., Zawicki R., 2004. Wstępne wyniki zastosowania technik GPS w pomiarach geodezyjnych na lodowcu Waldemara (NW Spitsbergen). Polish Polar Studies. XXX Międzynarodowe Sympozjum Polarne, Gdynia, 21-27.

Grześ, M. and Sobota, I., 2000. Winter snow accumulation and winter outflow from the Waldemar Glacier (NW Spitsbergen) between 1996 and 1998. Polish Polar Research, 21(1): 19-32.

Heucke, E., 1999. A light portable stream-driven ice drill suitable for drilling holes in ice and firn. Geografiska Annaler , 81 A (4): 603-609.

Hubbard, B. and Glasser, N., 2005. Field techniques in glaciology and glacial geomorphology. John Wiley & Sons, Ltd.

Kaser, G., Fountain, A. and Jansson, P., 2003. A manual for monitoring the mass balance of mountain glaciers. IHP-VI, Technical Documents in Hydrology, UNESCO, Paris, 59: 0-107.

Lankauf, K. R., 2002. Recesja lodowców rejonu Kaffiøyry (Ziemi Oskara II-Spitsbergen) w XX wieku. Prace Geograficzne, 183.

Østrem, G. and Brugman, M., 1991. Glacier mass-balance measurements: a manual for field and office work. National Hydrology Research Institute Science Report No. 4.

Sobota, I., 1999. Ablation of the Waldemar Glacier in the summer seasons 1996, 1997 and 1998. Polish Polar Studies, XXVI: 257-274.

Sobota, I., 2000. Ablation and discharge of the Waldemar Glacier, north-western Spitsbergen, in summer 1998. Polish Polar Research, 21(1): 3-18.

Sobota, I., 2004. Bilans masy lodowca (1996-2003) Waldemara i lodowca Ireny (2002-2003). Polish Polar Studies, XXX: 345-355.

Sobota, I., 2005. Struktura bilansu masy lodowców Kaffiøyry na tle lodowców Svalbardu. Kaffiøyra. Zarys środowiska geograficznego Kaffiøyry (NW Spitsbergen), 43-60.

RELATIONSHIP OF EQUILIBRIUM LINE ALTITUDE (ELA) AND ACCUMULATION AREA RATIO (AAR) WITH MASS BALANCE OF KAFFIØYRA GLACIERS, SVALBARD

IRENEUSZ SOBOTA

Department of Cryology and Polar Research, Institute of Geography, N. Copernicus University, Poland

A detailed analysis of both spatial and latitudinal changeability of the glaciers' mass balance was carried out. The position of the equilibrium line altitude (ELA) and the size of the accumulation area ratio (AAR) were established. Waldemarbreen, Irenebreen and Elisebreen are located in the northern part of the Oscar II Land, Kaffiøyra, north-western Spitsbergen.

In order to estimate the mass balance of Kaffiøyra glaciers the method of direct measurements was used. It was based on a set of ablation poles completed with the studies of the snow cover in the snow profiles. This method belongs to the most precise and most often used (Østrem and Brugman, 1991; Kaser et al., 2003). Twenty-two poles were placed on Waldemarbreen; Irenebreen and Elisebreen had ten poles installed each.

One of the aims of this paper was to work out the formula on the basis of which it would be possible to calculate the size of mass balance closest to the ones obtained the use of the glaciological method. Due to the fact that the direct method refers to the period 1996-2006, the author decided to try and estimate the mass balance of Waldemarbreen in the indirect way for a longer period of time, i.e. 1970-2004. Generally, it was based on the high correlation between mass balance and the equilibrium line altitude (ELA) and accumulation area ratio (AAR).

Due to lack of information on the value of both the ELA and the AAR in the period preceding the direct field studies, the establishing of their size was based on their dependency on the selected meteorological parameters. These research methods were called climatic methods. Climatic methods are widely applied for glacier investigations. They are based on the correlation of ELA and AAR with meteorological parameters and describe the influence of such elements as air temperature (PT-model) and PDD (PDD-model).

Thanks to the direct measurements, the average location of the equilibrium line on Waldemarbreen was estimated at the altitude of 397 m in 1996-2006. From 2002 to 2006 the annual equilibrium line altitude was 421 m a.s.l. for Irenebreen, while for Elisebreen it was 365 m a.s.l. (Figure 1). The equilibrium line altitude is correlated with the size of the mass balance of Waldemarbreen, and its course is an important indicator of the mass balance. Similarly, the accumulation area ratio AAR is significant; its values increase when the mass balance increases. The AAR coefficient for Waldemarbreen between 1996 and 2006 ranged from 0% to 48%.

For Irenebreen from 2002 to 2006, however, the values of AAR range from 29% to 10%.

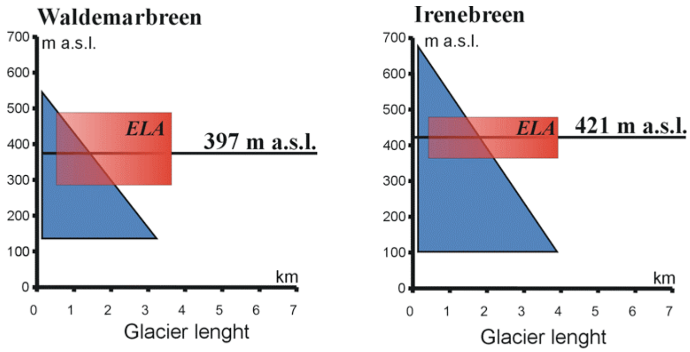

Figure 1. Equilibrium line altitude (ELA) on Waldemarbreen in 1996-2006 and Irenebreen in 2002-2006.

Significant interrelation was found between both the equilibrium line altitude (ELA) and the accumulation area ratio (AAR), and the mass balance of Waldemarbreen between 1996 and 2006. The correlation coefficient was 0.88 and 0.87, respectively.

High correlation between both the sizes of the ELA and the AAR, and the PDD and the mean air temperature between June and September brought the author to estimating the ELA and AAR values for a period of time between 1970 and 2004, i.e. longer than the direct field studies themselves. This, in turn, was the basis to estimate the mean altitude of the ELA, conditioned by the mean air temperature, to be at 353 m asl between 1970 and 2004, while between 1996 and 2004 it was 290 m a.s.l. This value for the latter period of time, based on the field measurements, amounted to 389 m asl. From PDD-model, the altitude of the ELA between 1970 and 2004 was 356 m a.s.l., while for the period between 1996 and 2004 it was 385 m a.s.l. It is clear that this method gives very similar results to those measured directly, and thus can be a substitute method for estimating the value of the ELA, used in the case when the direct measurements conducted on a glacier are impossible.

Taking the same interrelations into consideration, the author tried to estimate the value of the accumulation coefficient AAR for the period between 1970 and 2004. The received values were close to those based on the direct studies of the mass balance of the Waldemarbreen. The average value of the AAR coefficient based on the interrelation with the mean air temperature (VI-IX) for this period was 29%, while for the period of 1996-2004 it was 21%. Its measured value for that period was 22%. Considering the interrelation between the AAR and the PDD, the AAR mean value for this long-term period also amounted to 29%, while in the years 1996-2004 it amounted to 23%.

The estimated long-term values for 1970-2004 of both the ELA and the AAR, the parameters highly correlated with the measured mass balance. The mean ice mass balance for this long-term period, based on the correlation with the ELA, was -0.41 m w.e.; for the comparison period of time of 1996-2004 it was -0.52 m w.e. The measured mass balance for this period was -0.54 m w.e. The mass balance based on the correlation with the AAR was -0.40 m w.e. in the years 1970-2004, while in the years 1996-2004 it was -0.51 m w.e. It was, thus, similar to the sizes of the measured mass balance (Figure 2).

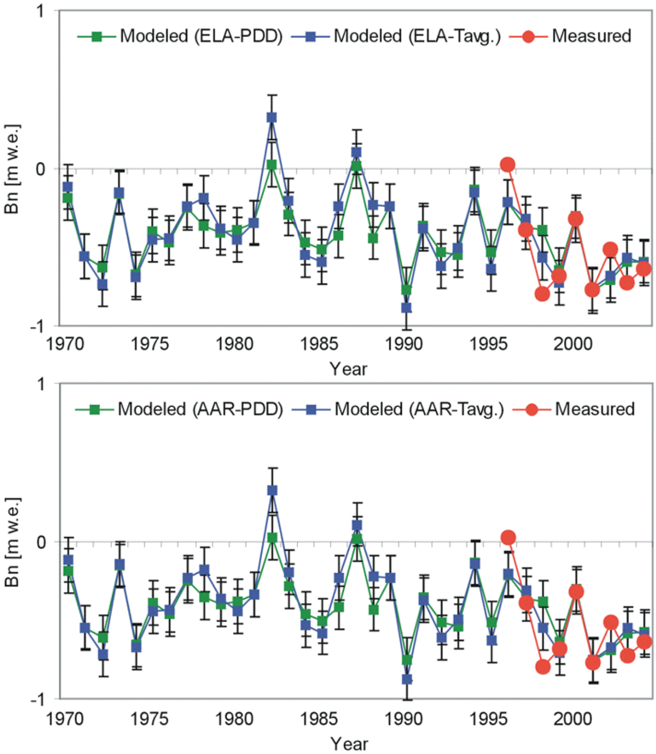

Figure 2. Mass balance of Waldemarbreen with error columns measured and modeled on the grounds of the relationship between ELA, AAR and the net balance of Waldemarbreen and the average air temperature (Tavg.) and positive degree-days (PDD) in June-September for the period of 1970-2004.

Direct glaciological investigations of the glacier mass balance, ELA and AAR are not always possible. Therefore, an attempt to assess the mass balance of Waldemarbreen through indirect methods was undertaken. The obtained results prove both validity and accuracy of these methods. They made it possible to define and recognise the variable elements of the glacier balance over dozens of years preceding the study period.
The resulting values of the mass balance of Waldemarbreen are similar to those of other Svalbard glaciers, which terminate on land and thus present the view of this phenomenon within the last decades.

References

Kaser, G., Fountain, A. and Jansson, P., 2003. A manual for monitoring the mass balance of mountain glaciers. IHP-VI, Technical Documents in Hydrology, UNESCO, Paris, 59: 0-107.

Østrem, G. and Brugman, M., 1991. Glacier mass-balance measurements: a manual for field and office work. National Hydrology Research Institute Science Report No. 4.

MASS BALANCE OBSERVATIONS ON SOME GLACIERS IN 2004/2005 AND 2005/2006 BALANCE YEARS, NORDENSKIOLD LAND, SPITSBERGEN

IRINA Y. SOLOVYANOVA[1] AND B.R. MAVLYUDOV[2]

[1] Arctic and Antarctic Research Institute. “FRAM” Arctic climate laboratory. St-Petersburg, Russia
[2] Institute of Geography Russian Academy of Sciences, Moscow, Russia

Significant climatic changes in the Arctic regions environments within the last decades are marked. The small mountain-valley glaciers of Spitsbergen are the fine indicators of these changes. Mass balance investigations on Spitsbergen glaciers located near to the Russian settlements, were on a regular basis realized by the Institute of geography of the USSR Academy of Sciences since 1974. Thus unique data about the archipelago glaciers conditions have been obtained. So for Vøring Glacier the length of the observational series of mass balance measurements is 25 years, and for Western Grønfjord Glacier - 10 years (Glaciology, 1985; Guskov, Gordejchik, 1978, Troitskij, 1988a,b). However these investigations have been stopped at the end of the 1980s. In 2003 spring mass balance investigations have been initiated on Aldegonda Glacier, in 2004 – on Western Grønfjord Glacier, and in 2005 are renewed on Vøring Glacier (Figure 1).

Figure 1. Position of studied glaciers.

Aldegonda Glacier is located on the western coast of Grønfjord 7 km southwest of Barentsburg (Nordenskiold Land). It has a west-east direction with length of about 3 km, width up to 2 km, and ice thickness up to 216 m. Within the 20th century the glacier has retreated from the seacoast over a distance of about 2 km. The lower point of the glacier tongue is located at 80 m asl, and the ridges around the glacier at about 600 m asl. The average elevation of glacier surface is about 275 m asl.

Western Grønfjord Glacier is located 12 km southwest of Barentsburg. The total glacier area is about 27 km^2. Within the 20th century the glacier has retreated about 3 km. The lower point of the glacier tongue is located at 60 m asl, and the ridges around the glacier at about 750 m asl. The average elevation of glacier is about 350 m asl.

Vøring Glacier is located on the western coast of Grønfjord 4 km to the west of Barentsburg. It has a west-east direction with length of about 1 km, and width up to 800 km. The glacier has lost almost half of its area from 1936. The lower point of the glacier tongue is located at 120 m asl, and the ridges around the glacier at about 600 m asl. The average elevation of a glacier is about 240 m asl. Melt water of this glacier feeds the Barentsburg drinking lake.

Because of all these differences it was assumed that these glaciers might have different mass balances. But our observations showed that all glaciers have strong negative net mass balances and almost the same shape of winter and summer mass balances curves. Why does this is happen? Probably due to position of these glaciers very close to the warm Atlantic Ocean current and air masses.

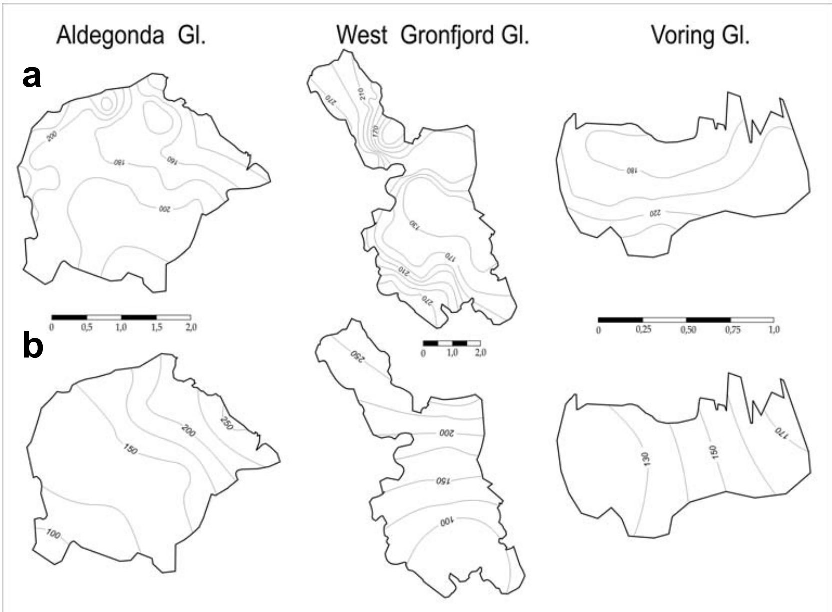

Figure 2. Mass balance investigations on studied glaciers; a) B_w in cm w.e., b) B_n in cm w.e.

Winter balance (B_w)

The winter balance of all glaciers was based on the results of snow surveys, which are performed in last week of April or in first week of May.

Aldegonda Glacier. The snow cover on the glacier surface in the spring of 2005 differed in uniformity; the snow cover thickness variation coefficient was about 0.17. Monotonous snow layering was caused by the glacier surface structure. There was insignificant increase in snow thickness on the periphery of the glacier that apparently was caused by avalanches action (Figure 2a). Average snow cover thickness on the glacier in May 2005 was 194 cm (133-261 cm). Snow density increased from the tongue to the upper part of the glacier from 0.29 to 0.39 g/cm^3 (average 0.34 g/cm^3). Accordingly values of general water stored in the snow cover slightly increased with glacier surface elevation increase. Average winter balance on the glacier was equal to 68 cm w.e. (Table 1).

Soft meteorological conditions in winter 2006 have determined the features of the snow cover distribution. Average snow thickness on Aldegonda Glacier surface was equal to 153 cm (121-190 cm). Snow density changed from 0.42 to 0.52 g/cm^3 (average 0.47 g/cm^3) which mainlu has been caused by increased snow water content. Average winter mass balance on the glacier was equal to 74 cm w.e.

Western Grønfjord Glacier. Snow cover distribution on the glacier has precisely expressed high-altitude dependence. In the spring of 2005 snow thickness on a profile changed from 88 cm in the lower glacier part (Figure 2a) up to 268 cm in its upper part at the elevation of 450 m. Average snow thickness value on the glacier was equal to 177 cm. Thus snow thickness increase at the glacial circus edges in the upper glacier part was also marked. Snow cover integrated density also increased upward on the glacier, and on average was equal to 0.37 g/cm^3. The vertical gradient of the general water-content in the snow cover in spring 2005 was equal to 30 cm w.e. at 100 m. Average value of the winter balance on Western Grønfjord Glacier was about 63 cm w.e.

A distinctive feature in the snow cover layering on Western Grønfjord Glacier surface in spring 2006 was the presence of a water layer up to 10 cm in the snow measured in prospect-holes at elevation up to 200 m. It has affected the snow cover density, which at the bottom of the prospect-holes was equal 0.53 g/cm^3. Water layer volume in mass balance calculations was not considered because of the impossibility of precise boundary definition of this layer spreading on the glacier surface. Snow thickness had an obvious high-altitude dependence. Average vertical gradient of snow cover water content on the glacier in spring 2006 was about 29 cm w.e. at 100 m. On average the glacier surface snow cover thickness was equal to 142 cm. The winter balance for Western Grønfjord Glacier in 2006 was about 93 cm w.e.

Vøring Glacier. The average snow cover thickness was equal to 186 cm. Value of integrated density in the upper part was lower than on the glacier tongue which was caused by the absence of consolidating wind action in isolated glacier circus. Average snow cover density on the glacier was equal to 0.33 g/cm^3 which is below corresponding values of other studied glaciers at similar elevations (Figure 2a). The winter glacier mass balance was about 54 cm w.e.

In connection with the inaccessibility of Vøring Glacier for transport in spring 2006 a study of the winter component of the mass balance was not made. Their values have been derived by the method of analogies. Estimated winter mass balance of the glacier was equal to 87 cm w.e.

Table 1. Surface mass balance data of research glaciers

	Aldegonda Glacier	Western Grønfjord Glacier	Vøring Glacier
		2002/2003	
B_w m w.e.	0.56		
B_s m w.e.	-2.10		
B_n m w.e.	-1.54		
ELA	700		
		2003/2004	
B_w m w.e.	0.52		
B_s m w.e.	-2.12		
B_n m w.e.	-1.63	-1.09	
ELA	700	650	
		2004/2005	
B_w m w.e.	0.68	0.63	0.54
B_s m w.e.	-2.09	-2.11	-1.81
B_n m w.e.	-1.41	-1.48	-1.27
ELA	>500	>600	500
		2005/2006	
B_w m w.e.	0.74	0.93	0.87
B_s m w.e.	-2.05	-1.99	-1.79
B_n m w.e.	-1.31	-1.06	-0.92
ELA	460	500	500

* Investigations of ice ablation begun only on 2003 July 17 and actual values of B_n and B_s were much higher.

Summer balance (B_s)

Melted thickness of the snow and ice layer for the summer season depends on air temperature, presence or absence of low clouds above the glacier surface. Ablation intensity also sharply increases with increase of liquid precipitation. For the determination of the summer ablation values on the investigated glaciers ablation sticks have been placed making it possible to characterize ablation at different elevation zones (Figure 2b).

Aldegonda Glacier. Ice and snow melting on Aldegonda Glacier in 2004/05 changed from -1.67 to -2.37 m w.e. At elevation interval of 200-300 m, covering the greatest part of the glacier area (55 %), the average ablation value was about -235 cm w.e. The value of the summer balance was about -209 cm w.e. In 2005/06 ice melting on Aldegonda Glacier changed from -31 cm w.e. above 475 m up to -200 cm w.e. and more at elevation less than 100 m. There is a clear elevation dependence of the summer ablation value on the glacier surface (R^2=0.8). Elevation ablation gradient is equal to -48 cm w.e. on 100 m.

Western Grønfjord Glacier. Average value of measured surface ablation by sticks during 2004/05 on the glacier was about -160 cm w.e. with a maximal absolute value at the glacier tongue at elevations less than 100 m of about -287 cm w.e. and minimal at elevation above 550 m of about -100 cm w.e. Average summer mass balance on glacier (ablation sum of snow and ice) was equal to -211 cm w.e.

Losses of glacier ice have consisted about 51.3 million M^3. Elevation ablation gradient was about -38 cm w.e. per 100 m.

A Linear function approximating the dependence of the summer ablation (A) on glacier surface elevation (x) for 2005/06 looks like A= -0.5592x + 288.45 (R^2 = 0.86). Thus the elevation ablation gradient was equal to -56 cm w.e. per 100 m. A feature of the 2006 summer season was the preservation of not melted snow spots up to the end of season on some parts of the upper elevation intervals, i.e. here the summer balance was positive. However, in the mountain pass area at an elevation of about 600 m the measured value of summer ablation was equal to about -18 cm w.e. Thus in spite of the presence of some areas with a positive mass balance, the average value of summer surface ablation in 2005/06 on Western Grønfjord Glacier was about -211 cm w.e.

Vøring Glacier. The 2004/05 summer mass balance on this glacier was about -181 cm w.e. The elevation ablation gradient was about -53 cm w.e. per 100 m. On the base of the investigated data, the 2005/06 value of the summer surface ablation on the glacier did not exceed -180 cm w.e. In spite of small difference in elevations of ice surface elevation the ablation gradient was about -62 cm w.e. per 100 m. The summer mass balance was equal to -171 cm w.e.

Net balance (B_n)

Annual mass balance (specific balance) was determined at the end of the ablation period as the algebraic sum of the summer and winter balances. In 2004/05 for Aldegonda Glacier it was equal to about -141 cm w.e., for Vøring Glacier about -127 cm w.e., and for Western Grønfjord Glacier annual balance was about -148 cm w.e. In 2005/06 the values of the annual mass balance of the investigated glaciers was about - 131, -92 and -106 cm w.e., respectively.

Discussion

A feature of all studied glaciers is that the degradation has similar characteristics: during the last two years the ablation on the glaciers has a little changed. In 2001-2004 ice melting has a general uniform distribution over the glaciers area. In 2005-2006 there is very clear elevation-ablation dependence and in the lower parts of the glaciers ablation intensity increased but in upper glacier parts decreased. We do not know the reasons for this phenomena but it is clear that it is connected with changes in air stratification above the glaciers.

The ELA is directly connected with the studied glaciers mass balance. ELA determination on the Spitsbergen glaciers was realized in 1960-1980 (Zinger, Mickhajlev, 1967, Glaciology, 1985) and varied between about 300-400 m asl. Continuous climate warming has led to the situation where during the years after this period ELA on the glaciers has essentially risen having reached elevations of about 700 m asl at the beginning of the 21st century (Mavlyudov, 2004) (Table 1). Long and multisnow winter 2004/2005 has affected the ELA. In 2005 the ELA position was fixed at a height of about 500 m asl for Vøring Glacier, at a height over 500 m for Aldegonda Glacier and at a height over 600 m for Western Grønfjord Glacier. In 2006 almost the same ELA values was found on the glaciers. In spite of the fact that in 2005 and 2006 ELA lowering was occurred in comparison with other years, the surfaces of almost all investigated glaciers still remained below ELA. It means that masses reduction occurred on all surface of glaciers.

Various references from the beginning of 20th century note retreating of Arctic glaciers tongues and glacial sheets located at small elevations. Comparison of mass balance data for Western Grønfjord and Vøring Glaciers for the last years with mass balance data for 2004/2005 and 2005/2006 allows to say that reduction of winter balance and increase of summer balance occurred and, as a consequence there was growth of annual glacial mass consumption. In contrast to some researchers (Dowdeswell et al., 1997) we can speak about essential glacier ablation increase. Probably such a positive trend in annual balance increase is traced only for rather small mountain-valley glaciers, which partially or completely lost their accumulation areas such the as investigated glaciers. It is possible that by consideration of general tendency of all archipelago glaciation change, the contribution of small glaciers to mass balance changes will not be so visible. However the objective estimation of archipelago glaciation change demands studying of these glaciers also.

Conclusion

The steady negative annual mass balance of the investigated Spitsbergen glaciers during last decades shows a proceeding warming in this Arctic sector. This conclusion is especially important since there are data about the onset of cooling of the global ocean, which can cause cooling of continents in future (Byshev et al., 2005). Probably noted ocean water-cooling is not very steady yet or still very small, or it has no direct influence on continents climate even on such seaside areas as the Spitsbergen archipelago.

Literature

Byshev V.I., Neumann V.G., Romanov Ju.A. (2005) About different directional changes of a global climate on continents and oceans. Reports of the Russian Academy of Sciences, 400(1), 98-104 (in Russian).

Dowdeswell J.A. et al. The mass balance of circum-arctic glaciers and recent climate change // Quat. Res. 1997. V. 48. P. 1-14.

Glaciology of Spitsbergen. Moscow, "Nauka", 1985, 200 p. (in Russian).

Guskov A.S., Gordejchik A.V. (1978) Water-ice balance of Spitsbergen glaciers in 1975/76 balance year. – Data of Glaciological Studies, 33, Moscow, 207-211 (in Russian).

Mavlyudov B.R. (2004) About degradation of Spitsbergen mountain-valley glaciers. - Complex researches of Spitsbergen nature, Iss. 4. Apatity, KNC RAS, 207-216 (in Russian).

Troitskij L.S. (1988a) Mass balance of different types glaciers on Spitsbergen. Data of Glaciological Studies, 63, Moscow, 117-121 (in Russian).

Troitskij L.S. (1988b) About mass balance of Spitsbergen glaciers in 1985/1986, 1986/1987 and 1987/1988 balance years. Data of Glaciological Studies, 63, Moscow, 194-197(in Russian).

Zinger E.M., Michajlev V.I. (1967) Snow accumulation on Spitsbergen glaciers – Data of Glaciological Studies, 13, Moscow, 86-100 (in Russian).

GEODETIC INVESTIGATIONS ON DYNAMIC PARAMETERS OF THE WEST GREENLAND INLAND ICE

MANFRED STOBER

Department of Surveying and Geoinformatics, Stuttgart University of Applied Sciences, Germany

Investigations on the inland ice

Since 1991 a glaciological geodetic program is performed in order to determine flow velocity, deformation and elevation change in the western part of the Greenland ice sheet.

There are two main test areas, SWISS-CAMP and ST2.

The first test field at Swiss-Camp (ETH/CU-Camp) was started in 1991. It consists of 4 stakes (triangle with 1 point in its centre). Swiss-Camp is situated 80 km East of the coastal village of Ilulissat (Jakobshavn), at latitude = 69° 34' 00" N, longitude = 49° 20' 00" W, ellipsoidal altitude = 1170 m near the equilibrium line (Reeh, 1989). It is a long-term project with a total of 9 field campaigns in years 1991, 1994, 1995, 1996, 1999, 2002, 2004, 2005 and 2006.

The second test field ST2 was established in 2004. It has the same net design than at Swiss Camp (4 stakes, triangle with 1 point in its centre). ST2 is situated at latitude = 69° 30' 28" N, longitude = 49° 39' 09" W, ellipsoidal height = 1000 m, so 170 m lower than Swiss-Camp, approximately 14 km south-west from Swiss-Camp. Here we have had three campaigns in 2004, 2005 and 2006.

The geodetic measuring program 2006 was similar to previous campaigns. All GPS measurements were done by 2 receivers Leica System 500 and 2 receivers Leica System 1200, with real-time equipment.

- Reference for all measurements is point EUREF 0112 on solid rock in Ilulissat.
- Static GPS baseline 65 or 80 km to ice reference station in test field.
- Measurement of the actual stake positions.
- Reconstruction and staking out of old stake positions from 1994, 1995, 1996, 1999, 2002, 2004 and 2005.
- Measuring actual heights at all these old positions by real-time GPS.
- Measuring of snow depth in order to reduce heights to ice surface.
- Topographical survey of snow surface by grid points every 200 meters and kinematic GPS profiling.

At the area **Swiss-Camp** elevation changes were derived from digital terrain models of the ice surface topography as well as from concrete previous point positions. Both methods result in the same average elevation change. Figure 1 shows the elevation change 1991 – 2006 from concrete (previous) stake point positions.

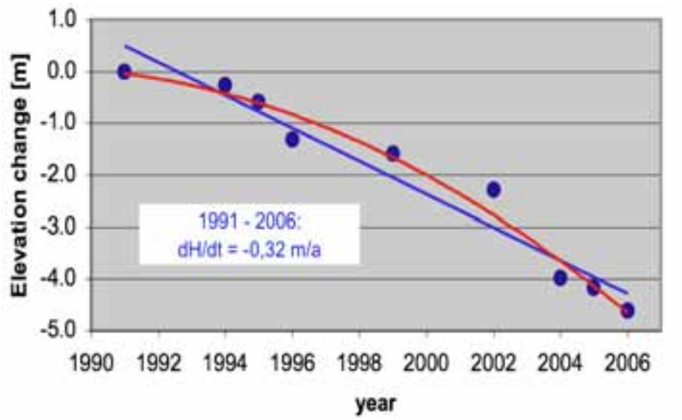

Figure 1. Elevation change of ice horizon at Swiss Camp 1991 – 2006.

The adjusted straight line over the whole period 1991 - 2006 shows an average elevation change of –0.32 m/a. Temporal variations up to a decrease of –0.85 m/a according to higher summer air temperature are clearly visible. All the extremely large elevation changes 1995-1996, 2002-2004 and also 2005-2006 coincide with the highest summer air temperatures (Steffen, 2005). In the last year we find an elevation decrease of –0.44 m/a. In the years 1991 until 2002 the linear trend was –0.22 m/a. In general, an increasing elevation decrease for future years is assumed (red line in Figure 1).

The ice flow velocity at Swiss-Camp in average is 0.317 m/d. We find continuously increasing values with years (Figure 2). That is also confirmed by comparison of two stakes in different years, but same local position (Table 1). The flow azimuth is still constant. The flow acceleration can be explained by increased basic sliding of the ice on the bedrock, due to the climate change (higher temperatures), which will affect more melt water on the glacier basin. A similar effect, caused by seasonal variation of temperature in summer or wintertime, was demonstrated by Zwally et al., 2002.

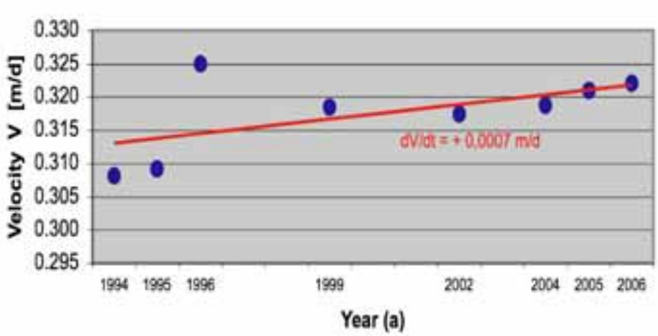

Figure 2. Swiss Camp: Ice flow velocity [m/d], 1991 – 2006.

The area **ST2** is situated in 1000 m altitude, 170 m lower than Swiss Camp. This test field was established in 2004 and re-measured first time in 2005 and again in 2006.

Table 1. Comparison of ice flow velocity at same position after 10 years

Point	Period	Flow velocity [m/d]	Flow azimuth [gon]
106.1	1994-1995	0.309	260.547
121	2004-2005	0.318	260.713

The elevation change was derived from digital terrain models over all the 1,6x1,6 km^2 area in 2004, 2005 and 2006, calculated from grid points every 200 meters and some kinematic GPS profiles. In average, between 2004 and 2005, we registered an elevation decrease –0.38 m/a. Between 2005 and 2006 the decrease was –0.30 m/a. Both periods are still too short for a long term interpretation. The average linear trend –0.34 m/a is in the same order and well agreeing with the results at Swiss-Camp.

The ice flow vector of area "ST2" in average gives the flow velocity of 0.20 m/d with a flow azimuth 266.4 gon. The flow velocity is significantly slower than at Swiss-Camp. This is in agreement with flow models, which indicate the fastest horizontal velocity at the equilibrium line (near Swiss-Camp)

Validation of airborne measurements

The very precise terrestrial surveys of the test fields Swiss-Camp and ST2 can also be used for validation of airborne measurements. In the period 1994-1999, Krabill (2000) has derived by laser altimetry (ATM) an annual elevation decrease of -0.2 to -0.3 m/a, and –0.6 m/a in the period 1997-2003 (Krabill et al. 2004). These values are well agreeing with the results in Figure 1. In the period 2002 – 2005 the ATM elevation change was about zero (not easily visible from coloured graphical display in Krabill et al. (2005)), less agreeing with the terrestrial measurements, which give here –0.6 m/a (Figure 1).

Flow velocity of glacier Eqip Sermia

The flow azimuth of Swiss-Camp and ST2 shows an ice flow towards the glacier Sermeq Avangnardleg ("North Glacier"), which is belonging to the catchment basin of Jakobshavn Isbrae glacier. This glacier is actually thinning and has doubled its speed in the last 10 years (Joughin et al. 2004, Maas et al. 2006). In order to compare flow velocities in different glaciers, we decided in 2005 to determine the flow velocity of the Eqip Sermia, situated only 80 km North from the Jakobshavn Glacier.

As measuring technique the terrestrial photogrammetry was applied with following features:

- Baseline for stereophotos = 120 m, on side moraine near glacier front
- Digital camera Canon EOS 350D, camera calibration by PhotoModeler 5.0,
- absolute and relative GPS-positioning of camera stations,
- repetition of measuring procedure after 7 days
- Evaluation by software Summit Evolution.

As preliminary result we obtain an average flow velocity of 3.1 m/d. Compared to 3.5 m/d in 1959 (Bauer, 1968) there is no significant change in velocity, contrarily to the recent velocity acceleration of the Jakobshavn Isbrae glacier.

The glacier front is compared by aerial photos from 1953 (Bauer, 1968), geodetic measurements in 1959 (Bauer, 1968) and LandSat satellite photo from 2001. In all the time the front was unchanged.

Summarizing the Eqip Sermia shows very stable behavior, while Jakobshavn Isbrae changes speed, thickness and front completely. In spite of similar climate change in the whole area, glaciers obviously react in very different way.

References

Bauer, A.: Le glacier de Eqe (Eqip Sermia) mouvement et variations du front (1959). Meddelelser om Groenland, Vol. 174, Nr. 2, Koebenhavn 1968.

Joughin, I., W. Abdalati, M. Fahnestock: Large fluctuations in speed on Greenland's Jakobshavn Isbrae glacier. Nature, 432, 608-610, 2004.

Krabill, W./ Abdalati, W./ Frederick, E./ Manizade, S./ Martin, C./ Sonntag, J./ Swift, R./ Thomas, R./ Wright, W./ Yungel, J.: "Greenland Ice Sheet: High-Elevation Balance and Peripheral Thinning", Science, Vol. 289, p. 428-430, 2000.

Krabill, W., E. Hanna, P. Huybrechts, W. Abdalati, J. Cappelen, B. Csatho, E. Frederick, S. Manizade, C. Martin, J. Sonntag, R. Swift, R. Thomas and J. Yungel: Greenland Ice Sheet: Increased coastal thinning. Geophysical Research Letter, Vol. 31, L24402, 2004.

Krabill, W. B., and R. H. Thomas (presented by H. Miller): Recent near-coastal elevation changes on the Greenland Ice Sheet from aircraft laser altimetry. 2nd International Alfred Wegener Symposium, Bremerhaven 2005.

Maas, H.-G., R. Dietrich, E. Schwalbe, M. Bäßler, P. Westfeld: Analysis of the motion behaviour of the Jakobshavn Isbrae glacier in Greenland by monocular image sequence analysis. IAPRS Vol. XXXVI, Part 5, 179-183, Dresden, September 2006.

Reeh, N.: Parametrization of melt rate and surface temperature on the Greenland Ice Sheet, Polarforschung 59 (3), 113-128, 1989.

Steffen, K. :Greenland climate Network (GC-NET), CIRES Boulder, Personal communication, 2005

Zwally, H.J., W. Abdalati, T. Herring, K. Larsen, J. Saba, K. Steffen: Surface melt-induced acceleration of Greenland ice-sheet flow. Science, 297, 218-222, 2002.

Estimation of the motion of Arctic glaciers with satellite L-band SAR data

Tazio Strozzi[1], Andreas Wiesmann[1], Urs Wegmüller[1], Charles Werner[1], Alexei Kouraev[2] and Aleksey Sharov[3]

[1] Gamma Remote Sensing, Gümligen, Switzerland
[2] Laboratoire d'études en géophysique et océanographie spatiale (LEGOS), Observatoire Midi-Pyrenées (OMP), Toulouse, France
[3] Joanneum Research, Graz, Austria

Many studies on Arctic and Antarctic glaciers and ice streams have demonstrated the invaluable potential of satellite Synthetic Aperture Radar (SAR) interferometry and offset tracking to map ice surface velocity fields without the expense of in-situ measurements. Most of these studies used data from the European Remote-Sensing Satellites ERS-1 and ERS-2 and from Canada's Earth observation satellite RADARSAT-1 at C-band (5.6 cm wavelength λ) with 1, 3 or 24 days acquisition time intervals. The experience with L-band SAR data with longer acquisition time intervals is, however, limited, in spite of the enormous amount of SAR data collected by the Japanese Earth Resources Satellite JERS-1 between 1992 and 1998 at λ = 23.5 cm and HH polarization.

In our contribution we discussed the motion of Arctic glaciers at Svalbard, Novaya Zemlya and Franz-Josef Land derived with offset tracking of L-band SAR data acquired by the JERS-1 satellite in winter with 44 days acquisition time interval. With offset tracking the registration offsets of two SAR images in both slant-range (i.e. in the line-of-sight of the satellite) and azimuth (i.e. along the orbit of the satellite) directions are generated and used to estimate the displacement of glaciers. The displacement maps show a number of clearly defined fast-flowing units with displacement larger than about 6 m in 44 days (i.e. 50 m/year). The estimated error of the JERS-1 offset tracking derived displacement is on the order of 20 m/year. Occasionally, azimuth streaks related to auroral zone ionospheric disturbances were detected and dedicated processing steps were applied to minimize their influence on the estimated motion pattern.

Our results demonstrated that offset-tracking of L-band SAR images is a robust and direct estimation technique of glacier motion. The JERS-1 results, obtained using SAR data acquired by a satellite operated until 1998, are significant in expectation of data from the PALSAR sensor onboard the Japanese Advanced Land Observing Satellite (ALOS) launched in early 2006.

Acknowledgements
Work supported by the FP6 EC INTEGRAL project (Contract No. SST3-CT-2003-502845) with Swiss contribution under BBW Nr. 03.0049. JERS-1 SAR data courtesy C1P.2611 (SIGMA, P.I. A. Sharov), © JAXA, processing Gamma Remote Sensing.

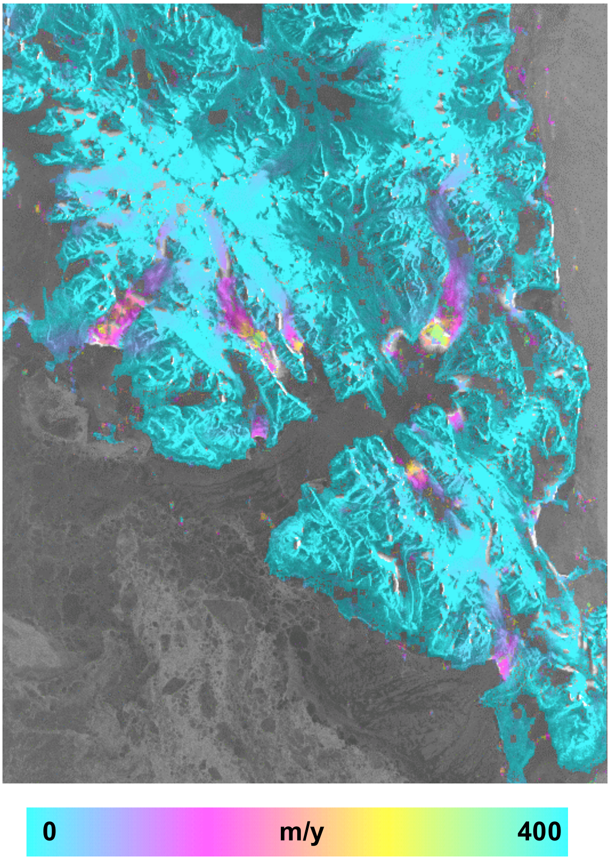

Figure 1. Horizontal surface displacement for South Spitsbergen (Svalbard) from JERS-1 offset tracking between SAR images of March 23 and May 6, 1994 with a perpendicular baseline of 310 m. Image width is ~80 km.

References

Gray, L., Mattar, K. & Vachon, P. (1998). InSAR results from the RADARSAT Antarctic mapping mission: estimation of glacier motion using a simple registration procedure. Proceedings of IGARSS 1998, Seattle, USA, 6-10 July

Strozzi T., Wiesmann, A., Sharov, A., Kouraev, A., Wegmüller, U. & Werner, C. (2006). Capabilities of L-band SAR data for arctic glacier motion estimation. Proceedings of IGARSS 2006, Denver, USA, July 31 - August 4

Wegmüller, U., Werner, C., Strozzi, T., & Wiesmann, A. (2006). Ionospheric electron concentration effects on SAR and INSAR. Proceedings of IGARSS 2006, Denver, USA, July 31 - August 4

Werner C., Wegmüller, U., Strozzi T., & Wiesmann, A. (2005). Precision estimation of local offsets between SAR SLCs and detected SAR images. Proceedings of IGARSS 2005, Seoul, Korea, 25-29 July

A NEW GLACIER INVENTORY FOR CUMBERLAND PENINSULA, CANADIAN ARCTIC, FROM ASTER DATA WITH ASSESSMENT OF CHANGES SINCE 1975 AND THE LITTLE ICE AGE EXTENT

FELIX SVOBODA AND FRANK PAUL

Department of Geography, University of Zurich, Zurich, Switzerland,

According to most climate change studies, the Arctic regions will experience a particular strong increase in temperature in the coming decades. The related potential increase in global sea level rise due to glacier melt from the strongly glaciated Canadian Arctic is difficult to assess as no complete glacier inventory exist (Raper and Braithwaite, 2006). Recorded glacier data and photographs acquired by the Canadian government in the late 70s are not readily available at present (Ommaney, 1998) and neither World Glacier Inventory (WGI) data (point information) nor digital glacier outlines (2D information) cover the whole area. The latter are also mandatory for a sound determination of individual glacier changes and, together with an appropriate digital elevation model (DEM), for calculation of the area-elevation distribution. With multispectral satellite data and well established methods both data sets (outlines and DEMs) can be generated and the related glacier inventory data can be derived automatically with modern geoinformatic techniques (e.g. Paul et al., 2002).

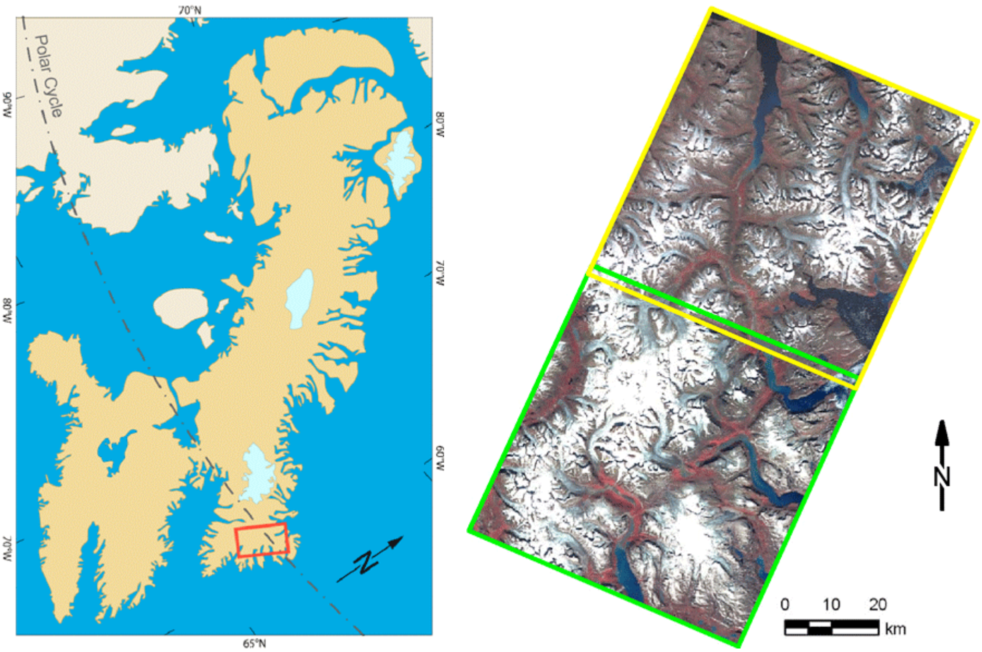

Figure 1. a) Location of the study site (red square) on Baffin Island, Canada, and b) false colour composite of the two used ASTER scenes.

In this study we present first results of a new glacier inventory for Cumberland Peninsula in south-eastern Baffin Island that has been generated within the framework of the GLIMS project from two ASTER satellite scenes acquired in August 2000 (Figure 1). The stereo capability from ASTER was used to derive two high resolution DEMs (30 m cells) which were also utilized to orthorectify the scenes. Especially on snow covered plains, in cast shadow, and on steep slopes the DEM was inaccurate (Figure 2). For automated glacier mapping we applied a threshold of 1.6 on a band 3/4 ratio image and additionally a threshold of 74 in band 1 for improving glacier classification in cast shadow. Debris covered glacier snouts and ice-divides had to be delineated manually. The latter were difficult to identify for many of the ice-clad mountain crests and ice caps. On snow covered areas the DEM could not be used to differentiate between glacier basins. In such regions the delineated ice-divides are more or less speculative.

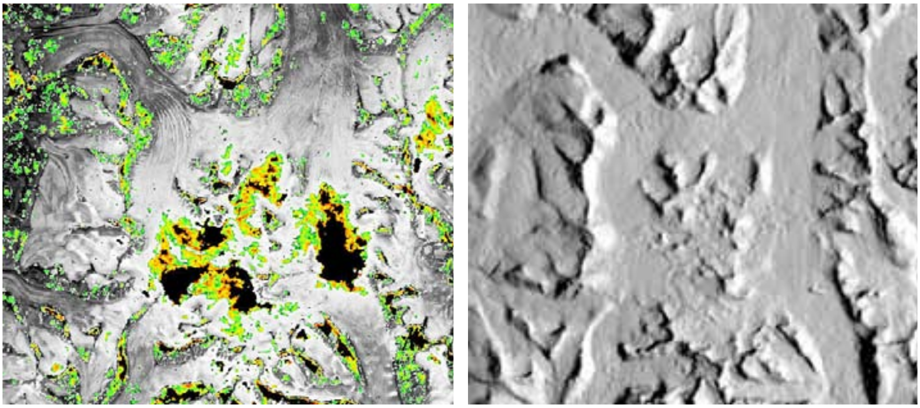

Figure 2. a) NIR channel overlaid by correlation of the DEM (black: 0, red: 0.1, yellow: 0.75, green: 0.9) and b) the corrected DEM (hill shade) for the same region.

For temporal comparison we obtained two additional satellite scenes from the GLCF. One TM scene from August 1990 and one MSS scene from end of July 1975. Moreover, we manually digitized the Little Ice Age (LIA) maximum glacier extent from well preserved moraines and trim lines in order to compare current rates of change with historic ones (Paul and Kääb, 2005). Since the TM image suffers from large amounts of seasonal snow and some clouds, it was excluded here. The MSS image suffers from the reduced spatial resolution (80 m pixels) and one clouded area. Despite the missing glacier mapping band in the short-wave infrared (ASTER band 4), we applied a threshold of 0.5 on a MSS band 3/4 ratio image, and additional brightness thresholds in the other bands. The result was quite accurate except for debris covered parts of the glaciers. All three mapped glacier extents are depicted in Figure 3.

Topographic glacier parameters were calculated from the ASTER-derived DEM and glacier changes (length, area) for the 1975 and the LIA extent. From the totally mapped 688 glaciers, about 40% could be extended with LIA outlines and about 15% were manually edited for debris cover. Including the delineation of glacier basins the work load was about 10 to 15 minutes per glacier. In particular the basin delineation was time consuming.

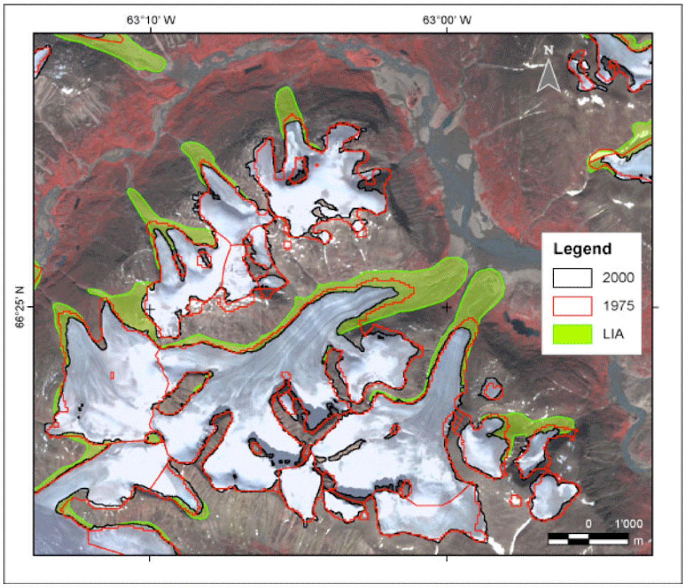

Figure 3. False colour ASTER image with the three different glacier extents.

The observed length changes since LIA (sample size 190) vary between 0 and -2500 m, with most values around -500 m. From 1975 to 2000 retreat values between 0 and -1200 m have been observed. In 2000 the mapped glacier area covers with 2480 km^2 around one third of the whole study area. The average glacier size is about 3.6 km^2. The relative change in area from the LIA until 2000 is about -22% (sample size 278), since 1975 it is -18% with respect to the 1975 area (sample size 492). The change in length and area indicate an acceleration of the retreat / area loss in the recent past. Most of the area changes took place at the terminus. There is virtually no change for smaller glaciers at high elevations, but this could be an artefact of seasonal snow that often hides the glacier perimeter. In principle, there is little dependence of glacier size on aspect, but mean elevation (as a proxy for the ELA) has some correlation with aspect (200 m higher in the south sector than in the north). The analyses of the results are still ongoing and glacier outlines and parameters will be provided to the GLIMS database in the future.

References

Ommaney, C. S. L. (1998). Monitoring and inventorying the glaciers of Canada: An historical review and personal comments. USGS Open-File Report, 98-0031 [Online: http://pubs.usgs.gov/of/of98-031/cdnglacinv.htm].

Paul, F. and Kääb, A. (2005): Perspectives on the production of a glacier inventory from multispectral satellite data in the Canadian Arctic: Cumberland Peninsula, Baffin Island. Annals of Glaciology, 42, 59-66.

Paul, F., Kääb, A., Maisch, M., Kellenberger, T. W. and Haeberli, W. (2002): The new remote-sensing-derived Swiss glacier inventory: I. Methods. Annals of Glaciology, 34, 355-361.

Raper, S.C.B. and Braithwaite, R.J. (2006): Low sea level rise projections from mountain glaciers and icecaps under global warming. Nature, 439, 311-313.

THERMAL REGIME CHANGES OF THE POLYTHERMAL MIDRE LOVÉNBREEN, SVALBARD

IAN C. WILLIS[1], DAVID M. RIPPIN[2] AND JACK KOHLER[3]

[1] Scott Polar Research Institute, Department of Geography, University of Cambridge, Cambridge, UK.
[2] Department of Geography, University of Hull, Hull, UK.
[3] Norwegian Polar Institute, Tromsø, Norway.

Introduction

Glaciers are retreating rapidly in response to global warming and are contributing to sea level rise (Dowdeswell and Hagen, 2004; Dyurgerov and Meier, 2004). The Arctic and the Antarctic Peninsular appear to have undergone greater than average global warming and are predicted to do so in the future (IPCC, 2007). Many Arctic glaciers are polythermal and many in the Antarctic Peninsular may be polythermal too. Since, a polythermal structure plays an important first order control on glacier mass balance, hydrology, dynamics, and the supply of solutes and sediments to proglacial streams and fjords, predicting how the thermal regime of polythermal glaciers will change in the future is an important research goal in glaciology.

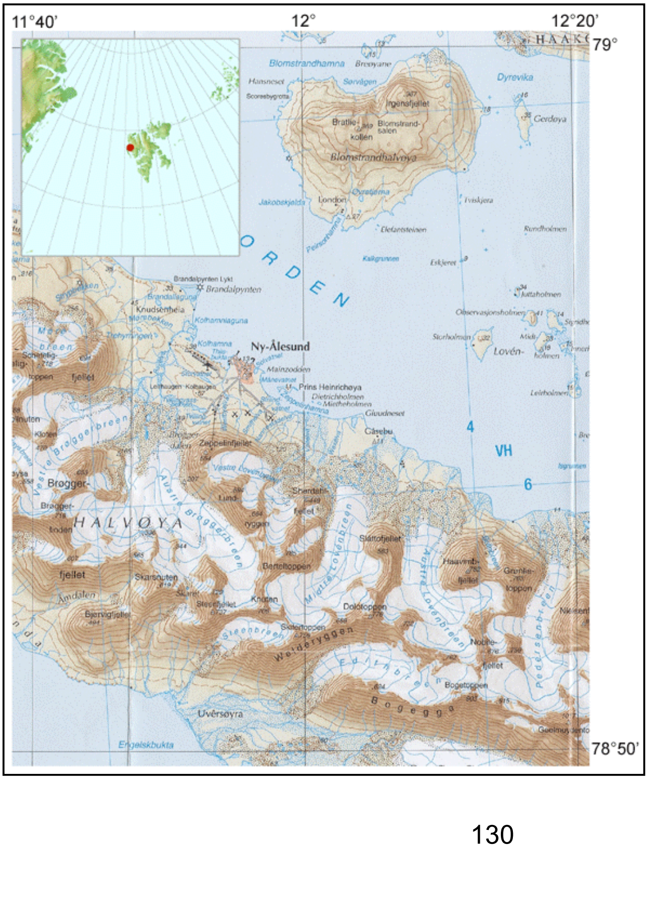

Figure 1. Location Map of Midre Lovenbreen, Svalbard. Source: Norsk Polarinstitutt 1:100 000 series. Svalbard – A7 Kongsfjorden, 2004.

Here we present some preliminary work documenting the changes to the thermal regime of Midre Lovénbreen, Svalbard between 1990 and 2006. Our longer-term aims are to use these data to help test a coupled thermo-mechanical glacier flow model capable of simulating changes in the thermal structure and dynamics of Arctic glaciers in the past, and into the future.

Midre Lovénbreen (78.538 N, 12.048 E) is a 6 km long alpine-type valley glacier with a maximum thickness of 180m (Rippin et al., 2003) (Figure 1). The glacier has a warm-based core, cold-based ice around its snout and margins, and cold ice at its surface, except in the upper accumulation area where warm ice extends to the surface (Björnsson et al., 1996; Rippin et al., 2003). The boundary between the warm-based and cold-based part of the glacier tongue acts as a thermal dam. Water is stored above the dam in spring/early summer but then breaks through the dam, flows beneath the cold-based margin, and emerges proglacially as a pressurized upwelling from mid-summer onwards (Hodson and Ferguson, 1999). The hydrology affects the glacier's dynamics (Rippin et al., 2005a; 2005b). Periods of fast flow during spring/early summer are due to reductions in basal drag beneath the upper tongue and increases in the longitudinal stress gradient over the lower tongue. During the water breakthrough event, fast flow occurs by reductions in basal drag beneath the lower cold-based tongue and increases in longitudinal stress coupling to the upper part.

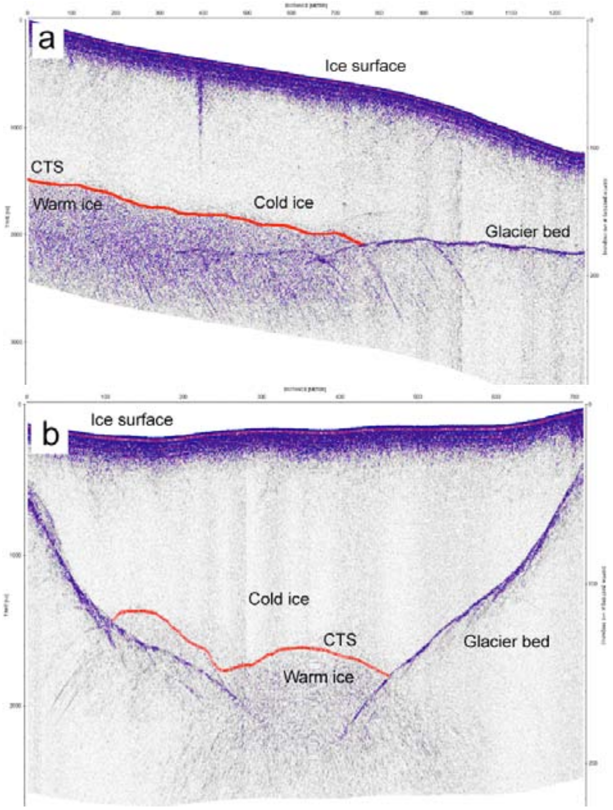

Figure 2. Longitudinal and cross profile GPR transects showing ice surface, glacier bed, and the cold-warm transition surface (CTS) marked by internal scattering.

Methodology

In April/May 2006, we carried out an extensive common-offset ground penetrating radar (GPR) survey of the glacier tongue. Radar data were collected continuously using a PulseEkko 100 system towed behind a skidoo. Approximately 10 800 m of data were collected at a 1 m step-size over the central portion of the glacier tongue, at a centre frequency of 50 MHz. The antennas were positioned parallel to one another and transverse to the survey direction, thus minimising offline reflections. At the same time, real-time kinematic GPS data were collected every 2 seconds to accurately locate the GPR system on the glacier. Subsequent processing of radar data was done using ReflexW, allowing us to pick the glacier surface, glacier bed, and the boundary between warm and cold ice along each transect.

Results & Discussion

Over much of the surveyed area, the surface and bed of the glacier are clearly visible, with minimal internal scattering (e.g. downglacier portion of Figure 2a and margins of Figure 2b). However, in a central portion of the surveyed area, there is a layer of ice above the bed in which internal scattering is present (e.g. upglacier portion of Figure 2a, and central part of Figure 2b). This basal scattering zone likely extends upglacier beyond the limits of our survey, but our data do not allow us to comment on this. We interpret areas of minimal scattering to be cold, water-free ice, and regions of intense scattering to be warm ice containing water.

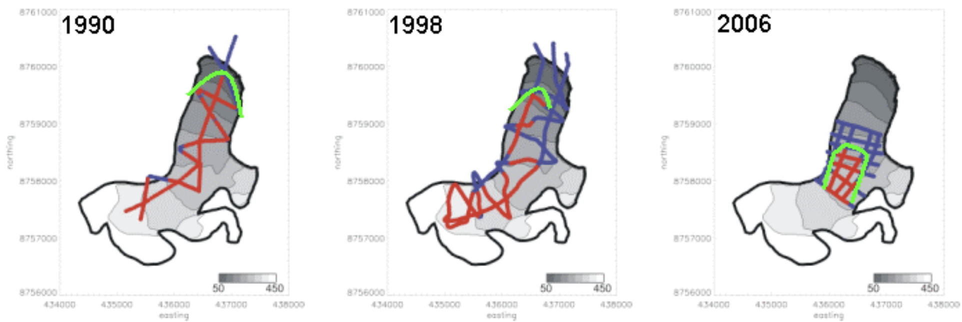

Figure 3. Maps showing areal extent of warm-based (red lines) and cold-based (blue lines) ice from GPR surveys in 1990 (Bjornsson et al, 1996), 1998 (John Moore, unpublished data) and 2006 (this study). The green line marks the boundary between the warm- and cold-based ice. Background map is based on DEM (elevations in metres) derived from 2003 Lidar data (Neil Arnold and Gareth Rees, personal communication, 2006).

The data allow us to map the lateral extent of warm-based and cold-based ice, which may be compared with similar maps based on previous GPR surveys collected in May 1990 (Björnsson et al., 1996) and May 1998 (John Moore, unpublished data) (Figure 3).

Figure 3 shows that boundary between warm- and cold-based ice has shrunk both laterally, but particularly longitudinally over the 16 years. In 2006, the thermal dam was ~1250m further upglacier than it was in 1990. To put this into context, the glacier average mass balance between 1990 and 2005 was -6.5 m w.e. (-11.5m w.e. since 1977), and the amount of snout retreat between 1995 and 2005 was 50m (550m since 1977).

Conclusions

Repeat GPR survey has been used to identify the thermal regime changes of the polythermal Midre Lovénbreen, Svalbard. The glacier has experienced significant shrinkage of its temperate core, as a consequence of sustained negative mass balance, thinning and snout retreat over recent years. The rate of basal cold/temperate boundary retreat was ~ 80m a^{-1} between 1990 and 2006, whereas the rate of snout retreat was only ~13m a^{-1} and the surface mass balance was only –0.4m w.e. a^{-1} over same period. This polythermal glacier is rapidly becoming a cold glacier, like its neighbour Austre Brøggerbreen. The data suggest that the thermal regime of Arctic glaciers varies sensitively to climate change. This will have important consequences for their hydrology and dynamics and will affect processes and rates of sediment and solute delivery to Arctic proglacial streams and shallow marine environments.

References

Björnsson, H. and 6 others. 1996. The thermal regime of sub-polar glaciers mapped by multi-frequency radio-echo sounding. J. Glaciol., 42(140), 23–32.

Dowdeswell, J.D. and Hagen, J-O. 2004 Arctic ice caps and glaciers. In Bamber, J. and Payne, T. (Eds). The Mass Balance of the Cryosphere. CUP.

Dyurgerov, M. and Meier, M. 2004. Glaciers and the study of climate and sea-level change. . In Bamber, J. and Payne, T. (Eds). The Mass Balance of the Cryosphere. CUP.

Hodson, A.J. and R.I. Ferguson. 1999. Fluvial suspended sediment transport from cold and warm-based glaciers in Svalbard. Earth Surf. Proc. Land., 24, 957-974.

IPCC. 2007. The Fourth Assessment Report of the United Nations Intergovernmental Panel on Climate Change. UNFCCC / WMO / UNEP.

Rippin, D., I. Willis, N. Arnold, A. Hodson, J.C. Moore, J. Kohler and H. Björnsson. 2003. Changes in geometry and subglacial drainage of Midre Lovénbreen, Svalbard, determined from Digital Elevation Models. Earth Surface Processes and Landforms, 28 (3), 273-298.

Rippin, D., I. Willis and N. Arnold. 2005a. Seasonal patterns of velocity and strain across the tongue of the polythermal glacier Midre Lovénbreen, Svalbard. Annals of Glaciology, 42, 445-454.

Rippin, D.M., Willis, I.C., Arnold, N.S., Hodson, A.J. and Brinkhaus, M. 2005b. Spatial and temporal variations in surface velocity and basal drag across the tongue of the polythermal glacier Midre Lovénbreen, Svalbard. Journal of Glaciology, 51(175), 588-600.

WORLD GLACIER MONITORING SERVICE – CALL-FOR-DATA FOR THE OBSERVATION PERIOD 2000–2005 AND INTERNATIONAL POLAR YEAR ACTIVITIES

MICHAEL ZEMP, MARTIN HOELZLE, FRANK PAUL AND WILFRIED HAEBERLI

World Glacier Monitoring Service, Department of Geography, University of Zurich, Switzerland

Worldwide collection of information about ongoing glacier changes was initiated in 1894 with the foundation of the International Glacier Commission at the 6th International Geological Congress in Zurich, Switzerland. Today, the World Glacier Monitoring Service (WGMS; http://www.wgms.ch) continues to collect and publish standardised information on ongoing glacier changes. WGMS is a service of the Commission for the Cryospheric Sciences of the International Union of Geodesy and Geophysics (CCS/IUGG) and maintains a network of national correspondents and local investigators in all the countries involved in glacier monitoring. In addition, the WGMS is in charge of the Global Terrestrial Network for Glaciers (GTN-G) within the Global Climate/Terrestrial Observing System (Haeberli et al. 2000). GTN-G aims at combining (a) in-situ observations with remotely sensed data, (b) process understanding with global coverage and (c) traditional measurements with new technologies by using an integrated and multi-level strategy (Haeberli 2004).

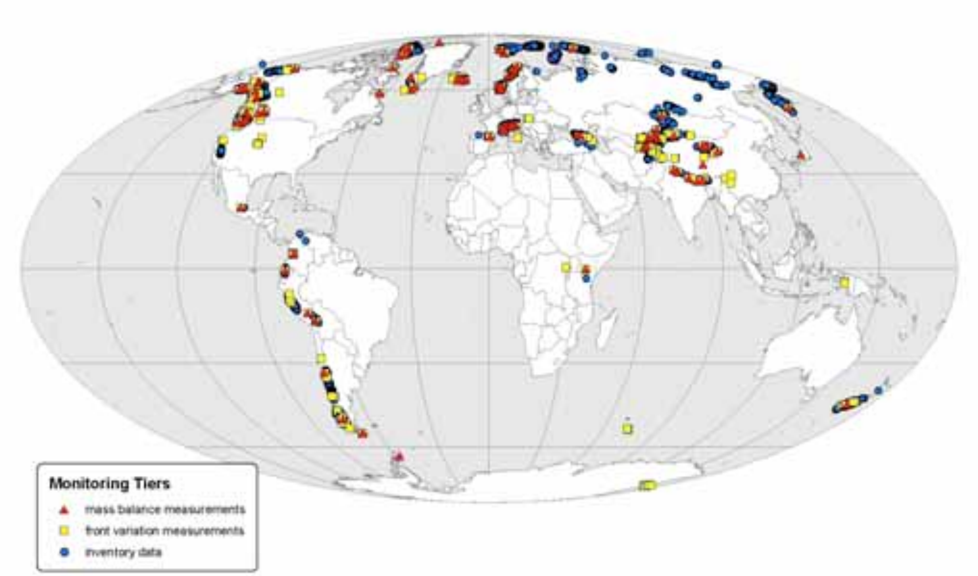

Figure 1. Worldwide glacier monitoring. Data source: WGMS.

Inventory (WGI 1989), there are information on location, classification, area, length, orientation and altitude range of over 71,000 glaciers available (mainly from aerial photographs and maps). The latter correspond to about 44% of total number and

23% of total area of all glaciers and ice caps worldwide (cf. estimates by Dyurgerov and Meier 2005). The Global Land Ice Measurements from Space (GLIMS; http://nsidc.org/glims) initiative was designed to continue this inventorying task (with space-borne sensors) in close cooperation with the National Snow and Ice Data Center (NSIDC; http://www.nsidc.org) and the WGMS. A new project (GLOBGLACIER), under the lead of F. Paul (University of Zurich), is proposed to the European Space Agency and aims at making a major contribution to the current GLIMS database (http://dup.esrin.esa.int/projects/summaryp98.asp).

At present, the WGMS is collecting information on glacier changes in mass, volume, area and length for the observation period 2000–2005. Out of the submitted data (due to by the 1st of March, 2007) the 'Fluctuations of Glaciers Vol. IX (2000–2005)' and the 'Glacier Mass Balance Bulletin No. 9 (2004–2005)' will be produced. First results from the submitted mass balance data of 30 reference mountain glaciers around the world, with continuous measurements since 1980, show an average annual ice loss of 0.6 m w.e. for the period of 2000–2005 which brings the cumulative mass loss since 1980 at about 9.6 m w.e. (Figure 2). This continues the trend in increasing ice loss (over reducing glacier surface areas) during the past 25 years and leaves no doubt about an ongoing climatic forcing.

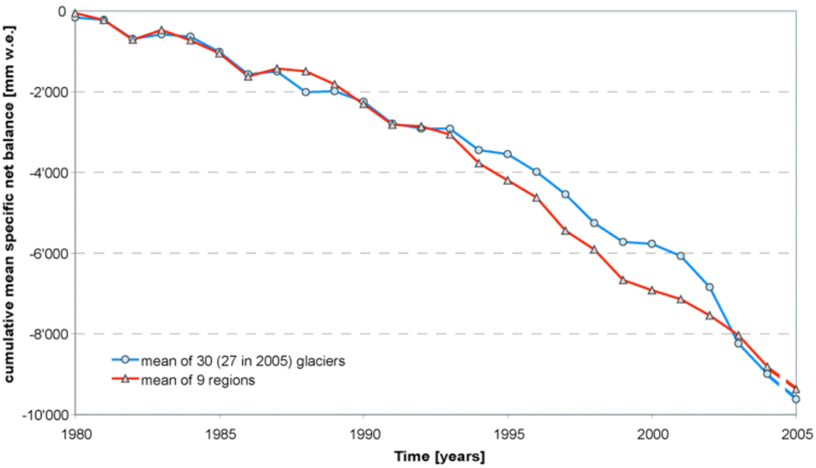

Figure 2. Cumulative mean specific net balance continuously measured on 30 glaciers in 9 mountain ranges for the period 1980 to 2004, and on 27 glaciers in 9 mountain ranges for 2005. The glaciers are Place (CA), South Cascade (US), Austre Broeggerbreen (NO), Midre Lovenbreen (NO), Echaurren Norte (CL), Gulkana (US), Wolverine (US), Engabreen (NO), Alfotbreen (NO), Nigardsbreen (NO), Grasubreen (NO), Storbreen (NO), Hellstugubreen (NO), Hardangerjoekulen (NO), Storglaciaeren (SE), Saint Sorlin (FR), Sarennes (FR), Silvretta (CH), Gries (CH), Sonnblickkees (AT), Vernagtferner (AT), Kesselwandferner (AT), Hintereisferner (AT), Careser (IT), No. 125 (CIS), Maliy Aktru (CIS), Leviy Aktru (CIS), Djankuat (CIS), Ts. Tuyuksuyskiy (KZ), Urumqihe S. No. 1 (CN). Data source: WGMS.

During the coming International Polar Year (IPY; 2007–2008), the WGMS will help to coordinate glacier related IPY-projects in cooperation with NSIDC, GLIMS and the IPY Data and Information Service (IPYDIS; http://nsidc.org/ipydis/). Scientists with glacier-related projects are invited to contact WGMS for available data, internationally approved standards for glacier monitoring, and for data submission guidelines. The WGMS will call for standardised glacier data measured during the IPY and aims at including an IPY-chapter in the 'Fluctuations of Glaciers Vol. X (2005–2010).

Acknowledgements

Our sincere thank goes to the national correspondents and principal investigators of the World Glacier Monitoring Service and all the contributing institutes and organisations for collection and free exchange of important data over many years.

References

Dyurgerov, M.B. and Meier, M.F. (2005): Glaciers and the changing earth system: a 2004 snapshot. INSTAAR 15 Occasional Paper, 58: 117 pp.

Haeberli, W., Cihlar, J. and Barry, R.G. (2000): Glacier monitoring within the Global Climate Observing System. Annals of Glaciology, 31: p. 241–246.

Haeberli, W. (2004): Glaciers and ice caps: historical background and strategies of world-wide monitoring. In: Bamber, J.L., Payne A.J. (eds.): Mass balance of the cryosphere. Cambridge University Press, Cambridge: p. 559–578.

WGI (1989): World glacier inventory – status 1988. In: Haeberli, W., Bösch, H., Scherler, K, Østrem, G. and Wallén, C.C. (eds.), IAHS(ICSI)–UNEP–UNESCO, World Glacier Monitoring Service, Nairobi: 458 pp.

Mass Balance of the Greenland Ice Sheet: Consistent Results on Near Balance to Negative

H. Jay Zwally, Anita C. Brenner, Scott B. Luthcke, Donghui Yi, Jun Li, Jack L. Saba, Mario B. Giovinetto, Helen G. Cornejo, Matthew A. Beckley, and Waleed Abdalati

NASA Goddard Space Flight Center, Greenbelt, USA

Summary

During the last year, various estimates of the mass balance of the Greenland ice sheet have been published, including estimates of an accelerated mass loss during approximately the last five years. Although some estimates of mass loss have differed by more than a factor of two, a subset of consistent results has emerged. From 1992 to 2002, the Greenland mass balance was slightly positive (+11 ± 3 Gt/yr) as shown by a combination of radar satellite altimetry and airborne laser surveys (ATM). This is consistent with a reinterpretation of the ATM results (-8 Gt/a) for approximately the same time period. Although the Greenland ice sheet was close to balance overall in the 1990's, it was thinning significantly below the Equilibrium Line Altitude (ELA) (-42 ± 2 Gt/yr) and growing inland (+53 ± 2 Gt/yr). Since 2000, some Greenland glaciers have accelerated mostly in the Southeastern and upper Western drainage systems, as shown by InSAR measurements of ice outflow velocity and seismic measurements of ice-quakes. Although several reports of mass losses based on GRACE satellite gravity data exceeded 200 Gt/yr, analysis of GRACE data with much better spatial and temporal resolution has given a smaller net loss of 101 Gt/yr for July 2003 to July 2005. The lower rate of loss is consistent with new results from ICESat data for about the same time period. The change of -112 Gt/yr from the small positive balance for the 1992-2002 period is also consistent the -117 Gt/yr change from the InSAR mass flux estimates, but is not consistent with the magnitudes for the respective periods (-81 Gt/y in 1996 and -198 Gt/yr in 2005). The ICESat results and the high-resolution GRACE results both shown an increase in thickening at higher elevations, an increase in thinning at lower elevations, and increased net losses in the Southeastern and upper Western drainage systems where glaciers have accelerated. The seasonal cycles in elevation and mass at lower elevations from the ICESat and GRACE data reflect increases in elevation and mass during the months of winter accumulation and decreases during the summer melting. The winter of 2004-2005 had a larger mass gain than the previous year and the summer of 2005 had an excess mass loss of about 95 Gt, corresponding to anomalously large precipitation and melting in those particular seasons.

GLACIODYN

What is GLACIODYN?
GLACIODYN deals with the dynamic response of arctic glaciers to global warming. It is an IPY lead project

Global warming will have a large impact on glaciers in the Arctic region. Changes in the extent of glaciers will affect sea level, and may lead to substantial changes in sediment and fresh water supplies to embayments and fjords.
In ACIA, a simple approach was taken to estimate the runoff of all glaciers in the Arctic for a set of climate-change scenarios. Changes in the surface mass balance were calculated without dealing with the fact that glacier geometries will change. It was also assumed that the rate of iceberg production at calving fronts would not change. However, there is now overwhelming evidence that the dynamic response of glaciers and ice sheets to changing surface conditions can be rapid and the consequences can be substantial. Studies on the relation between meltwater input, ice movement and calving rates are particularly needed.
GLACIODYN is an internationally-coordinated effort to study the dynamics of Arctic glaciers. The key elements of this effort are (i) to *make better use of observational techniques* to assess the detailed dynamics of a key set of glaciers, and (ii) to *develop models* that can be used to aggregate data and that are sufficiently robust to have predictive power. A set of target glaciers (see map below) have been identified for intensive observations (in situ and from space) for the period 2007-2010. This set covers a wide range of climatic/geographical settings and takes maximum advantage of prior long-term studies.

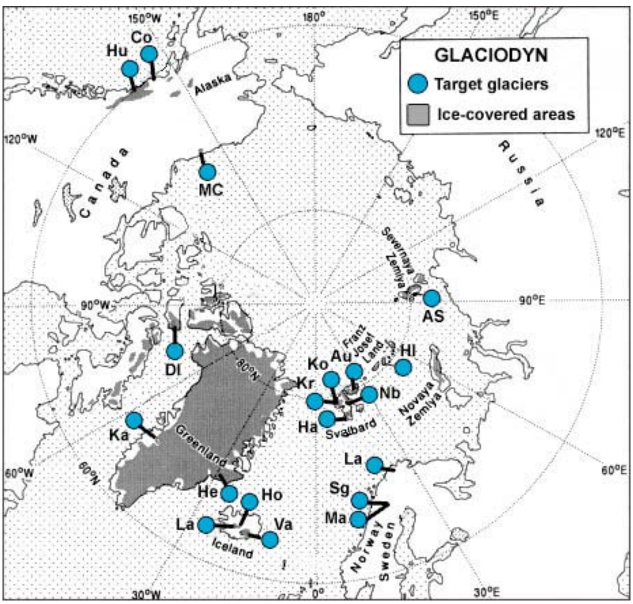

Among the target glaciers are glaciers for which information is available on length/area in historical times [reports, drawings, photographs, old maps, etc.]. This information will be combined with the newly derived maps to reconstruct glacier evolution from the Little Ice Age into the present. This will provide a better perspective for projecting changes in the coming century.

Special attention will be given to tidewater glaciers. We want to look carefully at the interaction between surface processes and dynamics (e.g. the influence of meltwater supply on ice velocities and consequently calving rates; interactions between terminal moraines, sediment flux, and ice velocities). In a warming world some glaciers will transform from cold to polythermal, or from polythermal to temperate. We want to study the effect of such transitions on glacier dynamics and related rates of retreat. Another important aspect of study is the surface albedo. Poor drainage of meltwater may lead to more extensive zones of soaked snow and supraglacial lakes (as seen in large parts of the Greenland Ice Sheet), thus enlarging the sensitivity of ablation rates to warming.

Model development will be conducted in parallel with the observational programmes. The modelling work will deal with processes acting on the smaller scale (e.g. parameterization of the calving process) and on the larger scale (e.g. global dynamics of tidewater glaciers, response to climate change, interaction with sediment dynamics).

Organizational structure of GLACIODYN

GLACIODYN has a simple and open organizational structure. It has a coordinator (J. Oerlemans, Utrecht University) and co-coordinator (J.-O. Hagen, University of Oslo). The IASC Working Group on Arctic Glaciology, in which there is a Committee of National Representatives, is used as forum for discussion and planning. When the need arises a smaller steering committee will be established.

Plans of individual research groups

In the first GLACIODYN planning meeting the emphasis was placed on the plans of individual research groups. It now appears that most of these plans have received funding in one way or another. The level of funding is very different for different countries, however. Substantial additional funds for projects contributing to GLACIODYN (directly or through other glaciological IPY projects) have become available in Canada, Norway, and Denmark. In some other countries, like the Netherlands, Poland, U.S.A., Sweden, U.K., support has been modest or decisions are still pending.
Concerning GLACIODYN it can be stated that the current level of funding is high enough to ensure a good start, with a large number of field activities in the spring/ summer of 2007.

Next planning meeting and workshops

The next GLACIODYN planning meeting will be held in early 2008 in Obergurgl, Austria. It will be combined with the general workshop of the Working Group on Arctic Glaciology.
It is planned to have the 2009 workshop in Canada.